CHALMERS
UNIVERSITY OF TECHNOLOGY

Timber Footbridge in Wendelstrand

An Iterative Design Process Combining Architecture and Engineering

Master's thesis in the Master's Programme Structural Engineering and Building Technology

ALEXANDER ANGRÉN
MARIA BRUZELL ROLL

Department of Architecture and Civil Engineering
Division of Structural Engineering
Lightweight Structures in collaboration with Architecture and Engineering
CHALMERS UNIVERSITY OF TECHNOLOGY
Master's Thesis ACEX30
Gothenburg, Sweden 2021

MASTER'S THESIS ACEX30

Timber Footbridge in Wendelstrand

An Iterative Design Process Combining Architecture and Engineering

Master's Thesis in the Master's Programme Structural Engineering and Building Technology

ALEXANDER ANGRÉN
MARIA BRUZELL ROLL

CHALMERS

Department of Architecture and Civil Engineering
Division of Structural Engineering
Lightweight Structures in collaboration with Architecture and Engineering
CHALMERS UNIVERSITY OF TECHNOLOGY
Göteborg, Sweden 2021

Timber Footbridge in Wendelstrand
An Iterative Design Process Combining Architecture and Engineering

Master's Thesis in the Master's Programme Structural Engineering and Building Technology

ALEXANDER ANGRÉN

MARIA BRUZELL ROLL

Examensarbete ACEX30
Institutionen för arkitektur och samhällsbyggnadsteknik
Chalmers tekniska högskola, 2021

Department of Architecture and Civil Engineering
Division of Structural Engineering
Lightweight Structures in collaboration with Architecture and Engineering
Chalmers University of Technology
SE-412 96 Göteborg
Sweden
Telephone: + 46 (0)31-772 1000

Cover:
Model in scale 1:20 of the proposed bridge design.
Department of Architecture and Civil Engineering
Göteborg, Sweden, 2021

Timber Footbridge in Wendelstrand
An Iterative Design Process Combining Architecture and Engineering
Master's thesis in the Master's Programme Structural Engineering and Building Technology

ALEXANDER ANGRÉN

MARIA BRUZELL ROLL

Department of Architecture and Civil Engineering
Division of Structural Engineering
Lightweight Structures in collaboration with Architecture and Engineering
Chalmers University of Technology

ABSTRACT

Wendelstrand is a new residential area in Mölnlycke planned with sustainability and wood as overall concepts. Adjacent to the area is the lake Landvettersjön, which today is cut off by a highly travelled country road. A footbridge over the road will link the lake and Wendelstrand and create a safe crossing for both residents and visitors to the area. In this thesis a proposal for such a footbridge is developed with emphasis on the relation to the timber and sustainability-concept of Wendelstrand, as well as the integration between architectural and structural qualities. An iterative design method is used to examine and develop possible solutions for a bridge proposal. Reference projects of existing timber bridges are used in the development of feasible bridge designs. Site-specific prerequisites, intentions from the developer Next Step Group, regulations from the local municipality and the Swedish Transport Administration are considered and integrated into the design. The proposal suggests a straight bridge across the road leading to a floating structure on the lake. The bridge supports are integrated into the superstructure and designed to limit the impact on the site. Physical models are used to verify the assembly process, as well as the structural concept and spatial qualities of the design. The design corresponds with Swedish and European standards concerning structural response. Simplified calculations are performed to verify the global and detailed design of the design proposal. A solution for an efficient structure in addition to an appealing architectural appearance is achieved by applying the principles of active bending in the superstructure.

Keywords: wood, timber, bridge, footbridge, conceptual, design, architecture, structure, active bending, Wendelstrand

Contents

Preface

In this study, an investigation of structural design for a site-specific bridge has been carried out. Our aim was, in addition to fulfilling the requirements of the client, to combine principles from structural engineering and architecture. We want to aspire to rethink and challenge standard solutions to contribute to the development of timber bridge design.

First, we would like to thank our examiner Robert Jockwer for supporting our ambition for the bridge design, for the enthusiasm during the process, and for contributing with important knowledge regarding structural design of timber structures. Our supervisor Prof. Karl-Gunnar Olsson is highly appreciated for his understanding and commitment to combine architecture with engineering, for emphasising on the importance of reference analysis, and for daring us to think boldly.

Thanks to Emelie Silverterna and Joakim Garfvé at Next Step Group, the developer of Wendelstrand, for the opportunity to collaborate and for insight in site-specific data, as well as valuable feedback on the design proposals. We would like to give thanks to Brosamverkan for the scholarship, who financed the material usage for our physical models. The scholarship enabled us to build models to verify the structural concept, validate the assembly method, and demonstrate the relation between the bridge design and Wendelstrand. Thanks to our opponent Vera Sehlstedt for numerous discussions and for support through the process.

At last, we would also like to address a special thanks to Burkard Walther, Miebach Ingenieurbüro, Camathias SA, werk1, and Wendelstrand for allowing us to use their photographs and illustrations in the thesis.

Göteborg June 2021

Alexander Angrén
Maria Bruzell Roll

1 Introduction

Close to Mölnlycke, outside Gothenburg, the Bråta gravel pit will be phased out and changed into a new residential area named Wendelstrand. This will be Northern Europe's largest residential area in wood and is developed by Next Step Group (E. Silverterna, personal communication, January 29, 2021). The area is situated right next to the lake Landvettersjön but the two are today separated by Boråsvägen, a heavily travelled country road (Wendelstrand, 2018). A timber bridge will facilitate a safe crossing, while the structure itself can be used to enhance the innovative ideas of Wendelstrand.

Interplay between nature and the buildings is an important part in the design of Wendelstrand. An approach in the direction of environmental sustainability is taken by choosing timber as the main structural material of the buildings (Garfvé, n.d.). In 2017 the Swedish parliament decided that Sweden should reach zero net-emissions of greenhouse gases by 2045 at latest, proceeding with negative emissions (Proposition 2016/17:146 Ett Klimatpolitiskt Ramverk För Sverige, 2017). Life Cycle Analysis studies show that when comparing timber frame buildings with non-timber alternatives, including concrete and steel, the former requires lower energy and releases less greenhouse gases (Dodoo et al., 2016). In other words, one way to reduce the environmental impact of structures is to increase the use of timber.

When designing timber bridges, emphasis must be laid on durable detail design preventing the superstructure from weathering, enabling the wood to dry out, and protecting the end-wood from exposure. Due to water absorption and the risk of rot, timber bridges need careful planning in order to limit the need for maintenance and frequent inspections than a bridge made out of steel or concrete (Pousette & Fjellström, 2004). Therefore, the maintenance costs of timber bridges are higher. On the other hand, timber has a high strength-to-weight ratio (Svenskt Trä, 2009). Consequently, a lighter construction can be achieved with less foundation work. However, the construction of timber bridge structures has evolved throughout the years. By learning from failure in timber bridges due to lack of careful detailing, poor choice of material, or lack of maintenance and cleaning, improved designs of modern timber bridges can be made (Pousette & Fjellström, 2004).

1.1 Aim

The aim of this thesis is to develop a design proposal for a timber footbridge in Wendelstrand. Focus lies on combining structural engineering knowledge with architectural visions.

The following research questions are formulated:

"In what way can a bridge proposal be achieved that meets the requirements and ideas of the client Next Step Group for the planned residential area Wendelstrand?"

"In what way can an iterative design method be used to develop a structural concept that enhances both engineering solutions and architectural qualities?"

1.2 Method

An iterative design method consisting of four stages is applied to answer the two research questions. In the first stage of contextualisation, an overview of the task is achieved by research of reference projects and identification of site-specific requirements. The second stage is a Conceptual design phase where possible solutions are examined and developed into one suitable proposal. This design proposal is further developed in the third stage and validated in the fourth and last stage. Figure 1.1 illustrates the design process from start to end.

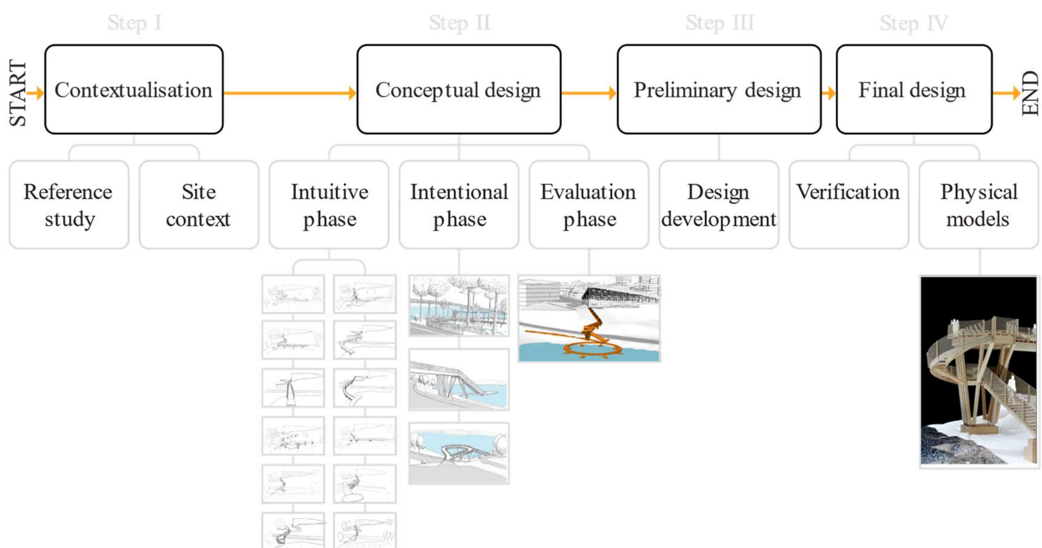

Figure 1.1 Design process.

To ensure fulfilment of the thesis aim, a set of evaluation criteria are formulated. These make the transition between the design phases, to ensure a correspondence between the final proposal and the thesis aim. The evaluation criteria include both external demands and requirements, and design criteria. The latter define expectations regarding both the visual appearance and the structural performance of the footbridge structure. Figure 1.2 illustrates the evaluation criteria, which are further explained in Chapter 5.

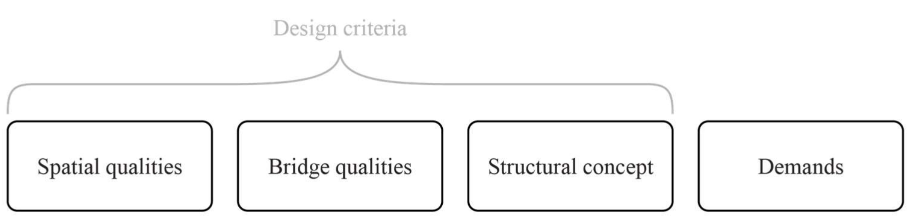

Figure 1.2 Evaluation criteria.

1.3 Limitations

The project is limited to a specific site, Wendelstrand, with real boundary conditions that the bridge design must comply with. Next Step Group is considered as the client, to establish a realistic context for the design project. They have stated clear demands regarding the bridge which will be prioritised in the design. The bridge design must consider the drastic elevation change in the landscape, as well as fulfilling non-negotiable requirements regarding shore protection, geological conditions, and standards from the Swedish Transport Administration and Eurocode.

The structural response of the final bridge design is roughly estimated, and dimensions are based on conservative calculations and available product dimensions. The chosen structural concept is based on experiments with physical models, combined with understanding gained from analysis of reference projects. A thorough investigation of the theory is outside the scope. Detailed investigation for optimisation of the connections and foundation elements is not performed. Moreover, the assembly method will only be tested in physical models, while considering the limitations of production, transport, and site conditions. To limit the thesis, no Life Cycle Analysis of the bridge proposal is performed. Groundwork and stabilisation of the hill is not considered in this thesis.

1.4 Outline

In Chapter 2 Design process, the design methodology with its different steps is further explained.

In Chapter 3 *Step I: Contextualisation – Reference study,* aspects when designing a timber bridge is stated and different timber bridge structures are introduced on a general level, as well as a detailed analysis of reference projects.

Chapter 4 *Step I: Contextualisation – Site*, contextualises the site Wendelstrand and identifies the client's and the Swedish Transport Administration's requirements and specifications. This will work as input for the design process.

In Chapter 5 *Step II: Conceptual design*, the iterative design process is initiated with a divergent exploration for possible concepts. Three possible solutions are the outcome of this process, which after consultation with the client and evaluation in relation to a set of criteria, are developed into one proposal.

This proposal is further refined with a suitable structural concept and rough dimensions in Chapter 6 *Step III: Preliminary design*. Thereafter, the structural concept is validated through calculations and the assembly method confirmed by a physical scale model in Chapter 7 Step IV: Final design .

At last, Chapter 8 *Discussion*, gives a critical evaluation and discussion of the work.

2 Design process

Iterative design is applied as methodology for the design study. The method is described in fib Model Code 2010 (International Federation for Structural Concrete, 2013) and adapted in the graduate course BOM170 Structural Design (created by Björn Engström and Morten Lund). The thesis methodology is based on the latter.

To initiate the design process, the task is established in a specific context. A large variation of improvised, possible solutions is developed. By an evaluation considering identified demands and contextual requirements, the proposed solutions can be narrowed down to one suitable design proposal. This is in turn developed through a precise and detailed design by the means of structural analysis and physical models.

2.1 Step I: Contextualisation

The intention of a contextualisation is to create an overview over the challenge and define the limitations of the task. This is achieved in two stages: firstly, an understanding of the current task is achieved by analysing solutions of similar challenges. Secondly, the specific problem is clarified by identifying challenges related to the site. This involves identification of different aspects of demands and definition of external requirements. The aim of the contextual stage is to create a foundation for the assessment of solutions in the following design process.

An analysis of reference projects helps broaden the understanding of different specific structures. These are collected in a data bank to identify possible solutions in existing structures that demonstrate their feasibility. These references support the development of design proposals in the Conceptual design phase.

2.2 Step II: Conceptual design phase

The Conceptual design phase is divided into three main steps: Intuitive phase, Intentional phase, and Evaluation phase (M. Plos, personal communication, September 2, 2020). By starting off in a broad and divergent generation of improvised concepts, qualities from these can then be merged into new and more specific concepts. The ideas are gradually developed and evaluated throughout the process to result in a final concept which fulfils the initially stated project intention.

2.2.1 Intuitive phase

The aim of the Intuitive phase is to generate as many different concepts as possible and investigate any idea related to the general context and demands. Every idea is possible in this phase, without any critical review or evaluation.

2.2.2 Intentional phase

The next phase aims to concretise the contextual requirements and to take the client's demands into account in the development of the structural design. This design is in turn evaluated in relation to the governing demands and requirements. As a result, the improvised concepts are developed and modified into a few, potential concepts.

2.2.3 Evaluation phase

The last part of the Conceptual design phase includes a review of the contextual demands. Conflicting demands are identified and prioritised after feasibility, fulfilment of client's intention and structural complexity. With a specified set of governing design criteria and demands, the most suitable structural concept can be defined and then brought into the next phase, the Preliminary design phase.

2.3 Step III: Preliminary design phase

Based on the result in the Evaluation phase, the final proposal is developed into a complete structural concept. This includes identification of the structural behaviour, determination of material and preliminary sizing of main structural elements. Reference projects with similar challenges are used to develop the solutions.

2.4 Step IV: Final design phase

The Final design phase includes a verification of the chosen structural concept. By detailed design of the structural elements, and calculations of the overall behaviour, the feasibility of the proposed concept can be proven. Physical models, in different scales, are also used to verify the structural design concept as well as the assembly method of the superstructure. This will allow for a verification of the detailed design as well as the relation between the overall structural design and its context.

3 Step I: Contextualisation – Reference study

As a literature study, reference projects of existing bridges are collected in a database and analysed. The reference projects will act as guidance for proper detailing, technical solutions, and ideas for structural concepts. An understanding of other qualities such structures hold is also gained from the reference analysis, such as the relation to the surroundings, consideration of pedestrians, or implementation of other functions. As these qualities are of subjective manner, the bridges are not analysed for this. Instead, it is used as inspiration in the next design step. Timber bridges make most of the studied bridges, but bridges in other materials are analysed as well. The reference data bank is illustrated in Figure 3.1, while the complete content can be found in Appendix A.

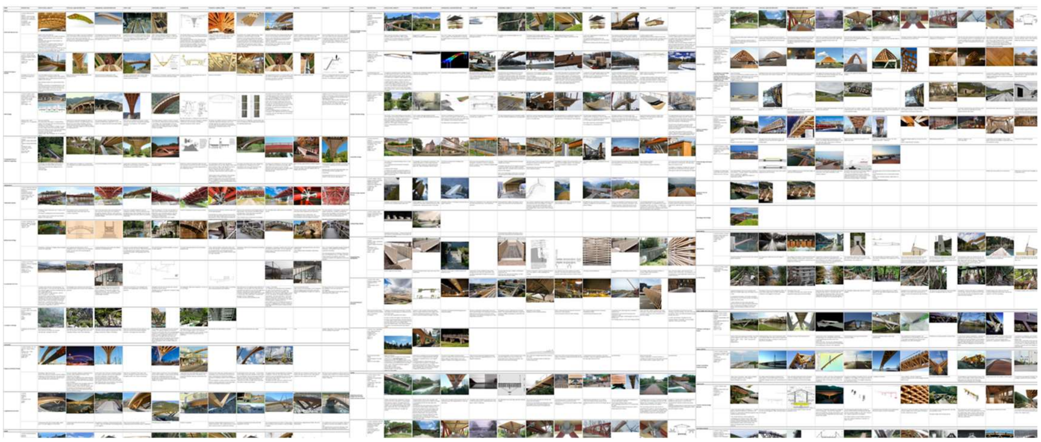

Figure 3.1 An overview of the complete bridge database.

3.1 Categorisation of timber bridges

The architectural appearance of a bridge is strongly linked to its structural concept. Each concept hols different benefits and limitations regarding maximum span length, superstructure dimensions, required foundation capacity, visual impact on the surroundings, material usage, and cost. The maximum span lengths vary considerably between the different bridge structures. Figure 3.2 illustrates different types of structural concepts applicable on timber bridges, categorised by span length.

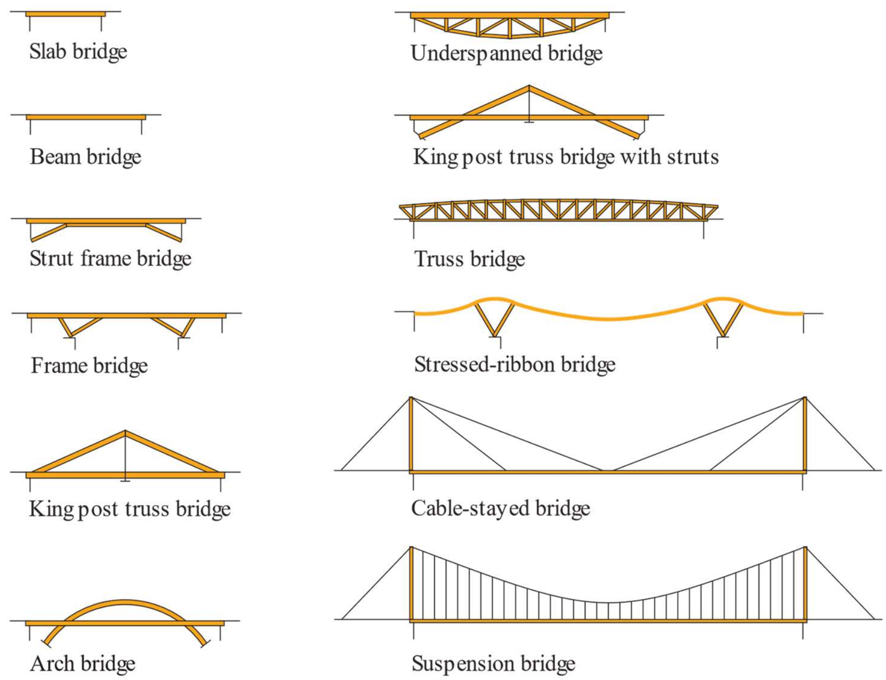

Figure 3.2 Different structural bridge types categorised by length.

Different structural systems carry loads in different ways. For example, a slab and beam bridge carry the load by bending, while a truss bridge globally transfers load by axial forces and bending as the local load transfer. A king post truss bridge uses bending, tension, and compression to distribute the load to the foundation, while a superstructure in a stressed-ribbon bridge works only in tension. Depending on required span length, desired visual impact and specific boundary conditions, a suitable structural concept can be applied and adapted to the specific site. Approximate span length and beam height for different structural systems are shown in Table 3.1.

Table 3.1 Approximate span lengths and beam heights for different timber bridge construction types. A compilation from (Gustafsson et al., 1996) *and* (Svenskt Trä, n.d.).

Construction type	**Span length,** L [m]	**Beam height,** h [m]
Slab bridge	20-30 (15)	L/20-L/30
Beam bridge		
- *Simply supported beam*	8	L/15-L/20
- *Simply supported round wood*	10	L/15-L/25
- *Simply supported glulam beam*	30 (40)	L/15-L/20
- *Underspanned beam*	10-50	L/8-L/12
- *Combined cross-sections*	50	L/15-L/20
- *Timber plated structure*	50	L/8-L/12
Strut frame bridge	40	L/15-L/20
Framework		
- *Truss*	30-75	L/12-L/18
- *Beam or glulam*	20-50	L/20-L/30

King post truss bridge	10-50	L/4-L/12
Arch bridge		
- *Arched walkway*	10-60	L/25
- *Hung walkway*	20-30	L/4-L/6
- *Post-supported walkway*	20-50	L/4-L/6
Truss bridge	100	L/10-L/15
Stressed-ribbon bridge	20-100	L/120
Cable-stayed bridge	20-100	L/4-L/8
Suspension bridge	20-100	L/4-L/8

3.2 Reference projects

In the following sub-chapters, an analysis of three structurally different and inspiring timber bridges are presented. The different studied aspects are:

- Structural concept
- Vertical load distribution
- Horizontal load distribution
- Rotational stability
- Point load
- Foundation
- Principle connections
- Production
- Assembly
- Material
- Durability

3.2.1 Neckartenzlingen Pedestrian Bridge

In Neckartenzlingen in south-west Germany a 96 m long cycle and pedestrian bridge spans over the Neckar river. The design and structure are created by Ingenieurbüro Miebach and completed in 2017. The bridge deck is 3 m wide and there are three spans where the mid span is 44.5 m and the other two 25.7 m (Miebach, n.d.). Figure 3.3 shows the continuous superstructure with its two parallel glulam beams.

Figure 3.3 Neckartenzlingen Pedestrian Bridge (Burkhard, 2017). *Used with permission. © www.hochbau-fotografie.de*

Structural concept

The Neckartenzlingen pedestrian bridge is a cantilever bridge with Gerber joints. These hinges transfer shear forces only and are located between the supports where the bending moment is close to zero. The superstructure consists of two parallel block-glued and bent glulam beams that cantilever out from the supports. To utilise the material, the cross-section height decreases towards the mid of the span. The glulam blocks are 2.1 m wide in the top layer and tapers down to 0.8 m at the bottom (Brandt, 2018). The bridge stretches out in a gentle S-shape.

Vertical load distribution

Vertically distributed load is transferred in the glulam blocks through bending to the supports. Due to reduction of the cross-section height in the span midpoint, the self-weight in the middle is also reduced. The largest cross-section height is found over the supports where the bending moments are the largest.

Horizontal load distribution

Transversal horizontal distributed load is handled by horizontal bending of the glulam blocks, and through axial forces in the transversal beams underneath the concrete slabs. The fact that the bridge is slightly S-shaped also contributes to the horizontal load capacity. Longitudinal horizontal loads are transferred by shear in the adhesive between the glulam block layers, down to the foundation and through the columns.

Rotational stability

The S-shape of the bridge provides global rotational stability.

Point load
A vertical point load is longitudinally and transversally distributed by the concrete slab and transversal beams down to the two main parallel glulam beams. From there the load is transferred through bending to the supports and foundation.

Foundation
Concrete piers support the superstructure on each side over the river, while concrete foundations anchor each bridge end. The glulam beams are connected to the supports and foundations by steel profiles that penetrates the structure (Brandt, 2018). The supports are considered as simply supported. Rotational movement is allowed at each bridge end.

Principle connections
The continuous beam is simply supported over the supports, which results in that no bending moment must be led down to the supports. The prefabricated bridge parts are connected to each other by Gerber hinges. These are located where the bending moment along the bridge is close to zero. The glulam blocks are individually fastened to each other with adhesives. Steel profiles connects the two parallel glulam beams. An exploded view illustrates the individual bridge parts in Figure 3.4.

Figure 3.4 *Exploded view drawing of the Neckartenzlingen Pedestrian Bridge* (Ingenieurbüro Miebach, 2017). *Illustration created by Ingenieurbüro Miebach. Used with permission.*

Production
Both the timber used for the glulam beams and the firm that manufactured the bridge components are local. Due to manufacturability the bridge cross-section has two parallel glulam beams. This creates a space where installation and electricity cables can be hidden (González, n.d.). The prefabricated wooden parts were transported to the site in different parts. The concrete slabs were pre-cast and transported to the site as well.

Assembly
The design allowed for sensible transport dimensions as well as a simplified assembly. The whole bridge took three days to assemble (Brandt, 2018). Two mobile cranes were used to lift the parts, standing on each side of the river. First the two outer spans were

lifted to its positions over the supports. Following, the beam over the mid span was lifted and connected with a Gerber hinge (Holzindustrie, n.d.).

Material
The superstructure is made of glulam beams while a pre-cast concrete slab with anti-slip surface constructs the decking. The railing and wires consist of stainless steel and the handrail is made of acetylated timber (Miebach, n.d.)

Durability
The 13 cm thick pre-cast concrete slab on top of the glulam beams gives a watertight protection (González, n.d.). The superstructure is protected by a 30 cm overhang of the concrete slabs. In addition, the glulam beams are tapered with 30° angle inwards which prevents rainfall from reaching the structure itself. Drainage channels made of steel are inserted under the concrete slab joints. To further protect the timber, a thin coat of glaze is applied (Brandt, 2018).

3.2.2 Punt Staderas

In the municipality of Laax, Switzerland, the slender bridge Punt Staderas spans over the country road Oberalpstrasse N19 to create a safe passing for bicyclists and pedestrians. The bridge design and structure are made by Walter Bieler with help of Stephan Berni and was completed in 2015 (von Büren, 2016). The main idea was to reduce the amount of wood and use the same cross-sectional dimension in all structural elements. This resulted in a slender superstructure with a total length of 115 m with nine spans of varying lengths. The longest span is found over the road and measures 24 m. The pathway is 2.5 m wide which allows enough space for both bikers and pedestrians, and has a slope of 6% (Ekwall, 2017). Figure 3.5 shows the largest span from below and the integration between the V-shaped supports in the structure.

Figure 3.5 Punt Staderas from below (Camathias SA, 2015b). *Used with permission.*

Structural concept
The superstructure is a Gerber girder built up as a Vierendeel girder. The webs in the Vierendeel frame builds up rectangular frames together with the upper and lower chords and with joints that can transfer bending moments into the webs. In contrary to a triangular truss with pinned connections to the upper and lower chord where the shear force is axially transferred through the diagonals (Wickersheimer, 1976). By using a Vierendeel girder a slender cross-section is achieved with a static height of 640 mm. The grid consists of two longitudinal layers with four beams each and an intermediate layer with transversal cross beams every 1.05 m (Ekwall, 2017). The concept is governed by the aim of using the same cross-sectional dimension for all structural elements, namely 160-by-240 mm and 14.5 m long (Guetg, n.d.). Since the span over the road is 24 m (longer than 14.5 m) glulam timber beams are used to ensure sufficient bearing capacity. The supports are V-shaped in both directions, with two considerable benefits. Firstly, the span lengths are decreased. Secondly, with an inwards V-shape, the bridge deck can provide weather protection of the support elements. In addition, the outer support beams stretch beyond the deck and enhance the railing design. The V-shaped supports improves the structural performance in two aspects. Firstly, the span lengths are decreased. Secondly, with a V-shape the V-shape allows for weather protection of the support elements by the bridge deck. The outer support beams stretch beyond the deck and enhance the railing design.

Vertical load distribution
A vertical, uniformly distributed load is lead through the Vierendeel girder to the supports by compression in the upper longitudinal layer and tension in the bottom longitudinal layer. At the supports the load is transferred through compression down to the foundation. Over the largest span the load is carried by bending moment through the glulam beams to the supports.

Horizontal load distribution
Horizontal capacity is provided by the transversal beams of the Vierendeel girder. A modest S-shape in the horizontal direction of the bridge path enhances the horizontal stability of the structure. The V-shaped supports are ordered in a 3-by-6 array with a steel bracing in the transverse direction. This geometry and additional bracing provide additional horizontal stability. For the longitudinal horizontal loads, the geometry of the V-shaped supports provide stability.

Rotational stability
The steel cross bracing inside the V-shaped supports provides global rotational stability (Figure 3.5). The local rotational stability comes from the stiff Vierendeel girder and connections between the members. With the use of a total of 2000 screws, each 80 cm long, the wooden elements are joined together (Oertli, 2018).

Point load
A vertical point load is transferred through the bridge deck down to the Vierendeel girder. The load is then transversally distributed by the cross beams to the longitudinal beams in the upper and lower layers of the girder. Then the force is carried by tension and compression through the girder to the supports, which in turn transfer the load through compression down to the foundation.

Foundation
Reinforced concrete abutments are placed at the two landing points. The V-shaped supports stand on concrete blocks.

Principle connections
Since the same cross-sectional dimension is used for all structural members, they match very well when connecting them together. The beam elements are assembled with fully threaded screws at an angle, which provides a shear proof behaviour. The connection stiffness was tested successfully at EMPA in Dübendorf beforehand (Oertli, 2018). The connections in the superstructure are covered by the bridge deck, while all other exposed connections are covered by boards that lead water away from the connection. Figure 3.6 shows the protecting boards and their influence in the visual appearance of the bridge.

Figure 3.6 Side view of Punt Staderas (Camathias SA, 2015a). *Note the cover board that leads water away from the structure. Used with permission.*

Production
The bridge consists entirely of locally cut wood. Walter Bieler personally assisted the forester in the search for suitable trees that could provide 14.5 m long beams (Guetg, n.d.). Both the Vierendeel and glulam girders were prefabricated and then transported to the site for assembly. The foundation abutments were casted on site.

Assembly
First the V-shaped load bearing supports were installed on the foundations. Thereafter the prefabricated girders were lifted to their position. During the assembly of the glulam beam spanning over the road, the road was closed and the beam could be lifted to its position (Standardname, 2015). The girders were then connected by screws. To make sure correct positioning of the structural parts, laser tools were used (Oertli, 2018).

Material
Originally the idea was to build a wooden bridge in larch with material from the immediate vicinity, but since spruce is the most widespread species in the area, it was

chosen as the main structural material. Larch was instead used in the exposed details. For the main span, glulam beams of strength class C24 are used. The paving consists of mastic asphalt.

Durability

The expected life span for the bridge is set to 80 years and the wood will start to turn grey until it finally becomes silverish (Oertli, 2018). Careful detailing has ensured a properly airy structure. Covering boards acts like small canopies for water where the water can drip off, and sufficient distance around allow the structure to dry out. The superstructure is protected by the covered pavement and the supports are tilted inwards. Weather-exposed surfaces consists of larch while the protected wood is spruce (Guetg, n.d.). The exposed railing and canopies that protect the superstructure are easy to replace.

3.2.3 Fussgängersteg Geheidgraben

In Olten, Switzerland, a conceptually interesting bridge is located. The design is made by the architecture firm werk1 with the engineers of Makiol Wiederkehr and was completed 2013. The bridge spans a little bit more than 7 m over a ditch which works as a retention basin, meaning that there seldom is any water in the ditch except from many days of rainfall (Makiol Wiederkehr, 2014b). The architectural idea is to have a wave-like pattern that is implemented both on the walking deck and railing, which can be seen in Figure 3.7.

Figure 3.7 Fussgängersteg Geheidgraben with its wave-like superstructure and railing (Makiol Wiederkehr, 2014b). *Used with permission.*

Structural concept

Statically, the bridge works as a simply supported beam bridge where the wavy decking is the main structural part. The longitudinally beams in the superstructure are actively bent, which creates a slab with good bending capacity both vertically and horizontally. It is assumed that the wavy handrails also to some extent contribute to the vertical bending moment capacity due to its height and actively bent members. As a simplification, the handrails can be read as a truss structure.

Vertical load distribution

Globally, a vertically distributed load is transferred through the wavy beams to the foundations by bending moment. The cross-sectional height of the wavy beams in the bridge deck provides the governing bearing capacity.

Horizontal load distribution

To create the waves, washers and nuts are used to spread and pull together the floorboards. They are mounted on two transversal steel rods above each other in a grid with 0.6 m spacing (Makiol Wiederkehr, 2014a). Together this makes a homogenous slab, which provides the horizontal capacity.

Rotational stability

The bridge has a relatively short span and a broad width, which provides global rotational stability. The railing with its integrated steel posts gives torsional stability.

Point load

A point load is transferred through one or two wavy beams towards the transversal steel rods, where the load then is transversally distributed to adjacent wavy beams and then finally longitudinally transported to the foundations.

Foundation

The bridge is resting on concrete foundations. Steel bearings of LNP profiles (120/120/10) connects the foundation and the timber superstructure. On one end of the bridge there are elongated holes in the connection between support and beam, which allows for swelling and shrinkage. Rotation is allowed in one bridge end. The steel bearings on respective side of the ditch have a height difference of 0.6 m (Makiol Wiederkehr, 2014b).

Principle connections

Washers and nuts provide the necessary distance between the thin beams to create a wave pattern in the deck. The distancers are mounted on threaded steel rods in tension. The railings are constructed by laying boards with similar wave pattern created by distances, see Figure 3.8. RRW steel profiled posts penetrate the laying boards. The distances also protect the steel posts.

Figure 3.8 Railing structure with distancing (Makiol Wiederkehr, 2014a). *Used with permission.*

Production

The bridge is prefabricated, and the decking and railings are preassembled separately. The curvature of the waved boards is made by screwing the nuts on the threaded bars to wanted position, and then the nuts themselves work as distancing to the next layer board.

Assembly

The preassembled decking and railings are joined together, and then the bridge is lifted to its position on the concrete foundation in one piece (Makiol Wiederkehr, 2014a).

Material

Decking and railing is made of massive rough-sawn oak boards. Steel is used for the threaded rods, nuts, washers, posts in railing and supports. The foundation abutments are in concrete.

Durability

Due to the wavy character, water can drip through the structure, and the structure is also easily dried. A consequence of the weather exposed structure is an aged appearance with rust and weather torn wood (Makiol Wiederkehr, 2014a). The steel posts in the railing are protected by the distancing steels parts. An extra board is mounted on top of the railing to cover the fastenings. The fact that pedestrians walk directly on the unprotected superstructure, will shorten the service life of the bridge. It is also difficult to replace single elements without demounting the whole bridge.

4 Step I: Contextualisation – Site

When designing a bridge, there are several aspects to consider. The context of the specific site needs to be analysed and studied such as required span lengths, foundation possibilities, and surrounding scenery and buildings, and connection existing paths. When these aspects are formulated, a structural concept can be explored and developed. This concept should fulfil the identified requirements connected to the context.

In the following chapter, general demands based on client's expectations are formulated. These consider both the visual appearance of the bridge, the purpose of the footbridge, and the feasibility of the proposal. Geotechnical and topographical conditions outline the site-specific context. These are in turn are affected by requirements stated by the municipality and Swedish Transport Administration. The above-mentioned aspects are identified by a study of public documents and site-specific investigations. An early visit to the site contributed to a perception of the current site concerning characteristics in the terrain, scenery, and surroundings. The project background, main challenges, and governing demands are formulated in this chapter.

4.1 About the site

The chosen site is a planned development area named Wendelstrand, situated east of Mölnlycke outside of Gothenburg (Figure 4.1). The current gravel pit will be transformed into a residential area by 2026-2030, initiated by Next Step Group. Wendelstrand is planned to hold 850 new residences and public buildings, such as a nursery school, elderly home, and shops (Härryda Kommun, 2020). The community building, named Lakehouse, will be in the centre of the area, housing services such as restaurants, co-working offices, and gym. The building outlines the main square of the area, which holds the most important social services in the area (Härryda Kommun, 2020).

Figure 4.1 The specific site in relation to Gothenburg (Google maps, 2021).

The general intention of Next Step Group for Wendelstrand is to develop a sustainable residential area, where the buildings adapt to the landscape and the architecture involves a high presence of timber (Härryda Kommun, 2020). A view over Landvettersjön and adjacent nature reserve is found in the southeast corner of the main square, while the roof of Lakehouse offers the most spectacular view, see Figure 4.2. The architect aims to make Landvettersjön present and visible throughout the whole area. With an increasing building height further away from the lake, the residents can see the lake from their apartments, see Figure 4.3.

Figure 4.2 Birds view of Wendelstrand (Wendelstrand, n.d.-b). *Photo: Snøhetta. Used with permission.*

Figure 4.3 Wendelstrand from Landvettersjön (Wendelstrand, n.d.-a). *Photo: Snøhetta. Used with permission.*

4.2 Clients demands

As the architecture of Wendelstrand enables a view of the lake anywhere in the area, the only missing link to the lake is the physical one. The client, Next Step Group, envisions a bridge that connects Lakehouse and the main square of Wendelstrand with the lake, both physically and visually. The road Boråsvägen must be considered, with the priority of making the lake accessible for the residents and visitors of Wendelstrand. Furthermore, the client wishes for a bridge structure with a high presence of timber that correspond with the sustainability profile of the development project. In addition to this, the client envisions a design that offers qualities other than merely a connection between A and B, that can be combined with the expected experience of Wendelstrand and Lakehouse.

4.3 Site-specific boundary conditions

The site-specific boundary conditions mainly concern the surrounding topography. Public regulations stated by the Swedish Transport Administration, and site-specific regulations regarding shoreline adds to the list of restrictions that must be considered in the bridge design.

The required height clearance of 5.3 m over the road is stated by the Swedish Transport Administration (Härryda Kommun, 2019). Furthermore, the supports must be placed with a clearance of 2 m from the walkway (Trafikverket, 2021).

The county administrative board in Västra Götaland has defined a shore protection area, stretching 100-200 m from the shore of Landvettersjön. The purpose of the expanded restriction is to keep the shorelines clear from permanent structures to enable public access to the water, in addition to protecting the geological conditions in and around the lake (Sektorn för samhällsbyggnad, 2020). The area between Landvettersjön and Wendelstrand lies within the shore protection and is thereby protected. Early site-investigations on behalf of Next Step Group has identified the possibility of excluding a short strip of land along the load, to make space for possible bridge foundations (E. Silverterna, J. Garfvé, personal communication, March 11, 2021). The further development of the timber footbridge will consider this explicit area as excluded from shore-protection regulations, that is, a 4.5 m wide strip along the road. As a compromise, the bridge design is limited to a maximum of two landing points on the lakeside of the road.

In the initial planning process of the area of Wendelstrand, several technical investigations were performed on behalf of Härryda municipality. Important for the footbridge design is the investigation of geotechnical conditions of the site. The investigation proposes the supports to be constructed as either ground slab, drill pipe or a combination of both as the soil layers generally consist of sand with elements of silt, gravel, and solid rock (Norconsult, 2018). Furthermore, in the latest local plan, a risk of minor landslides in the steepest terrain southeast of the area right next to Boråsvägen, is identified (Härryda Kommun, 2020). The evaluation has estimated it as a non-critical situation with a ten-year risk. However, stabilisation of the terrain in question is outside the scope of the current project.

Governing topographical conditions are identified as the following and illustrated together with the requirements from the Swedish Transport Administration in Figure 4.4:

- 19 m height difference between Lakehouse and Landvettersjön.
- Steep slope in the terrain (21°).
- Boråsvägen has a varying width of 7-11 m including pavement.
- Required height clearance of 5.3 m and 2 m width clearance.

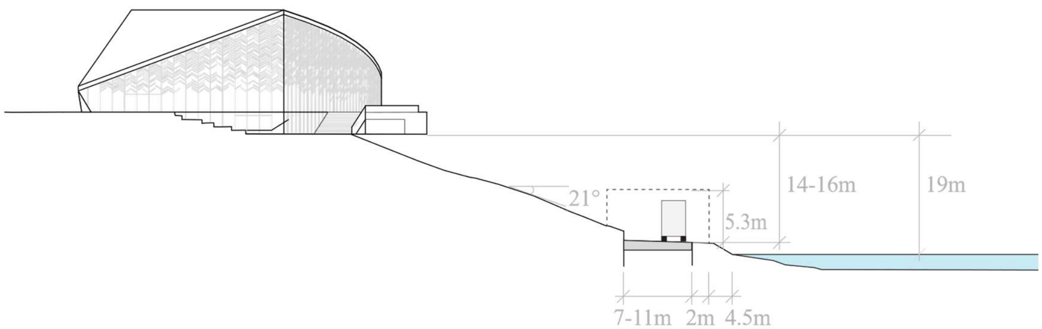

Figure 4.4 Governing boundaries of the site.

4.4 Summary of contextualisation

From the site contextualisation, the following demands and requirements are identified. The public requirements are considered non-negotiable and must be fulfilled for the proposal to be feasible. In addition, to achieve an attractive bridge proposal, the client's demands must be met.

- Clients demands
  - Physical and visual relation between Wendelstrand and Landvettersjön
  - Make the lake accessible for residents as well as visitors
  - Footbridge design with a high presence of timber
  - Proposal for additional qualities in the design
- Public regulations
  - The Swedish Transport Administration
  - Västra Götaland County Administration
- Shore protection
  - Västra Götaland County Administration

Following, the contextualisation reveals numerous unspecified design aspects that will affect the bridge design. These design aspects will guide the development of possible solutions in the next design phase. Each aspect will be investigated both separately and combined, with the aim of enabling a large variety of design proposals:

- Path and landing points
  - As the exact landing points of the bridge are not specified by the client, the movement of the bridge path is free to investigate.
- Length and inclination of the path
  - The length of the bridge path is related to the inclination. The inclination is regulated, thus governing the total length of the path.

- Integrated functions
    - A general expectation for the bridge design includes additional functions in the structure. These are not stated specifically from the client.
- Architectural appearance
    - The client expects a bridge design that relates to the profile of Wendelstrand. No further demand is stated and is therefore part of the design investigation.
- Structural concept
    - A free investigation of the most suitable structural concept for the bridge is allowed.

5 Step II: Conceptual design

When the specific site and different criteria are defined, the search for a suitable bridge concept, which is an answer to these, can begin. The search starts broad with many various suggestions and is then narrowed down into a suitable concept. To create a framework for the design proposals a set of general design criteria are formulated. These are based on qualities which are strived for and include contextual limitations and challenges, and clients demands. In addition to this, the designers aim of combining architectural qualities with structural engineering knowledge is considered in the design criteria.

As stated in Chapter 2.2 the *Conceptual design phase* includes three sub-phases: *Intuitive*, *Intentional* and *Evaluation*. The Intuitive phase focus on exploring the possibilities on the site with less consideration of the design criteria. Any subjective opinion is set aside during this design process to allow for a large variety in the generation of the first ideas. Combined with a thorough review of the expected design qualities, three concepts are developed from the initial proposals in the Intentional phase. Each concept is developed to a certain level to enable a thorough comparison of the proposals and to determine the feasibility of the designs. In the last part of the Conceptual design phase, the three concepts are evaluated in relation to the stated design criteria and identified demands. The result is an appropriate solution for a footbridge in Wendelstrand.

A set of defined evaluation criteria creates the transition between each design phase. The evaluation criteria are categorised into design criteria and demands, with the purpose of securing fulfilment of the contextual requirements in the design development, and inclusion of expected design qualities. To enable a large variation in the proposals, a reduction in the evaluation criteria is exercised in the transition between the first two phases to discover qualities in other solutions. The evaluation criteria used are illustrated in Figure 5.1. The proposed design will fulfil every stated evaluation criterion before being developed in the Preliminary design phase.

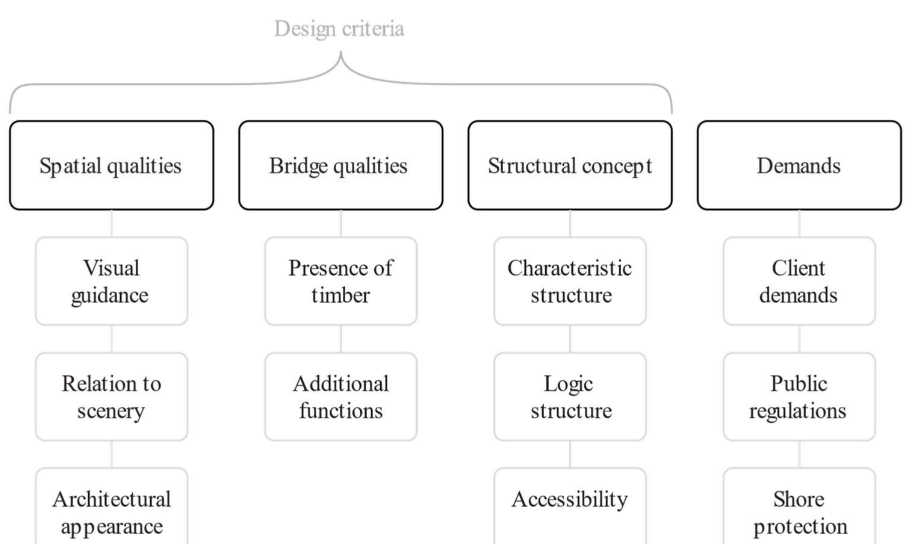

Figure 5.1 Illustration of the governing evaluation criteria.

5.1 Design criteria

The design criteria are divided into three main categories: spatial qualities, bridge qualities, and structural concept. The different aspects of the categories are explained in the following three subchapters.

5.1.1 Spatial qualities

The spatial qualities consider the architectural aspect of the structure and its relation to the surroundings. This is implemented in different aspects, which are stated below.

Visual guidance
The client requests a visual and physical connection between Lakehouse and Landvettersjön. The design aims to establish a reachable structure with a sense of predictability for the users. In addition, the design should invite visitors from other areas and enable approach from different directions. The design criteria can be met either partly or completely, such as only a visible landing point, path extending from the city square, or a straight bridge path from Lakehouse to Landvettersjön.

Relation to scenery
As for all built structures, the relation to the scenery is of great importance. The architecture of Wendelstrand follows the same manner and blends in with the surroundings. It is therefore of interest to develop a bridge design with similar characteristics. As the purpose of the bridge is to connect the residential area and the lake, the design of the bridge must relate to the characteristics of both the residential area and the nature around the lake.

Architectural appearance
Furthermore, the structure should hold certain architectural qualities. This is not necessarily directly related to breath-taking design with large visual impact. On the contrary, such qualities can be found in careful detailing of functions such as water drainage, hand railing or torsional stability. It can also be found in a design that relates to a specific site characteristic. Although this design criterium is rather vague, the assessment is grounded on substantial arguments. The aim is to develop a structure that holds architectural qualities and simultaneously relates to its surroundings. The criteria r*elation to scenery* and *architectural appearance* therefore determines a level of accepted visual impact.

5.1.2 Bridge qualities

The bridge qualities consider the architectural aspect of the design in relation to its form and concern the following aspects.

Presence of timber
As Wendelstrand will become Northern Europe's largest residential area in timber, it is expected that the bridge proposal aims for a high presence of timber with an obvious timber structure. Yet, a large amount of timber is not necessarily the most suitable interpretation of this design criterium but rather a careful design of the different structural members with the resulting visual expression as governing criterion. This

aspect is also related to the design category regarding *Structural concept* which will be elaborated further in the next subchapter.

Additional functions
The common function of a bridge is to be part of a traffic flow. In this case, the bridge will be part of a pathway where the landing point is the goal. In addition to the sole purpose of connecting Lakehouse and Landvettersjön, it is of interest to develop a design that adds other qualities to the site. For instance, integrated seating or permanent furniture as an extension of the superstructure, a viewing platform expanded from the bridge path, a pier stretching out over the water, or weather protection underneath the bridge.

5.1.3 Structural concept

The third and last category incorporate design criteria into the structural design.

Characteristic structure
First and foremost, the structural design of a bridge is related to the visual appearance of the bridge. Consequently, the choice of structural concept affects the design criterion of *Spatial qualities* and *Architectural appearance*, and vice versa. The intention is to develop a bridge design where both architectural and engineering qualities are considered, with the aim of contributing to the development of timber bridge design. Therefore, a conscious consideration of these aspects is required, which ultimately will result in an enhancement of the qualities rather than compromising.

Logic structure
The structural concept of the bridge must be logic in the sense of the utilization and purpose of the structural members. All members will contribute to the structural performance of the bridge, which is related to both the structural and architectural aspects of the design. Form follows function, and function follows form. Whichever is governing is determined by the other evaluation criteria. Furthermore, the bridge design aims for a high presence of timber. A structural concept best suited for timber will be developed, as timber will not be chosen for the sole purpose of timber presence. An investigation of the most suitable timber product is necessary.

Accessibility
As Wendelstrand will lodge residents in the span from children to elderly, the bridge aims to be accessible for everyone. An inclination of 2° or less is stated as the requirement for wheelchair users (Göteborgs Stad Trafikkontoret, 2017), which is challenging to combine with the large height difference. For this reason, the bridge design will aim to meet the inclination requirements to an extent where everyone can utilize the main functions of the bridge. Whether or not the whole bridge design will meet the accessibility requirements depends on how the concept meets the other design criteria stated in this chapter.

5.2 Intuitive phase

The *Intuitive phase* focus on generating a diversity of possible solutions. Figure 5.2 shows the evaluation criteria which are the most emphasised in this phase.

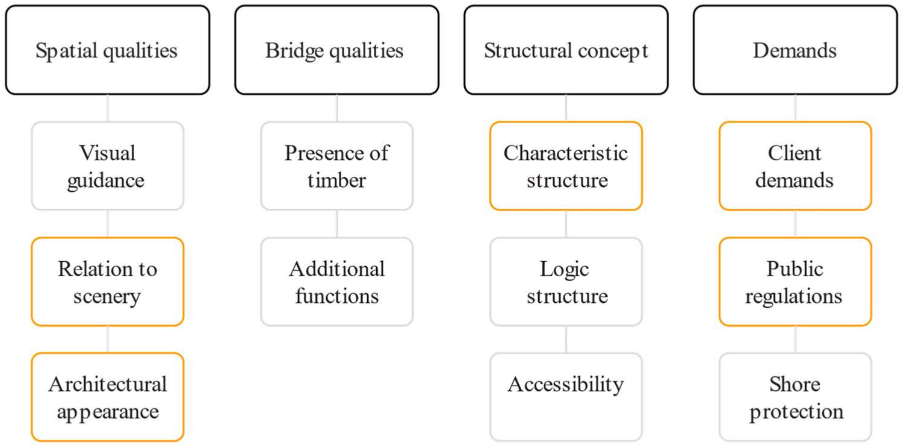

Figure 5.2 Emphasised evaluation criteria in the Intuitive phase are highlighted in orange.

As neither the starting- or landing points are explicitly stated by the client, an exploration of different movement patterns with corresponding qualities and consequences are explored.

Three main aspects are identified as governing for the movement pattern of the bridge. Firstly, the path must connect to Lakehouse, preferably as an extension of the adjacent seating platform. Secondly, it should be possible to access the bridge from the bicycle and pedestrian lane on Boråsvägen, from both directions. As illustrated in Figure 5.3, a parking space is located along the road, which will be used by visitors to Wendelstrand. Third and last the bridge should connect to Landvettersjön. Both a physical and visual connection to the water will be explored. Figure 5.3 illustrates the three landing points to be considered.

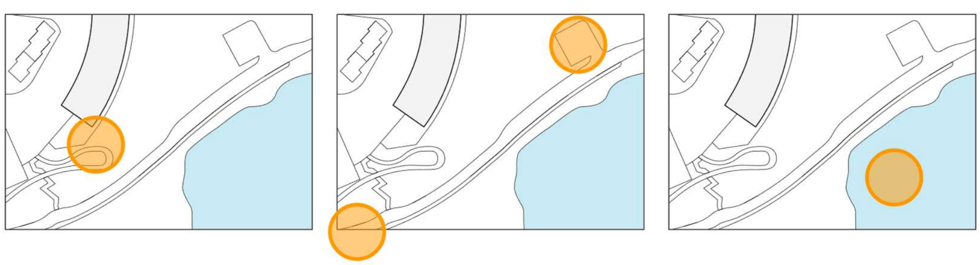

Figure 5.3 Landing points. Lakehouse, Boråsvägen with parking and Landvettersjön.

Depending on the chosen path, the design criteria are fulfilled to different extents. As a result, varying spatial qualities are explored. For instance, to what extent the starting point connects to Lakehouse, whether the bridge is accessible from the road and in which direction, or whether the bridge has a physical connection with the water. A selection of possible movement patterns is illustrated in Figure 5.4.

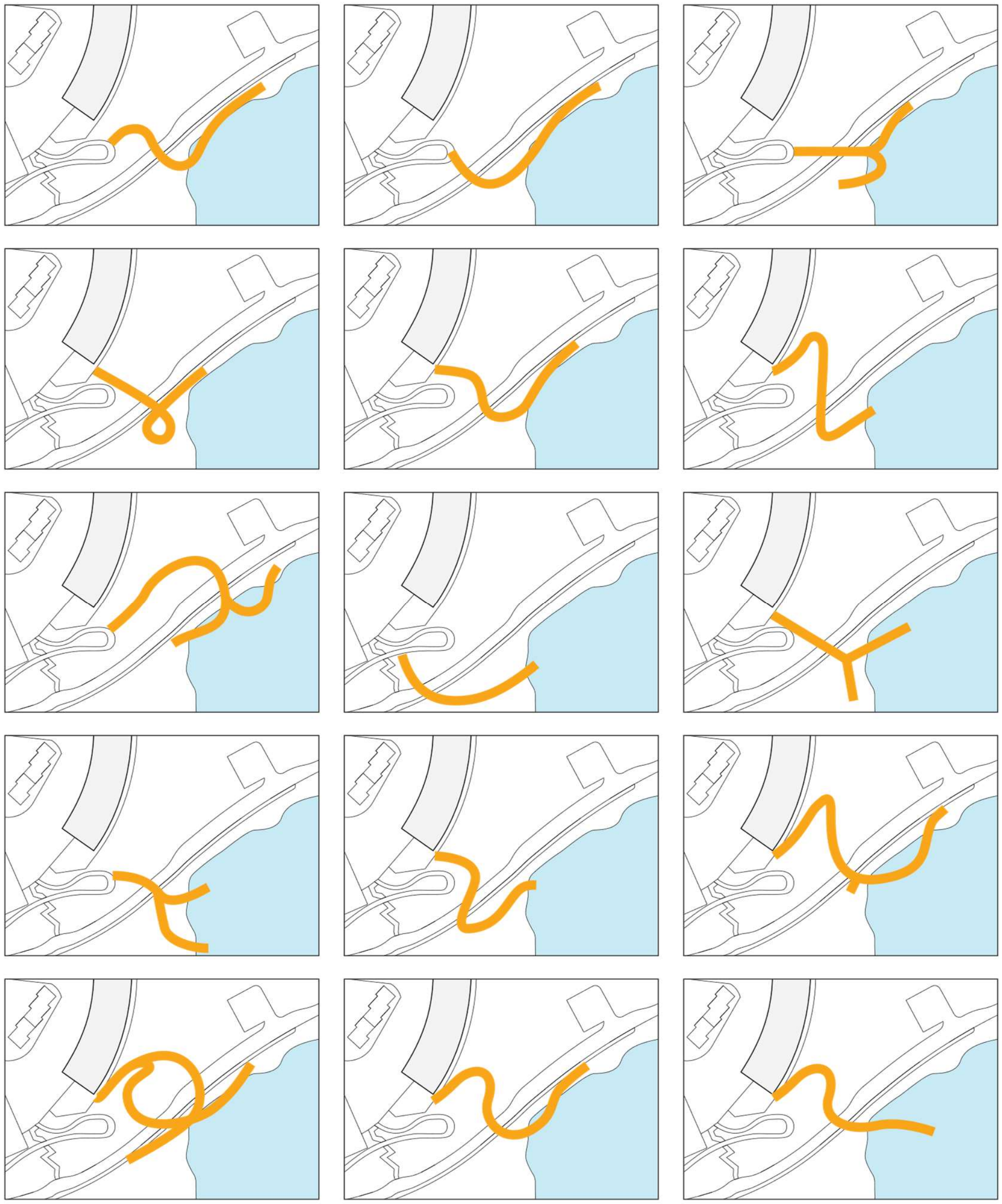

Figure 5.4 Variation of movement patterns.

The Intuitive design phase aims to explore the possibilities of the site, which is made possible with a large variation of ideas. Based on the exploration of possible patterns in Figure 5.4 different structural bridge concepts are assigned to the different paths. As the idea of a structural concept is formulated, the design is developed with principal sections and connections. The result is twelve different design concepts, illustrated in Figure 5.5.

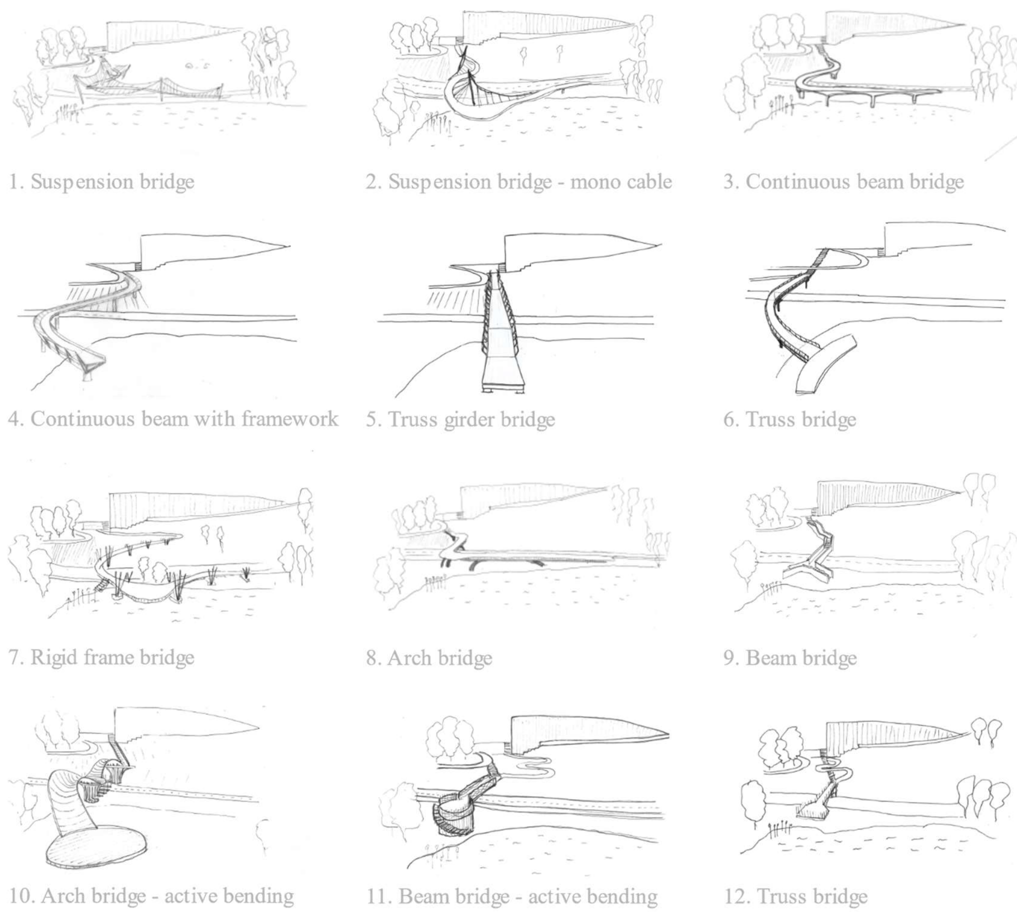

Figure 5.5 Initial proposals.

Summary of the Intuitive phase

The design proposals developed in the Intuitive phase are generated through conscious consideration of:

- Spatial qualities
    - Investigate different options of movement pattern when connecting Lakehouse, Boråsvägen and Landvettersjön.
    - Explore the possibilities and limitations of the site when considering the movement of the bridge.
- Structural concept
    - Explore the possibilities of the movement patterns by applying different structural concepts, both inspired by reference projects and developed from the movement pattern itself.
    - Explore the possibilities and limitations of the movement patterns when considering the structural concepts.

5.3 Intentional design phase

The Intentional phase aims to develop the intuitive proposals and narrow them down to three structural concepts. This is done by considering the aspects of the evaluation criterions highlighted in Figure 5.6.

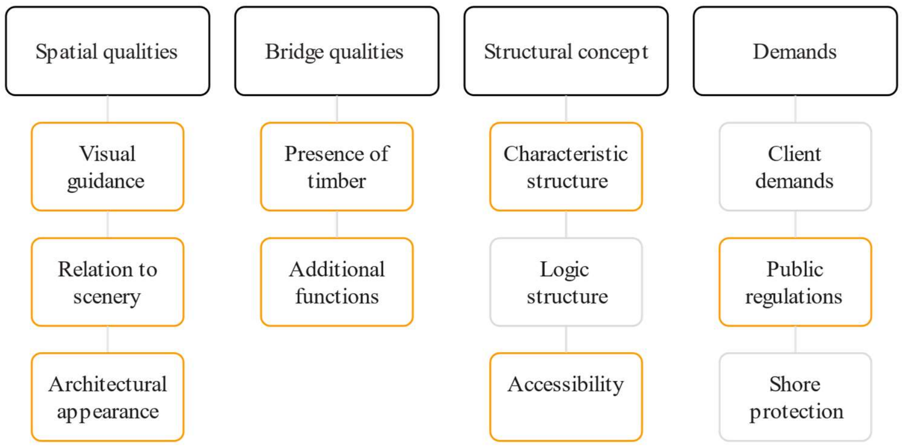

Figure 5.6 Emphasised evaluation criteria in the Intentional phase are highlighted in orange.

Focus lies on how the desired qualities can be met for different movement patterns. The study aims to determine whether one pattern is superior in meeting the design criteria, or if different movement patterns meet the desired criteria on an equal level.

A variation of spatial qualities is found for different movement patterns, where different paths meet the design criteria on different levels. An exploration of different movement paths results in a large variation between the design proposals in the Intentional phase. Three different movement patterns are chosen for further development. They are illustrated in Figure 5.7 and differs in the following sense:

- Accessible ramp
- Direct or curved path
- Ramp in one or two directions
- Bridge reaching out over the water
- Bridge reaching into the water

Figure 5.7 Three different proposals with three different movement patterns.

Next, the proposals from the Intuitive phase are evaluated for the chosen evaluation criteria of the current phase. As the criteria are not prioritised, the proposals are not being rated in a matrix. Instead, they are evaluated in relation to each other and to which extent they satisfy the design criteria:

- Does the bridge relate to the scenery?
- Is the presence of timber high?
- Does the design integrate additional functions in the structure?
- Does the structural design add an architectural quality?
- How is the impact on the surroundings?
- Does the design create a physical and visual connection between Lakehouse and Landvettersjön?
- Is it possible to comply with the accessibility requirement?

Three keywords are formulated to give impact on the development of the design proposals: *nature*, *embracing* and *sweeping*. *Nature* as in relation to the surroundings, or resemblance of the characteristics of the site. *Embracing* as a quality in the bridge, which can be achieved in the design of the railings or integrated seating, and implementation of timber presence. *Sweeping* describes the movement of the bridge, which resembles a natural path. These keywords represent the essence of the design criteria formulated in Chapter **Error! Reference source not found.**. In the further development of the proposals, characteristics from these keywords are implemented to a different extent to ensure a variation in the proposals.

The movement pattern governs the development of the design, where each path is assigned with a suitable structural solution. The proposals are developed to enhance a conceptual idea rather than searching for the one most suitable solution. To enable an evaluation of the proposals in the next phase, divergence is strived for. Reference projects are of great importance to support the design development. Three resulting bridge proposals are presented in the following part of this chapter.

Proposal 1

The aim of this concept is to create a path that winds among the trees in two levels, where the delta on the southwest side of Landvettersjön is explored. This area is outside the local plan, but holds a lot of potential and qualities. Figure 5.8 shows a conceptual illustration of the proposal. The essence of this proposal is the relation to the scenery. The structure blends with the trees and with supports resembling tree trunks and a movement resembling a natural path.

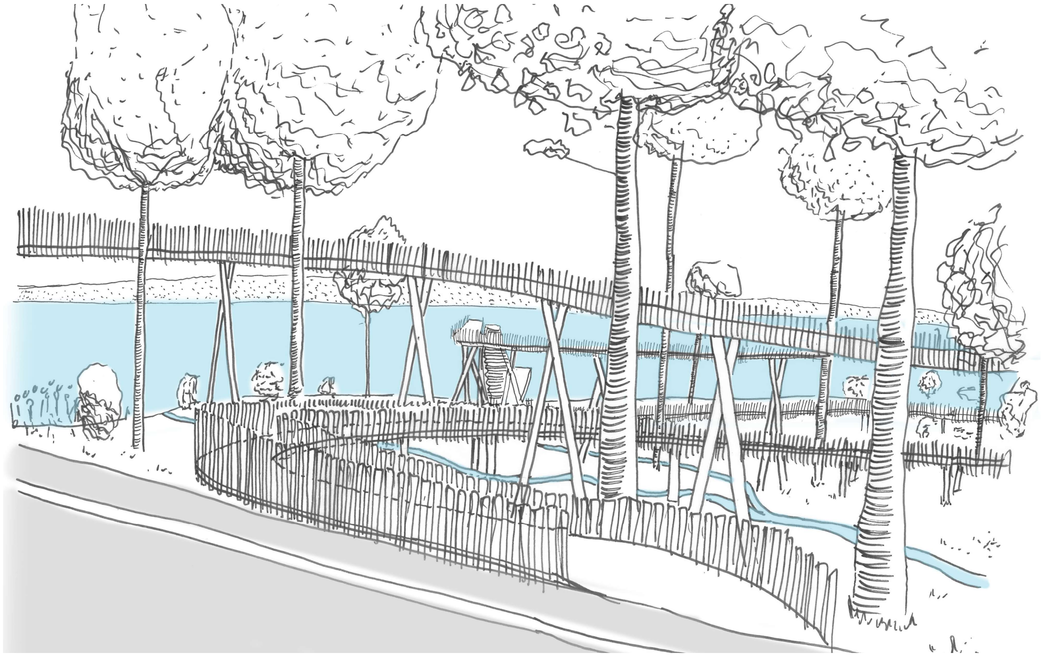

Figure 5.8 Bridge proposal 1 seen from the road.

The structure consist of paths in two planes; an upper leading the visitor from Lakehouse across the road, and a lower path from the road with an accessible inclination. The upper path lands in an elevated platform above the water, while the lower path stretches out in a pier below the platform, which is seen in Figure 5.9. The two paths are connected with a staircase.

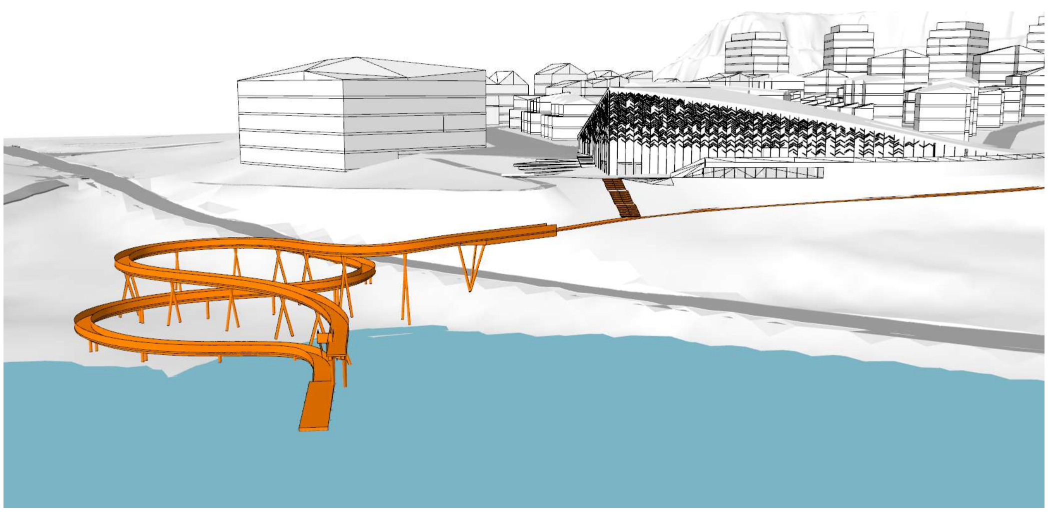

Figure 5.9 Perspective of proposal 1.

The load-bearing system consists of a curved glulam beam with Gerber hinges. There are inclined supports every 10^{th} meter. The torsional stiffness comes from transverse rigid steel frames. Over the road, the span of 15 m is carried by two larger parallel glulam beams with intermediate diagonal glulam beams, creating a truss.

Proposal 2

The second proposal is a bridge that follows the straight line of sight from the road that go towards the square outside Lakehouse, across Boråsvägen, into the water, landing in a long pier, see Figure 5.10. The large height difference impose the design to include stairs to access the bridge. An accessible ramp is integrated as an extension between the pier and the road. The aim of the design is to create a clear visual and physical connection to Lakehouse, with an characteristic structure that adds an architectural quality.

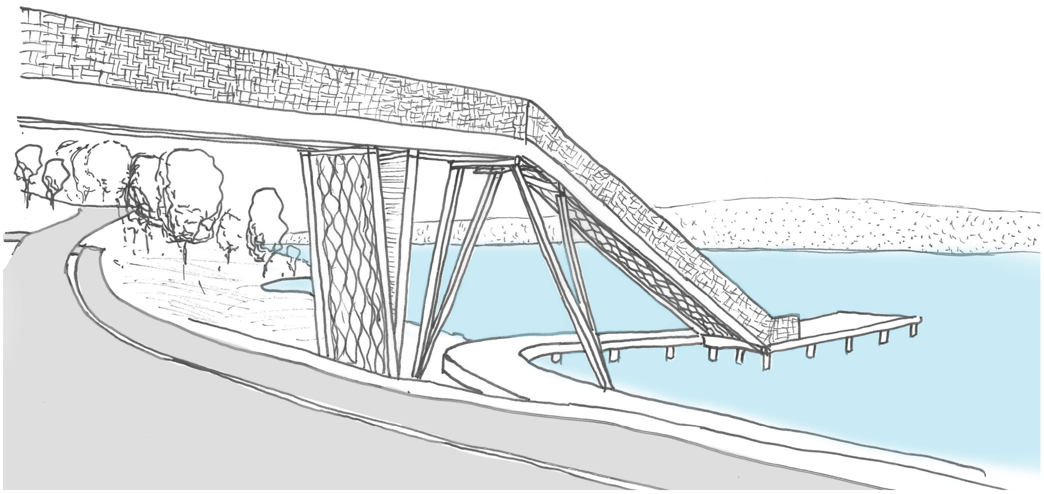

Figure 5.10 Bridge proposal 2 seen from the road.

The structural concept of the second proposal's superstructure is characterised by beams in a sinus pattern. The beams are rigidly connected to create interaction for vertical and horizontal bending. A perspective of the proposal is seen in Figure 5.11.

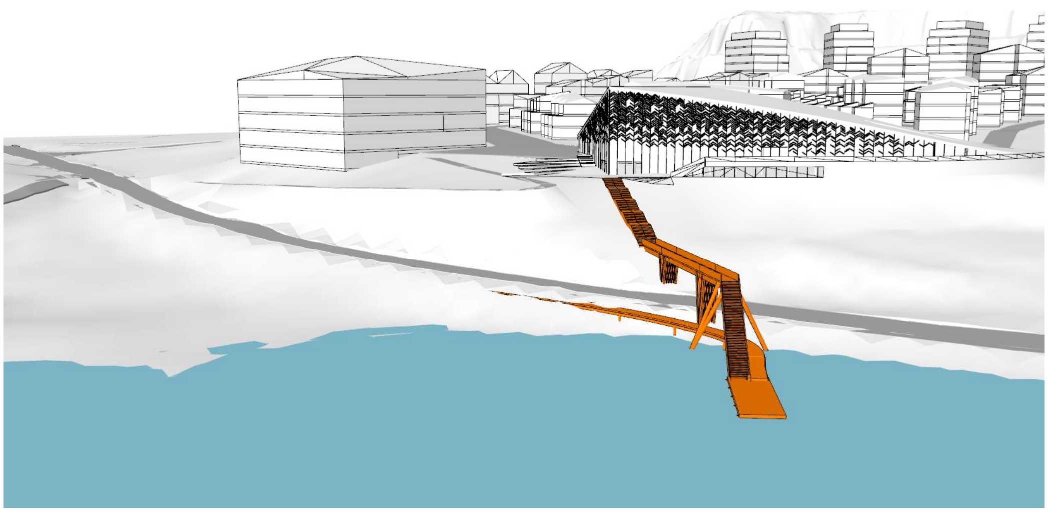

Figure 5.11 Perspective of proposal 2.

To emphasise the concept of curved beams, the railing consists of thin wood elements woven and stacked ontop of each other, which in turn adds to the torsional stability of the bridge. The superstructure is protected by a bridge deck, but is exposed on the lower side. The same structural concept is applied on the stairs leading down to the pier, as well as the vertical support elements. The visible structure adds an architectural quality and experience for the visitors approaching from the road.

Proposal 3

The third proposal aims to establish a clear visual and physical connection to Lakehouse, but does not have a physical connection to the water. Instead a platform is reaching out over Landvettersjön, see Figure 5.12, to create a visual connection. The pathway widens over the water, to give space for seatings on the bridge deck.

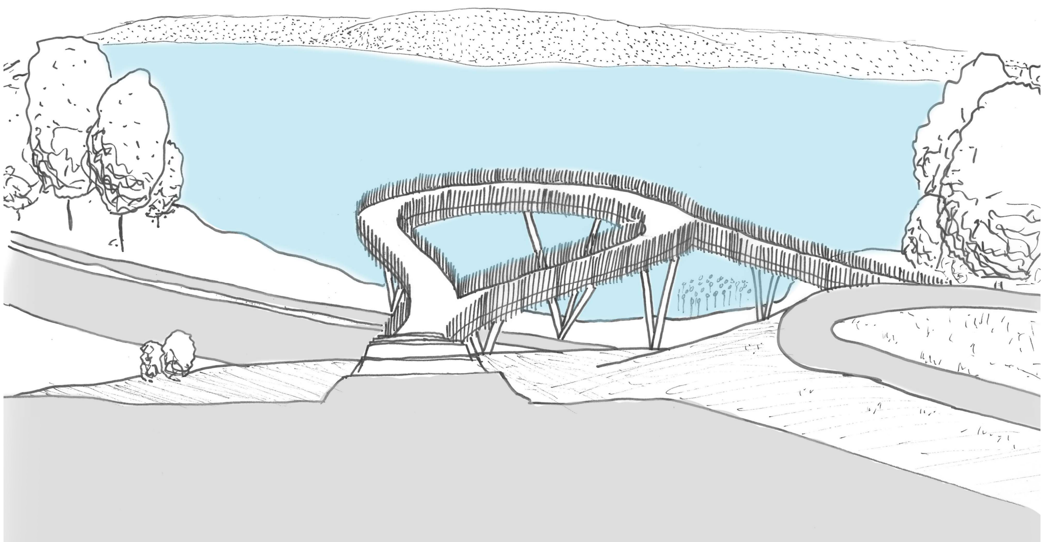

Figure 5.12 Bridge proposal 3 seen from Lakehouse.

The structrual design resembles reeds found along the lake, lifting the structure. The goal is to have slender columns, concentrated at few points, to achieve an airy appearance. A perspective of the bridge is shown in Figure 5.13.

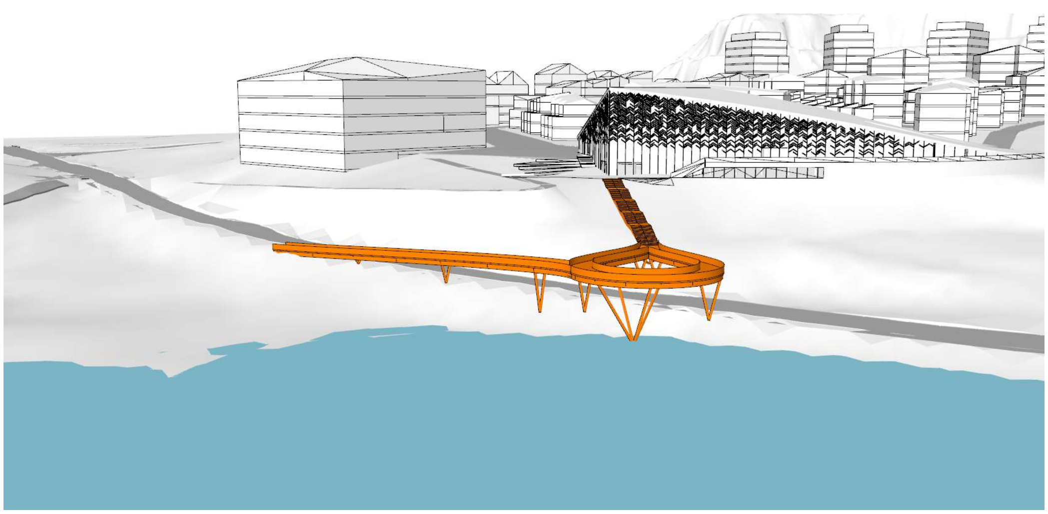

Figure 5.13 Perspective of proposal 3.

The structural concept is described as a beam-column system. The main load-bearing capacity is provided by two outer glulam beams with intermediate diagonal glulams beams in a zig-zag pattern. Beams of smaller dimensions are perpendicularly connected to the zig-zag beams. This will not only contribute to the horizontal stiffness, but it will create a characteristic pattern from beneath.

Summary Intentional phase
The design proposals developed in the Intentional phase focus on exploring the possibilities of the site outside of the local plan and investigate which additional qualities that could be included in the bridge design. The accessibility requirement played a larger role in the design proposals, as well as the intention of including visitors from every direction. The intuitive concepts are developed with emphasis on the following characteristics:

- *Nature*: relation to scenery
- *Embracing*: additional quality in the bridge, implementation of timber
- *Sweeping*: movement of the bridge and relation to scenery

5.4 Evaluation phase

In the last phase of the Conceptual design, the bridge proposals are evaluated in relation to the design criteria, contextual requirements, and the client's demands. The aim is to narrow down the proposals into one, suitable concept.

Client evaluation
As the footbridge in Wendelstrand is requested by Next Step Group, the three intentional design proposals were pitched in a meeting on March 11, 2021. The presentation was customised to communicate the bridge concepts as a fictive design competition, considering Next Step Group as a client. Our understanding of the project Wendelstrand and analysation of the site were introduced. The three bridge proposals were presented as solutions, with their different possibilities and qualities. Already built reference projects were shown to support the arguments.

From the discussion afterwards, feedback from Next Step Group focused on how to involve visitors as well as residents. As Wendelstrand aims to attract visitors from the surrounding area, a bridge structure connected to the water will be included in the overall experience of the area. It is therefore of interest to include visitors approaching the bridge and lake from Boråsvägen as well as from Lakehouse. Physical contact with the water is of greater interest than initially communicated, and the client also emphasised on including additional functions in the bridge design, to offer an experience to the public. The client also wanted suggestions for possible activities in the lake as an extension of the bridge.

Moreover, the client focused on how the bridge design is affected by the Swedish Transport Administration, shore protection and private landowners of the areas outside the local plan. The demands from the Swedish Transport Administration are non-negotiable and are therefore complied with as requirements. The extent of the shore protection area was vaguely defined and was therefore not strictly incorporated as an evaluation criterion. From this meeting, it is clarified that there is a small area excepted from the shore protection regulations. A maximum of two support foundations are allowed within this area. The impact on the seabed should be limited, where floating solutions should be aimed for. The delta area is outside the local plan of Wendelstrand, owned by private individuals and the municipality. To get permission to build something here is rather difficult to achieve. The client cannot plan for a project relying on agreement from outside parties with unpredictable interests.

Based on this discussion, proposal 2 and 3 are found to be the most feasible bridge proposals to be developed, according to the client. These consider the shore protection to some extent and have a clear visual and physical connection between Lakehouse and Landvettersjön. Next Step Group emphasises on the physical connection to the water, as well as the accessibility from the road. Proposal 1 is disregarded because it is located outside the local plan.

Summary of the Evaluation phase

As a summarize of the client's meeting it can be concluded that the final bridge proposal must fulfil the following:

- Contextual demands:
    - The proposal must be within the borders of the local plan.
    - Respect the shore protection regulations and minimise the amount of supports along the shoreline.
    - Avoid supports in the lake.
    - Respect the demands of the Swedish Transport Administration.
- Design demands:
    - Strong visual connection to Lakehouse, preferably in a straight line from the city square. Aim to create a sense of predictability for the users.
    - Establish a physical connection with the water. Not necessarily continuous from Lakehouse to the water.
    - The bridge design should include a proposal for additional functions.
    - The whole bridge does not have to be accessible from Lakehouse to the lake, since there already is a planned accessible path close to the planned bridge. However, the water must be accessible from Boråsvägen.
- Design ambition:
    - Relate to scenery, both in aspects of nature and architecture.
    - Clear presence of timber.
    - Architectural quality in the structure.
    - Resemblance of a natural path.

The development of the final bridge design is determined by the following aspects regarding spatial and bridge specific qualities:

- Limited area for a landing point on the shoreline can complicate the stair connecting the bridge and the ground.
- Visual expression of the pier in relation to the bridge structure and surrounding architecture.
- Relation between the pier and pedestrians approaching both directions along Boråsvägen.
- Possibility for a variation in additional functions on the pier.

6 Step III: Preliminary design

The conclusions drawn from the evaluation phase specify the framework for the final design proposal. This is a tool to develop the concept to where it meets every defined evaluation criterion. Physical models are used to investigate the feasibility of the chosen structural concept. The aim of this phase is to develop the final design proposal to an extent where it can be verified and proven in the last design step: Final design.

6.1 Final design proposal

The final design proposal is a development of design proposals 2 and 3, where a straight path from Lakehouse ends in a platform, creating visual connection to the lake. A physical connection to the lake is made possible by stairs. Figure 6.1 illustrates the final concept in its context and the following subchapters describes the concept more in detail.

Figure 6.1 Conceptual model of the final design.

6.1.1 Overall bridge design

The client's wish for a strong physical and visual connection to the water is recognised by the straight sight line from the residential streets and the small square in front of Lakehouse. The bridge is accessed by stairs in the hillside. The straight path ends in a wide viewing platform, enabling a pause for the pedestrians. Stairs wind down to the ground and lands on the floating pier. A plan view of the final design proposal is seen in Figure 6.2.

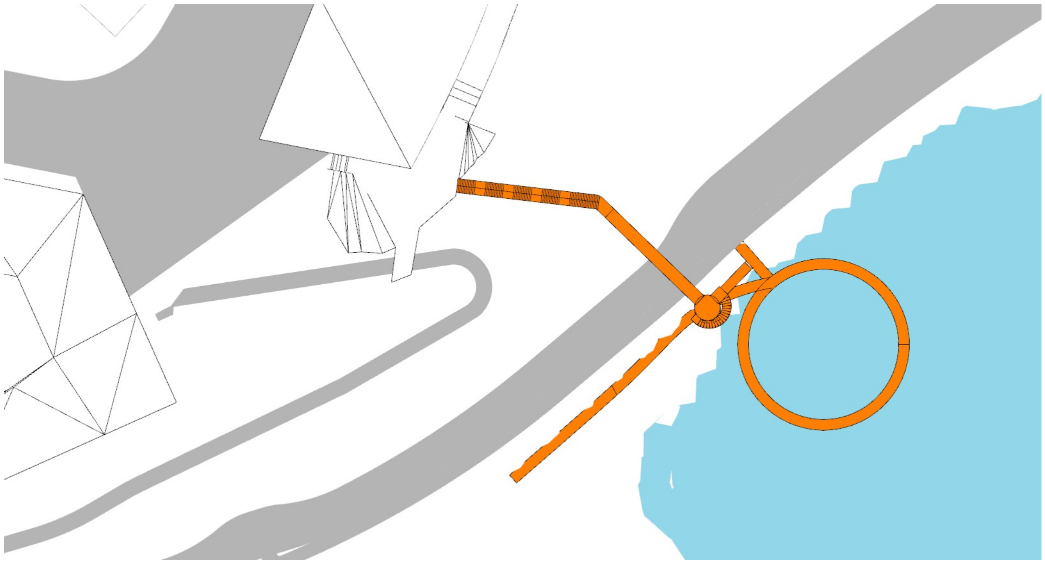

Figure 6.2 Plan view of the final design proposal illustrating the sight line from the city square and Lakehouse to the lake.

The connection between the bridge and the pier is established by a curved staircase, which ensures a landing point within the specified area along the shoreline. An accessible ramp follows the topography and is then led parallel with Boråsvägen down under the viewing platform and then onto the floating pier. Pedestrians that approach from the other direction can access the pier by stairs down from the walkway.

As the client specifically requested, the bridge must offer something more than just a physical connection to the water. A circular floating pier is chosen to be an extension of the accessibility ramp and is proposed to facilitate different possible activities to meet the client's requests. The pier is inspired by the sculpture *The Infinity Bridge* by Gjøde & Povlsgaard Arkitekter in Aarhus. The circular pier offers an inner pool, as well as the possibility to anchor floating saunas, restaurant rafts and canoe rental. Additionally, the circular shape relates to the design language of the curved staircase and ensures a smooth transition for visitors approaching from three directions. Visitors can pause at any point on the circular pier, instead of being led on a straight path out in the water.

6.1.2 Structural concept

The structural concept is a beam bridge with inclined columns, with a total span of approximately 27 m. The superstructure is built up by two outer straight beams and a horizontal truss action is achieved by actively bent beam in a sinus pattern. It is assumed that the internal stresses from active bending provide more horizontal stiffness to the superstructure than pre-bent beams with the same dimensions and geometrical pattern.

The vertical supports are V-shaped in the longitudinal direction. Structurally this will lead to smaller span lengths, and an architecturally visually resemblance of reeds that stretches up along the shoreline. Figure 6.3 shows a side view of the bridge.

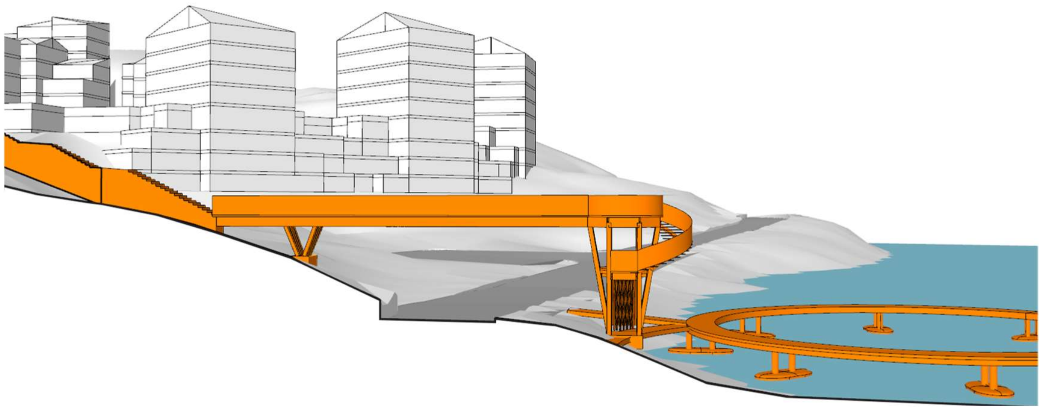

Figure 6.3 Side view of the bridge illustrating the V-shaped supports, the circular staircase, and the floating pier.

To minimise the total length of the staircase, which has a height to length ratio of 1:2, the staircase winds down to an intermediate platform and is then led down straight to the ground. In addition to this, the straight staircase provides global horizontal stability to the bridge structure. The statical concept is visualised together with the bridge structure in Figure 6.4.

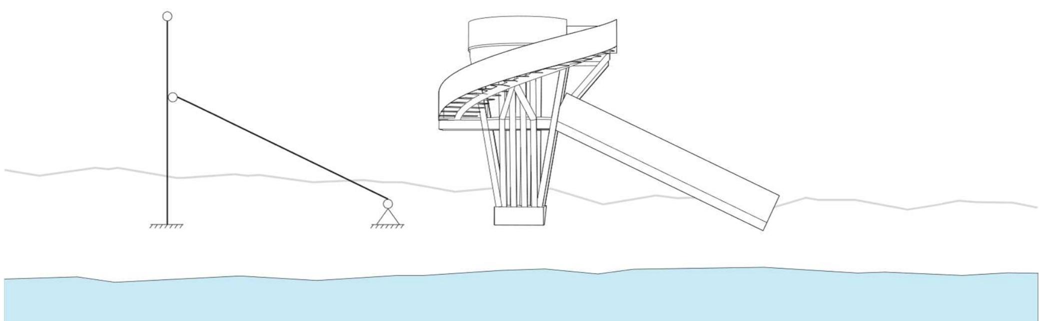

Figure 6.4 Concept for horizontal stability of the viewing platform.

The floating pier is supported by pontoons, which are anchored to the same abutment as the staircase on land. Spacing between the pontoons and the pier deck allows for sunlight to reach the seabed and ensure healthy biotope conditions in the lake.

6.1.3 Experiment with active bending

As the production and assembly method is part of the bridge design the concept of using active bending in the superstructure needs to be tested and verified. The assembly of this structural concept is assumed to be rather complex compared to a simple beam bridge. Instead of performing another literature study, an investigation of physical models is used to gain understanding of active bending. First small and simple conceptual models of actively bent members are built to understand the forces and failure modes better. Then larger and more complex models are built to test the assembly method.

To begin with, small strips of cardboard and paper are bent and attached to each other in different combinations. Figure 6.5 shows four models that actively bends the strips in different ways. The cardboard has much more stiffness than what paper has and is therefore referred to as the *stiffer* part in the observation. The bridge proposal suggests having two outer straight elements, here referred as *beams*, and inner bent elements, here referred to as *lamellas*.

a) Stiff frame, less stiff panels

b) Same stiffnes on beams and panels

c) Stiff transversal beam, less stiff panels

d) Same stiffnes on transversal beams and panels

Figure 6.5 Experimental models of actively bent cardboard and paper strips.

In Figure 6.5a, a stiffer straight beam frame is used with less stiff bent lamellas. The lamellas are connected to each other, layer after layer. Without the frame, the lamellas lay parallel to each other, and active bending is first introduced when the two outer lamellas are stretched out and connected to the stiffer straight beam frame.

In Figure 6.5b, same stiffness on the outer beams as well as the inner bent lamellas is used. The curvature of the lamellas is achieved when the lamella is longitudinally pushed together and attached to the straight beam. The adjacent lamella is equally pushed and connected to the neighbouring lamella, until the outer straight beam is attached and force the deformation in the opposite direction. This method results in buckling of the lamellas. As a conclusion, the curved lamellas must have a significantly smaller stiffness than the outer beams.

In Figure 6.5c, stiffer transversal beams are used with less stiff bent lamellas. The lamellas are attached together in the same manner as in Figure 6.5a, but instead of being anchored to a stiffer frame, transversal elements push the lamellas apart causing the curvature.

The model in Figure 6.5d has used same stiffness on transversal beams and lamellas, in this case cardboard instead of paper. This model generates the best result, where an even curvature is achieved. As a result, the curved elements interact and create a continuous element. The resulting stiffness generated by the interaction of the curved lamellas is sufficient to maintain a desired shape for an external force and resembles the behaviour of a truss.

A conclusion from this test is that a combination of a stiffer, outer frame and transverse distancing elements is considered as optimal. It is easier to control the deformation of the lamellas with the help of transversal stiffeners. It can also be observed that the curved shape of the lamellas can be achieved in two ways: either induced by a transversal distancing force or by buckling caused by a longitudinal compressing force. Without any transversal or longitudinal force, the lamellas will automatically lay flat against each other. If looking at the boundary conditions instead, a longitudinal force can be represented in fixed connections at the ends of the curvature, while a transversal force can allow for a roller support at one of the ends. A combination of these can of course be done to reduce the residual forces required at the boundary conditions. The correlation between boundary conditions and shape is illustrated in Figure 6.6.

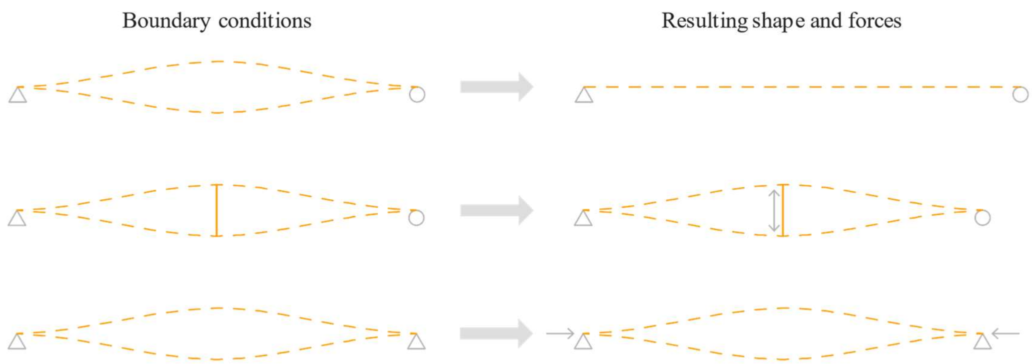

Figure 6.6 Observations of different boundary conditions and resulting shape and forces due to active bending.

The aim of using actively bent elements is to mimic a truss and thereby create horizontal stability in the superstructure. As seen in Figure 6.7 the bent elements resemble a truss, and forces can diagonally be transported. The inclination of the structs can be altered to achieve different visual appearances.

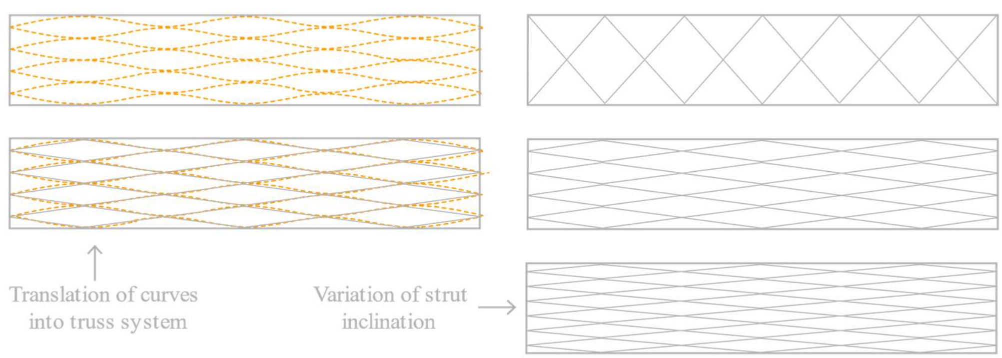

Figure 6.7 Theoretical perception of the structural behaviour of beams in a sinusoidal pattern.

6.2 Model development of structural concept

Based on the knowledge gained from the previous small experiment, the next step is to build a concept model in wood to simulate a more realistic assembly method and to test the structural behaviour of the actively bent elements.

The assembly method of the conceptual model is illustrated in Figure 6.8 and can also be described as the following:

1. A thicker element is used as outer beam and a thinner element for the curved panels. The elements are predrilled, with a few millimetres offset in the panels.
2. Threaded steel bars are inserted through one of the outer straight beams and fastened with nuts on the outside.
3. A straight panel is mounted on the threaded bars. Deformation of the panel is induced due to the offset of the holes as well as from nuts placed at desired transversal distance on the bars.
4. The rest of the panels are assembled in a similar way, creating the waved truss.
5. Lastly, the other straight beam is assembled, and secured by nuts on the outside.

Figure 6.8 Diagram of the assembly method of the concept model.

Evaluation of the concept model

As can be seen in the second step of the assembly method in Figure 6.8, the outer beam started to deform due to the built-in longitudinal forces as described in the previous subchapter. This deformation got larger for each new panel added. To attach the last straight beam, large amount of external force was required. The predrilling of the holes had a relatively large offset, creating large amplitude of the sinus curves. As a result, the position of the nuts was adjusted thereafter, resulting in unprecise spacing. Buckling of the threaded bars could also be observed. Ideally the bars should be in tension, but in this model, they are in compression because no spacers were used.

As a conclusion from these observations, compression members should be used to secure the deformation of the panels, allowing the threaded bar to be in pure tension. Secondly, the panels should be mounted on the bars as straight elements with compression spacers at specified positions. Thereafter, as nuts in each end of the threaded bars are screwed tighter, forced compression is induced on the wood elements. With specifically placed compression distancers, the sinusoidal pattern is created. This method will ensure an even deformation and stress distribution in the structure. Regarding the pre-drilling, the position of the holes should be more accurate and measured beforehand, so the right spacing is achieved. The holes in the bent panels can preferably have larger dimension than the dimension of the threaded bars to secure some tolerance during assembly.

Concerning the structural behaviour of the structure, it works well in vertical and horizontal bending. The torsional stiffness is however weak. This can be increased by using an extra layer of threaded bars, in addition to an increased height of the wooden elements. On the other hand, interaction of the curved panels is secured by pre-tensioning the superstructure. This phenomenon will increase when the threaded bars work purely in tension, and the deformation is secured by separate compression members. Applied force in horizontal direction proves that the curved panels act like a truss, which distributes the forces in compression and tension to the straight, thicker beams.

Continuing from this, the concept model is developed according to the observed results. The superstructure is built in a model in scale 1:10 to verify the new assembly method as well as attempt to increase the torsional stiffness. A model of the complete bridge structure is built in scale 1:20 to verify the production method of the whole bridge structure. Moreover, this model will demonstrate the connection between the superstructure and columns as well as the horizontal stability from the straight staircase. Spatial qualities and the bridge's context in its surrounding is demonstrated in a landscape model in scale 1:400. These models are presented in the next chapter.

7 Step IV: Final design

The final bridge design proposal is a straight bridge deck across the road, V-shaped column supports, a circular staircase, and a circular, floating pier. The bridge deck ends in a viewing platform, with the staircase winding around and underneath the structure. Simultaneously, an accessible ramp from the road is led through the V-shaped platform columns, underneath the staircase. Any visitor will be able to experience the bridge structure from underneath, where every path leading to the floating pier is interplayed with the bridge structure. As a result, the bridge design proposal offers both a transport route, a destination, and an experience. The overall concept together with its context is shown in Figure 7.1 and Figure 7.2.

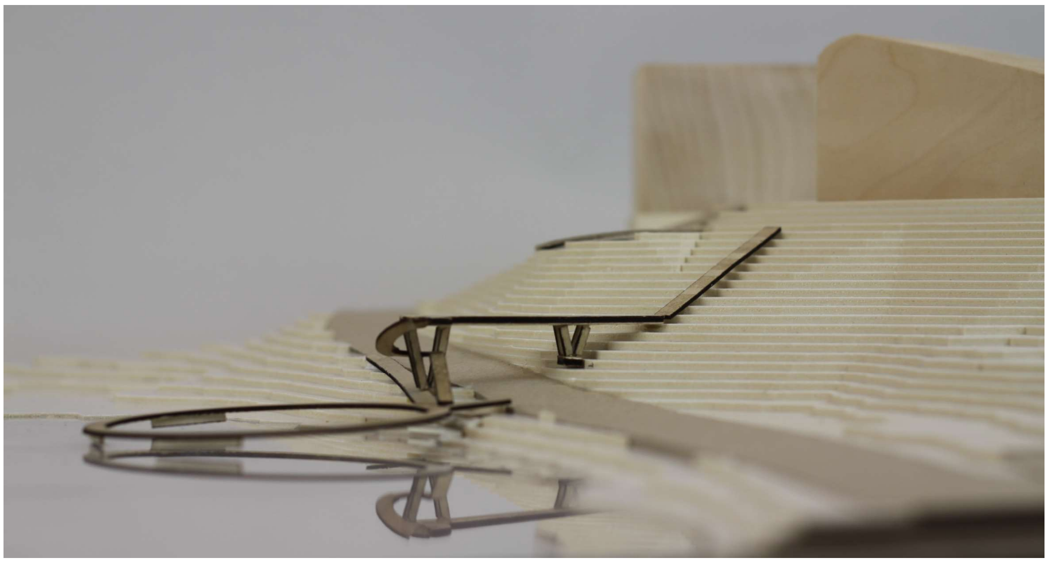

Figure 7.1 Scale model in 1:400 of the proposed design in its context.

Figure 7.2 The whole bridge model in scale 1:20.

The structural concept of the bridge deck is developed to decrease the effective height of the deck, while maintaining, or increasing, the horizontal and vertical capacity. Panels of Laminated Veneer Lumber (LVL) are actively bent into a sinusoidal pattern, secured by two outer, parallel straight LVL-beams and pre-tensioned with threaded steel bars into a uniform element. Active bending is applied to achieve the wanted performance of the deck, where built in stresses allow the curved panels to interact in a truss-like behaviour giving both vertical and horizontal stiffness. The superstructure with its actively bent lamella panels can be seen in Figure 7.3.

Figure 7.3 The bridge superstructure seen from the intermediate platform.

V-shaped column supports decrease the span-lengths of the bridge and as a result reducing the governing forces in the superstructure. The columns go up into the superstructure and the bent panels are spread to give room to the connection. This creates a homogeneous meeting between the bridge and supports and enhances the architectural appearance of the concept. The connection is in the mid height of the superstructure, generating no extra cantilevering point. The integrated meeting between columns and superstructure is shown in Figure 7.4.

Requirements on the site concerning clearance from the road and shore protected area determine the chosen landing points. The direction of the bridge is on the other hand determined by the visual connection between the lake and Lakehouse, but also by the challenges of connecting the bridge with a staircase. The design aims to limit the impact on the ground, while simultaneously achieving the required stability of the global bridge structure. The straight staircase is anchored on the shore strip in a perpendicular direction to the superstructure to achieve global horizontal stability. To reduce the total length of the straight staircase it starts at the intermediate platform, which is seen in Figure 7.5.

Figure 7.4 *The supports are integrated into the superstructure creating a homogeneous appearance.*

Figure 7.5 *Viewing platform and pathway down to the ground level. The straight staircase also contributes to the horizontal stability.*

7.1 Bridge dimensions

A land section of the final bridge design with its correlation to Lakehouse and Landvettersjön is illustrated in Figure 7.6. An overview of the governing dimensions, and clearance is given in Figure 7.7. To ensure water drainage along the bridge, an inclination of 2% towards Lakehouse is applied.

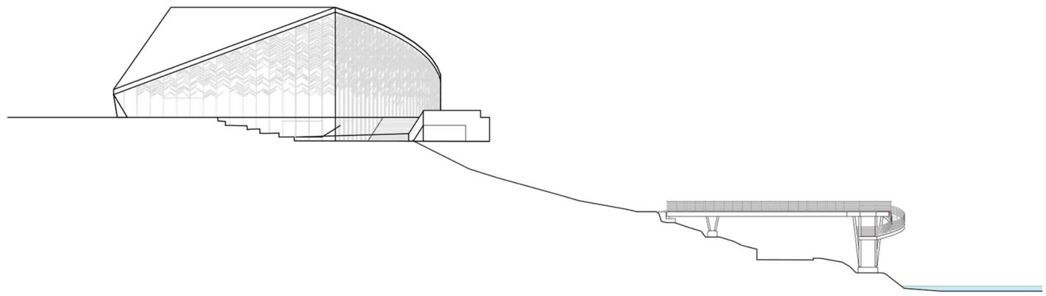

Figure 7.6 Side view of the bridge in relation to Lakehouse and Landvettersjön.

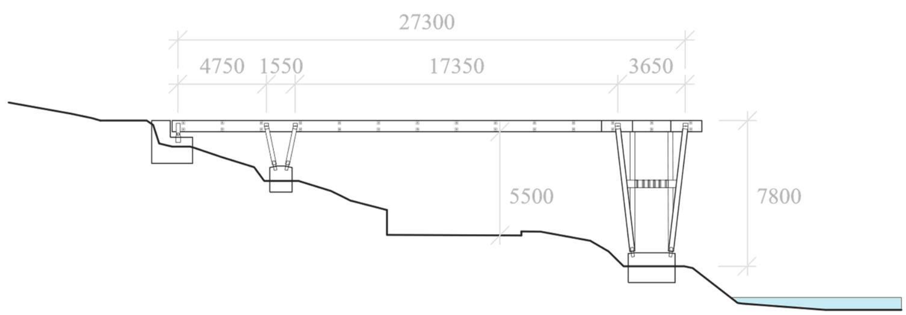

Figure 7.7 Land section with main dimensions.

A cross-section of the bridge is illustrated in Figure 7.8 with labels of the structural elements and governing dimensions of the bridge deck. The specific dimensions of the load-bearing elements are summarised in Table 7.1, while dimensions of the bridge deck components such as floor beams and railing are summarised in Table 7.2. The dimensions of the support columns are presented in Table 7.3. The foundation elements are suggested to be in reinforced concrete but required dimensions are not calculated. A rough estimation of the required capacity of these elements is presented in Table 7.22.

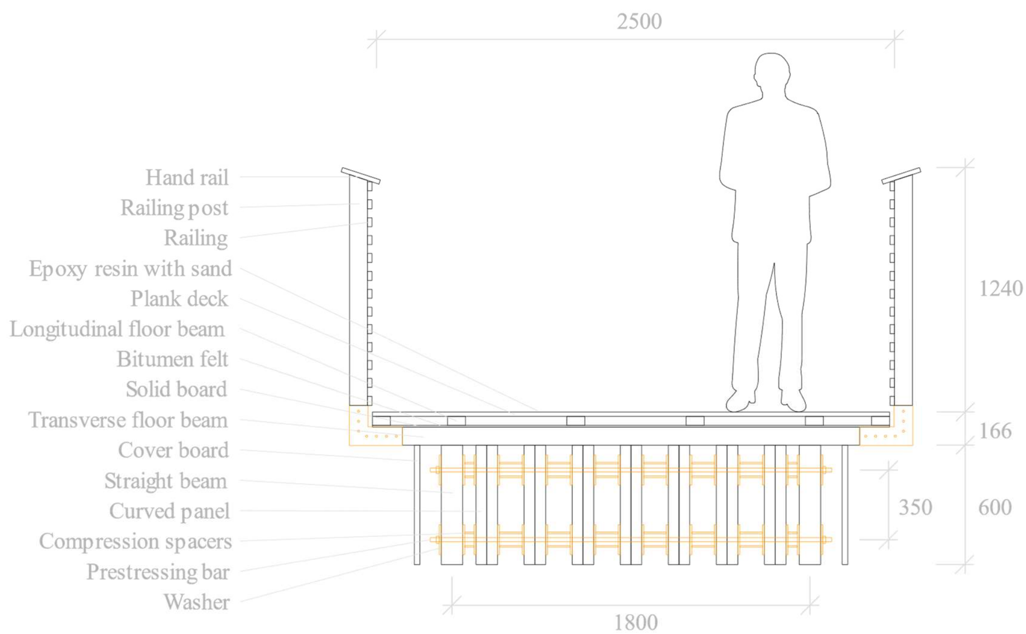

Figure 7.8 Cross-section of the superstructure and bridge deck with corresponding materials and dimensions.

Table 7.1 Dimensions of the load-bearing elements.

Element	**Material**	**Dimension**	**Value** [mm]
Straight beams	LVL, Kerto-S	w x h	108 x 600
Curved panels	LVL, Kerto-S	w x h	54 x 600
Compression spacers	CHS	d, t	76.1, 8
Prestressing bar	Dywidag, 26WR	d	26.5

Table 7.2 Dimensions of bridge deck components.

Element	**Material**	**Dimension**	**Value** [mm]
Transverse floor beams	Solid timber	w x h, c-c	75 x 90, 600
Longitudinal floor beams		w x h, c-c	90 x 45, 600
Plank deck		w x h, c-c	195 x 22.5, 210
Railing		w x h, c-c	120 x 70, 1200
Solid board	Plywood	t	9
Bitumen felt	YEP 2500	t	2

Table 7.3 Dimensions of support elements.

Element	**Material**	**Dimension**	**Value** [mm]
Support columns intermediate	LVL	w x h	216 x 260
Support columns platform		w x h	270 x 260

The design of the staircase is performed as a simply supported beam subjected to vertical load according to the load cases calculated for the superstructure. The structure is built up similarly as the bridge superstructure, with two outer straight beams and actively bent LVL panels. The final dimensions of the staircase structure are presented in Table 7.4.

Table 7.4 Dimensions of the load-bearing elements of the staircase.

Element	**Material**	**Dimension**	**Value** [mm]
Straight, outer beams	LVL, Kerto-S	w x h	108 x 400
Curved beams	LVL, Kerto-S	w x h	54 x 400
Compression distancers	CHS	d, t	76.1, 8
Prestressing bar	Dywidag, 18WR	d	17.5

7.2 Input data

To verify the bridge design with its cross-sections hand calculations and a simplified FE analysis are performed. The overall bridge design is based on European Standards and Swedish Standards. General requirements for timber footbridges are formulated by the Swedish Transport Administration. Overall bridge design concerning the capacity is covered in *Bärighetsberäkning av broar* and states which European standards that are used to determine the capacity of the structure (Ronnebrant, s2020). Detailed design of the bridge is covered in *Krav Brobyggande* (Krona, 2019). To ensure a more concise writing, EC5-1 will be used as abbreviation for Eurocode SS-EN 1995-1 etc.

The following standards are used for the different calculation aspects:

- Design material properties for LVL: EC5-1-1 (SS-EN 1995-1-1:2004)
- Bridge specific properties: EC5-2 (SS-EN 1995-2:2004)
- Dimensioning with the partial factor method: EC0 (SS-EN 1990:2010)
- General loads
    - Wind load: EC1-1-4 (SS-EN 1991-1-4:2005)
    - Snow load: EC1-1-3 (SS-EN 1991-1-3:2003)
- Bridge specific loads: EC1-2 (SS-EN 1991-2:2003), with corresponding partial factors
- Load combinations: EC1-1 (SS-EN 1991-1-1:2005)
- Bridge details: The Swedish Transport Administration, *Krav Brobyggande* (TDOK 2016:0204)

7.2.1 Partial factors

The timber bridge is dimensioned according to EC0 where the partial coefficient method is applied. On the load side partial factors are used to consider exposure, load duration, load situations and -combinations. The material related partial factors are taken from EC5.

Material properties

The characteristic material properties are adjusted with partial factors that considers exposure, load duration, material, and element size according to EC5-1, which gives the design material properties:

$$f_d = k_{mod} \frac{f_k}{\gamma_M} \; [MPa] \tag{7.1}$$

The correlation factor k_{mod} considers the load duration and moisture content of the structural material. The bridge is classified as service class 3 according to EC5-1. However, if the main structural members can be sufficiently protected against rain, service class 2 can be applied. In this case, a conservative approach is chosen and thereby service class 3 is used. Self-weight is classified as permanent load while imposed loads such as wind load (EC5-1) and traffic load from pedestrians (EC5-2) are considered short-term loads. According to EC5-1, combination of loads of different duration should be determined for the shortest load duration, which in this case is short-term load duration. For LVL exposed to short-term load duration in service class 3 (EC5-1), the correlation factor is set according to

$$k_{mod} = 0.7 \tag{7.2}$$

The partial factor γ_M is determined by the specific material and differs for control of capacity and control of deformation. For LVL, the partial factor according to EC5-1 is:

$$\gamma_M = 1.2 \tag{7.3}$$

For LVL with rectangular cross-section and majority of the veneers are oriented in the same direction, the size effect in bending and tension must be considered. For LVL in bending, the reference height is 300 mm. For any element height in bending other than 300 mm, the characteristic bending strength $f_{m.k}$ should be multiplied with the factor k_h according to EC5-1. For LVL in tension, the reference length is 3000 mm. For any element length other than 3000 mm, the characteristic value $f_{t.0.k}$ should be multiplied with a factor k_l according to EC5-1. The design capacity of the LVL beams and panels are determined for veneers in the same direction.

The dimensions determining the size effect factors for LVL in bending and tension, and the resulting factors are summarised in Table 7.5.

Table 7.5 LVL size effect.

Load action		**Value**
Element height in bending	h_{lvl}	0.6 [m]
Element length in tension	L	27.3 [m]
Size effect for bending	$k_{h.lvl}$	0.92
Size effect for tension	$k_{l.lvl}$	0.876

Load combinations

As the risk of personal injury in the case of structural collapse is considered serious, the bridge is categorized as safety class 3 according to 13 § in Boverket EKS 10 (Boverket, 2016). The partial coefficient considering the safety of a load bearing structure is set according to 14 § EKS 10:

$$\gamma_d = 1.0 \tag{7.4}$$

The timber bridge is verified in Ultimate Limit State (ULS) for deformation of the structure, STR: “Internal failure or excessive deformation of the structure or structural members, including footings, piles, basement walls, etc., where the strength of construction materials of the structure governs” (Chapter 6.4.1, EC0).

Load combinations in ULS considering the capacity of the structure is calculated according to Equation 6.10a and b in EC0. For unfavourable permanent loads *G*:

$$LC_G = \gamma_d \cdot \gamma_G \cdot G_k \tag{7.5}$$

For variable loads $Q_{k.i}$, the loads are combined as follows:

$$LC_{Q.i} = \gamma_d \cdot \gamma_Q \cdot Q_{k.i} \tag{7.6}$$

For interacting variable loads $Q_{k.i}$ and $Q_{k.j}$, where $Q_{k.i}$ is the main load, the loads are combined accordingly:

$$LC_{Q.ij} = \gamma_d \cdot \gamma_Q \cdot Q_{k.i} + \gamma_d \cdot \gamma_Q \cdot \psi_{0.1.i} \cdot Q_{k.j} \tag{7.7}$$

The partial factors for load combinations are found in Table 7.6 according to EC0 and Boverket EKS 10. Relevant load factors are found in Table 7.7, extracted from Table A2.2 in EC0.

Table 7.6 Partial factors for load combinations.

Type of load		**Characteristic**	**Frequent**	**Quasi-permanent**
Permanent load	γ_G	1.2	1.0	1.0
Variable load	γ_Q	1.5	1.0	1.0
Risk class 3	γ_d	1.0	1.0	1.0

Table 7.7 Load factors for load combinations.

Type of load	**Characteristic** $\psi_{0.i}$	**Frequent** $\psi_{1.i}$	**Quasi-permanent** $\psi_{2.i}$
Traffic load	0.4	0.4	0
Wind load	0.3	0.2	0
Snow load	0.7	0.5	0.2

7.2.2 Material properties

Laminated Veneer Lumber, LVL, is chosen as the main structural material of the load-bearing elements in the bridge. Kerto-S beam is chosen for both the outer straight beams and the curved beams, with all lamellas oriented with the same fibre direction. Usually the majority of the lamellas in Kerto-S are oriented with fibre direction along the beam and the rest in vertical direction. The stiffness can be increased with a few lamellas perpendicular to the length, but this is not accounted for in the following capacity calculations.

Characteristic material properties for Kerto-S beam are extracted from the dominating European Supplier of LVL, Mestä Wood, according to manufacturer’s declaration of performance (Eurofins Expert Services Oy, 2020). The straight beams are built up by 9 times 3 mm veneer sheets glued together from 4 lamellas. The curved panels are built up by 2 lamellas.

The characteristic material properties of the Kerto-S beam, and the resulting design strength properties adjusted with corresponding partial factors, are listed in Table 7.8 according to producer's certificate (Eurofins Expert Services Oy, 2020).

Table 7.8 Design properties of LVL.

Design strength properties		**Value** [MPa]
Bending edgewise	$f_{m.0.edge.d}$	16.9
Bending flatwise	$f_{m.0.flat.d}$	28.8
Tension parallel to grain	$f_{t.0.d}$	12.8
Compression parallel to grain	$f_{c.0.d}$	14.6
Compression perpendicular to grain, edgewise	$f_{c.90.edge.d}$	2.50
Compression perpendicular to grain, flatwise	$f_{c.90.flat.d}$	0.92
Shear edgewise	$f_{v.0.edge.d}$	1.71
Shear flatwise	$f_{v.0.flat.d}$	0.96
Characteristic material properties		**Value**
Size effect parameter	s	0.12
Elastic modulus, parallel to grain	$E_{0.k}$	11600 [MPa]
Elastic modulus, parallel to grain, mean	$E_{0.m}$	13800 [MPa]
Elastic modulus, perpendicular to grain, edge, mean	$E_{90.edge.m}$	430 [MPa]
Elastic modulus, perpendicular to grain, flat, mean	$E_{90.flat.m}$	130 [MPa]
Density, characteristic	ρ_k	480 [kg/m^3]
Density, mean	ρ_m	510 [kg/m^3]

7.2.3 Loads

7.2.3.1 Permanent loads

The self-weight of the bridge deck components is calculated according to the following equation. L_i is the length of the element and n_i is the number of elements on the bridge:

$$G_{k.i} = \rho_{k.i} \cdot g \cdot n_i \cdot w_i \cdot h_i \frac{L_i}{L_{tot}} \ [kN/m] \qquad 7.8$$

The resulting permanent loads are listed in the table below, where non-load-bearing elements include floor beams, plywood and construction boards, plank deck, epoxy resin cover, and railing.

Table 7.9 Permanent loads

Characteristic permanent load		**Value** [kN/m]
Straight beams	$G_{k.lvl.s}$	0.61
Curved beams	$G_{k.lvl.c}$	2.14
Distancers	$G_{k.dis}$	0.50
Non-load-bearing elements	$G_{k.deck}$	1.14
Total permanent load	G_k	4.39

7.2.3.2 Variable loads

The variable loads working on the bridge structure are identified as:

- Traffic load from pedestrians only, as no service vehicle can access the bridge.
- Wind load on the bridge deck and on the support columns.
- Snow load as the bridge must be manually cleared. This load will only be included in the load combinations if it exceeds the permanent load.

Temperature deformations are discharged from the calculations as the expansion coefficient for timber is small.

Traffic load, vertical

Load Model 4: "Crowd loading", is applied according to EC1-2. As the bridge is likely to be subjected to an even flow of pedestrians rather than a continuous dense crowd, the characteristic value of uniformly distributed load is set according to:

$$Q_{fk} = 2.0 + \frac{120}{L + 30}\ [kN/m^2] \qquad 7.9$$

$$2\frac{kN}{m^2} \leq Q_{fk} \leq 5\frac{kN}{m^2} \qquad 7.10$$

According to EC1-2, the uniformly distributed load should be applied in the most unfavourable parts of the surface, in both longitudinal and transverse direction. A conservative approach is chosen where the load is applied as uniformly distributed over the cross-section.

Traffic load, horizontal

For footbridges only, a horizontal force Q_{flk} should be considered, acting along the bridge deck axis at the pavement level, according to EC1-2:

$$Q_{flk} = 0.1q_{fk}[kN] \qquad 7.11$$

The horizontal force is considered to act simultaneously with the corresponding vertical load.

Wind load on the bridge structure

The transverse, horizontal wind load is calculated according to EC1-1-4. The vertical wind load is determined for both uplift and downwards. According to EC1-1-4 does the vertical wind load only have significant effect on the structure if the force exceeds the permanent load of the bridge. In this case, the downward vertical wind load will not be of the same order as the dead load and is therefore disregarded in the capacity calculations of the bridge. The uplifting force will be considered in the detailed design of the bridge connections.

The force in transverse direction $F_{w.x}$ is determined by the simplified method according to EC1-1-4, ρ being the air density:

$$F_{w.x} = \frac{1}{2}\rho \cdot v_b^2 \cdot C_x \cdot A_{ref.x}\ [kN] \qquad 7.12$$

For structures in terrain category II, the wind load factor C_x can be defined with interpolation of table 8.2 in EC1-1-4, determined by the reference height z_e which is altitude above sea level plus bridge height.

For load combinations without traffic load and plain webs, the reference area is calculated as:

$$A_{ref.x} = L \cdot d\ [m^2] \qquad 7.13$$

The reference height d for an open parapet and open safety barrier is set accordingly, d_{tot} being the total height of the bridge deck:

$$d = 0.6m + d_{tot}\ [m] \qquad 7.14$$

The wind velocity is defined according to EC1-1-4:

$$v_b = c_{dir} \cdot c_{season} \cdot v_{b.0} = 26.0\frac{m}{s} \qquad 7.15$$

The fundamental values used to calculate peak velocity pressure depends on the geographical conditions of the bridge in question. The fundamental value for Wendelstrand is $v_{b.0} = 25.0\ m/s$ (Boverket, 2019b). The directional factor c_{dir} and seasonal factor c_{season} are set to 1.0. The basic velocity pressure is calculated as

$$q_b = \frac{1}{2}\rho \cdot {v_{b.0}}^2 = 0.39\frac{kN}{m^2} \qquad 7.16$$

Longitudinal wind forces depend on the horizontal wind forces and the geometry of the bridge. For plated bridges, the longitudinal wind force is 25% of the transverse wind forces (Chapter. 8.3.4 in EC1-1-4). The wind force along the bridge is set to:

$$F_{w.y} = 0.25F_{w.x}\ [kN] \qquad 7.17$$

Wind load on column supports

Wind load on columns are calculated according to Chapter 7.6 in EC1-1-4. The design situation is assumed to be wind blowing in the transverse direction of the bridge. The wind force on a rectangular column is calculated as

$$F_w = c_s \cdot c_d \cdot c_f \cdot q_p \cdot A_{ref}\ [kN] \qquad 7.18$$

The seasonal factors c_s and c_d are set to 1.0. The peak velocity pressure is calculated as follows, with $c_e(z)$ depending on the terrain category for the bridge structure.

$$q_p = c_e(z) \cdot q_b\ [kN] \qquad 7.19$$

The force coefficient for rectangular cross-sections with sharp corners is determined as

$$c_f = c_{f.0} \cdot \psi_\lambda \tag{7.20}$$

The end-effect factor ψ_λ is determined by Figure 7.36 in EC1-1-4 and depends on the solidity ratio φ and the slenderness λ. These in turn depend on the dimensions of the projected column. The force coefficient $c_{f.0}$ is determined by linear interpolation of Figure 7.23 in EC1-1-4.

Snow load
Snow load on bridge decks is calculated with the same method as for roof structures, according to Chapter 5 in EC1-1-3. The snow load is calculated as:

$$s = \mu_i \cdot C_e \cdot C_t \cdot s_k \ [kN] \tag{7.21}$$

The exposure coefficient C_e is conservatively set to 1.0 for normal conditions. The thermal coefficient C_t is not relevant for pedestrian bridges and is set to 1.0. The shape coefficient μ_i depends on the inclination of the bridge structure, and is set to 0.8 according to Table 5.2 in EC1-1-3. The characteristic value of snow on the ground is determined by the geographical conditions on the site and is given by Boverket EKS as $s_k = 1.5\ kN/m^2$ (Boverket, 2019a).

Total variable load
The resulting variable loads are listed in Table 7.10.

Table 7.10 Variable loads

Characteristic variable load		Value
Traffic load, vertical	$Q_{fk.z}$	10.2 [kN/m]
Traffic load, horizontal	$Q_{fk.x}$	27.9 [kN]
Wind load, horizontal	$F_{w.x}$	2.32 [kN/m]
Wind load, along	$F_{w.y}$	15.8 [kN]
Snow load	q_{snow}	3.0 [kN/m]

7.2.3.3 Accidental load

Due to traffic under the bridge, accidental design situations must be included in the dimensioning of the support columns according to EC1-2. For stiff columns and roads in urban areas, the impact force is set to:

$$F_{dx} = 500\ kN \tag{7.22}$$

$$F_{dy} = 250\ kN \tag{7.23}$$

The impact forces are assumed to not occur simultaneously. The impact height is determined to $h_d = 1.25\ m$ with the impact area depending on the vehicle. This cannot be wider than the width of the support, according to EC1-2. The column capacity is tested for accidental actions without the influence of variable loads.

7.2.4 Load combinations

Load model 4 is applied to calculate the bridge capacity. This includes characteristic values, frequent values, and quasi-permanent values for a uniformly distributed load according to Table 2.1 in EC1-2.

The following subchapters present the design load combinations used to calculate the capacity of the bridge superstructure and columns in ultimate limit state and serviceability state.

Design load combinations – bridge superstructure
The governing load combinations on the bridge superstructure are illustrated in Figure 7.9. The design load combinations used to calculate the capacity of the bridge superstructure in ultimate limit state are summarised in Table 7.11. Snow load is disregarded in the load combinations as it does not exceed the permanent load on the bridge.

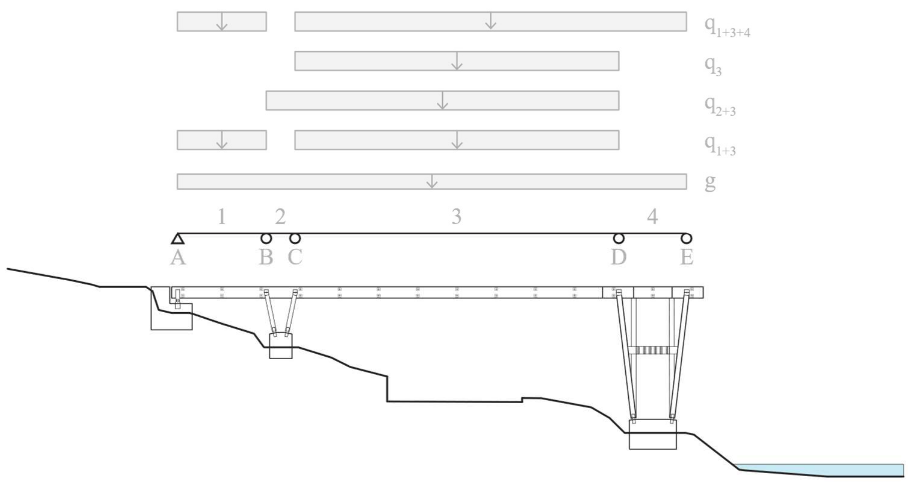

Figure 7.9 Governing load combinations on the superstructure.

Table 7.11 Design loads for capacity calculations

Load combination		Value
Vertical load *Self-weight + traffic load*	$q_{d.z.uls}$	20.6 [kN/m]
Transverse load *Wind load*	$q_{d.x.uls}$	3.48 [kN/m]
Longitudinal load *Wind load + traffic load*	$q_{d.y.uls}$	4.11 [kN]

The design loads used to calculate the instantaneous and final deformations of the bridge in serviceability state are summarised in Table 7.12.

Table 7.12 Design loads for deformation calculations

Load combination		**Value** [kN/m]
Vertical load *Self-weight*	$q_{d.sls.G}$	4.39
Vertical load *Traffic load*	$q_{d.sls.Q}$	10.2

Design load combinations – support columns

The largest reaction force in the support columns depend on how the variable load is distributed on the bridge. The load response of the bridge in terms of reaction forces is illustrated in Figure 7.10.

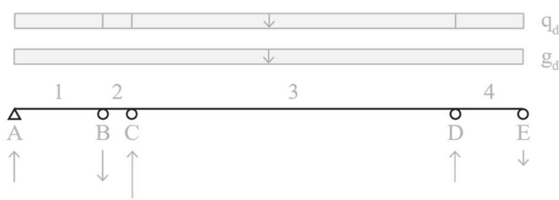

Figure 7.10 Load response from distributed load along the bridge.

The most critical load case is applied for the largest reaction force in each column, which is summarised in Table 7.13.

Table 7.13 Critical load cases for each column support

Column	**Load combination** Span	**Reaction force, vertical** [kN/m]	**Reaction force, horizontal** [kN/m]
Column B	*3*	-260	-44.8
Column C	*2+3*	459	78.4
Column D	*1+3+4*	308	52.1
Column E	*1+3*	-82.9	-15.8

These reaction forces are combined with wind load acting on the columns. Furthermore, the support columns are verified for the accidental load due to traffic under the bridge. These are only combined with the permanent loads on the bridge.

The design loads used to calculate the capacity of the support elements in Ultimate Limit State are summarised in table Table 7.14 and illustrated in Figure 7.11.

Table 7.14 Design loads for capacity calculations

Design load combination		**Value**
Transverse load, column B, C	q_w	1.45 [kN/m]
Transverse load, column D, E	q_w	1.89 [kN/m]
Accidental load, column C *Longitudinal vs transverse direction*	q_{dx} q_{dy}	741 [kN/m^2] 308 [kN/m^2]
Accidental load, column D *Longitudinal vs transverse direction*	q_{dx} q_{dy}	593 [kN/m^2] 308 [kN/m^2]

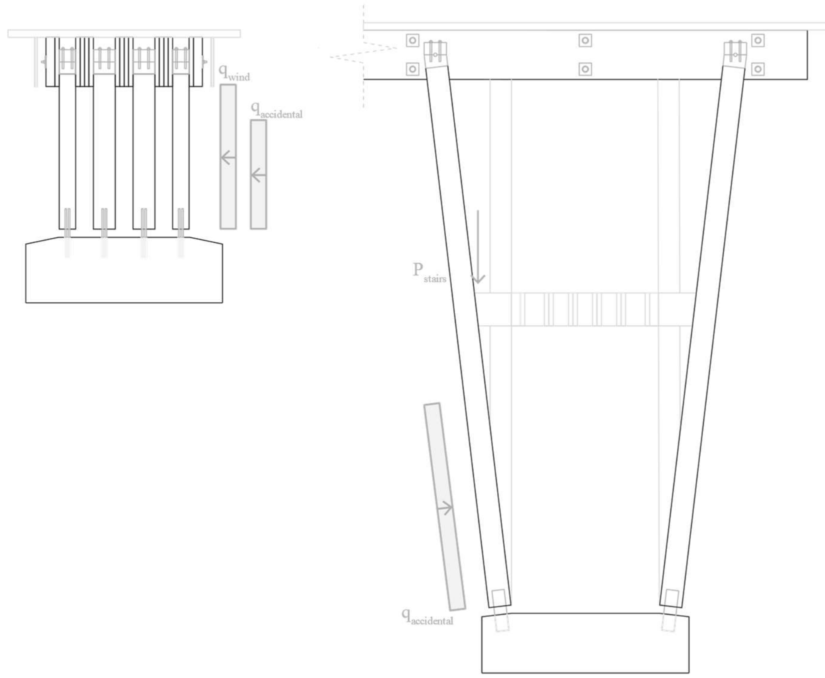

Figure 7.11 Variable load on the supports. Hill-side columns to the left, and lake-side to the right.

7.3 Global design

In the following subchapters the calculated response in ULS and SLS of the superstructure and columns are presented.

7.3.1 Superstructure in ULS

Maximum load effects

The maximum load effects on the bridge structure is calculated for a continuous beam in four unequal spans. The maximum load effects calculated for load in vertical direction are summarised in Table 7.15 and illustrated in Figure 7.12.

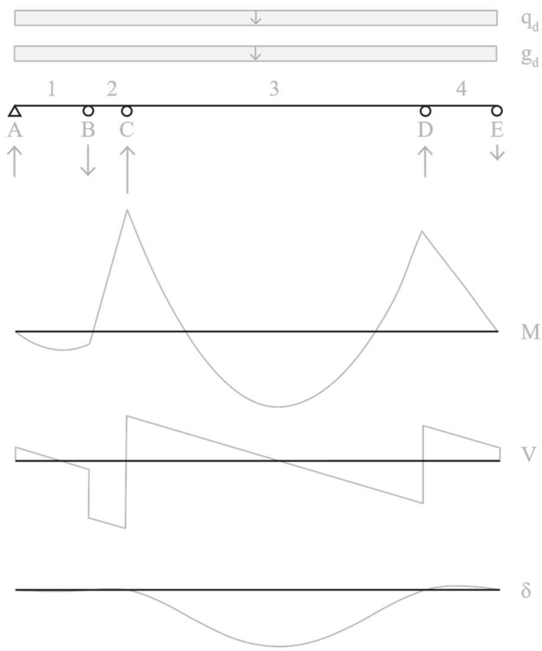

Figure 7.12 Load response due to uniformly distributed load

Table 7.15 Load effects, vertical load.

Load effects	**Critical load case** Span		**Value**
Bending moment, largest span	*1+3*	$M_{f.max}$	294 [kN/m]
Bending moment, intermediate support	*2+3*	$M_{s.max}$	477 [kN/m]
Shear force, intermediate support	*2+3*	$V_{4.max}$	281 [kN]
Reaction force, platform support	*2+3*	$R_{5.max}$	459 [kN]
Maximum deflection, largest span	*1+3*	δ_{max}	-25.1 [mm]

The maximum load effects on the bridge structure in transverse direction are summarised in Table 7.16.

Table 7.16 Load effects, transverse load.

Load effects	**Critical load case** Span		**Value**
Bending moment, largest span	*1+3*	$M_{f.max}$	49.7 [kN/m]
Bending moment, intermediate support	*2+3*	$M_{s.max}$	80.8 [kN/m]
Shear force, intermediate support	*2+3*	$V_{4.max}$	48.2 [kN]
Reaction force, platform support	*2+3*	$R_{5.max}$	78.4 [kN]

Bending stresses due to induced deformation

The induced deformation of the LVL panels leads to bending stresses parallel to the grain, between the lamellas. The stresses depend on the lamella thickness, radius of the curve and stiffness of the material. The radius is decided through iterative parametric design, based on lamella thickness, desired curvature length and interaction with bending and axial compression.

The bending stresses are verified for the bending capacity of the LVL according to EC5:

$$\sigma_{m.flat.d} \leq k_r \cdot f_{m.0.flat.d} \qquad 7.24$$

In bent glulam elements, the reduced capacity is considered by applying a reduction factor k_r. As a conservative approach, the capacity of the bent LVL elements is reduced in the same manner. The reduction factor is determined as follows, where t is the thickness of the bent panel and r_{in} is the inner radius of the curve:

$$k_r = \begin{cases} 0.76 + 0.001\dfrac{r_{in}}{t}, & \dfrac{r_{in}}{t} < 240 \\ 1, & \dfrac{r_{in}}{t} \geq 240 \end{cases} \qquad 7.25$$

The stresses in the curved zoned for bent lamellas are calculated according to the following equation, t being the lamella thickness:

$$\sigma_{m.90.d} = \frac{E_{0.k}t}{2r_{in}} \qquad 7.26$$

The chosen geometry and resulting bending stresses are presented in the table below:

Table 7.17 Curvature of the LVL panels and resulting bending stresses.

Factor		Value
Inner radius of curved panels	r_{in}	14.5 [m]
Bending stresses in lamellas	$\sigma_{m.90.d}$	10.8 [MPa]

Verify capacity

The bending, compression and shear capacity of the bridge is verified stepwise to monitor the structural response of the load-bearing element. The design bending stresses in the whole cross-section are verified for the design bending capacity in the respective direction according to Chapter 6.1.6 in EC5 for k_m = 0.7 for LVL. The compression stresses parallel to the grain are verified according to Chapter 6.1.4 in EC5 for the whole cross-section, the straight beams, and the curved beams respectively.

The effect of combined bending and axial compression is controlled for both the whole cross-section and the straight beams according to:

$$\left(\frac{\sigma_{c.0.d}}{f_{c.o.d}}\right)^2 + \frac{\sigma_{m.y.d}}{f_{m.y.d}} + k_m\frac{\sigma_{m.z.d}}{f_{m.z.d}} \leq 1 \qquad 7.27$$

$$\left(\frac{\sigma_{c.0.d}}{f_{c.o.d}}\right)^2 + k_m\frac{\sigma_{m.y.d}}{f_{m.y.d}} + \frac{\sigma_{m.z.d}}{f_{m.z.d}} \leq 1 \qquad 7.28$$

As the curved panels are designed for the bridge deck to work as a horizontal truss, the combined bending and compression capacity of the panels are checked in z-direction only. Due to induced deformations in the panel, the compression strength is reduced with a buckling factor $k_{c.z}$ determined according to Chapter 6.3.3 in EC5. Partly interaction is assumed for the induced bending stresses in the panels, with an interaction factor k_{curve} set to 0.7. As the design of the curved panels fulfils the criteria "lateral displacement of its compressive edge is prevented throughout its length and torsional rotation is prevented at its supports" (EN 1995-1-1, Chapter 6.3.3 (5)), the buckling factor k_{crit} is set to 1.0. The curved panels are checked according to the following equation:

$$\frac{\sigma_{c.0.d}}{k_{c.z} \cdot f_{c.0.d}} + \left(\frac{\sigma_{m.z.d}}{k_{crit} \cdot f_{m.z.d}}\right)^2 + k_{curve}\frac{\sigma_{m.90.d}}{f_{m.y.d}} \leq 1 \qquad 7.29$$

The bridge deck is verified for the combined effect of induced bending stresses, bending in two directions and axial compression. The buckling factors $k_{c.z}$ and $k_{c.y}$ are defined conservatively for the whole bridge deck, where the buckling length in vertical direction is set equal to the length of the largest bridge span and transverse direction equal to the spacing between the compression distances. Slenderness ratios larger than 0.3 reveal that the stresses in each direction will increase due to deflection, and should therefore be verified according to Equation 6.23-24 in EC5:

$$\frac{\sigma_{c.0.d}}{k_{c.y} \cdot f_{c.0.d}} + \frac{\sigma_{m.y.d}}{f_{m.y.d}} + k_m\frac{\sigma_{m.z.d}}{f_{m.z.d}} + k_{curve}\frac{\sigma_{m.90.d}}{f_{m.y.d}} \leq 1 \qquad 7.30$$

$$\frac{\sigma_{c.0.d}}{k_{c.z} \cdot f_{c.0.d}} + k_m\frac{\sigma_{m.y.d}}{f_{m.y.d}} + \frac{\sigma_{m.z.d}}{f_{m.z.d}} + k_{curve}\frac{\sigma_{m.90.d}}{f_{m.y.d}} \leq 1 \qquad 7.31$$

The shear stresses are verified according to Chapter 6.1.7 in EC5. The resulting utilisation ratios in ULS are presented Table 7.18.

Table 7.18 Utilisation ratios in ULS

Design stress	**Utilisation** [%]
Superstructure	
Bending, vertical main	49
Bending, transverse main	35
Axial compression	0.8
Bending + compression, vertical main	49
Bending + compression, transverse main	35
Bending + compression + induced deformation, vertical main	86
Bending + compression + induced deformation, transverse main	72
Shear, vertical load	26
Shear, transverse load	8
Straight beam	
Bending capacity ratio, vertical load	27
Bending capacity ratio, transverse load	23
Axial compression	0.4
Bending + compression, vertical main	40.2
Bending + compression, transverse main	35.1
Curved panel	
Bending capacity ratio, vertical load	53.9
Bending capacity ratio, transverse load	93.5

Induced deformation	51.8
Axial compression	0.85
Bending + compression, main direction	34.0
Bending + compression + induced deformation, vertical	70.2

Observation of the results show that the curved panels handle most of the bending stresses in the superstructure and are more utilised than the straight beams. Second order effects of the panels are not considered in the calculations.

7.3.2 Superstructure in SLS

The maximum deflection is calculated for traffic load and permanent load only, according to Chapter 7.2 in EC5-2.

Deformations

The deformations in a structure subjected to loads and moisture must be verified according to Chapter 2.2.3 in EC5. The final deformations are calculated for quasi permanent load combinations, while the instantaneous deformation is calculated for characteristic load combinations in SLS. As the bridge deck is composed by members with equal modulus of elasticity and shear modulus, the final deformation is calculated as

$$u_{fin} = u_{fin.G} + \sum u_{fin.Q.i} \qquad 7.32$$

The final deformation due to permanent load G and variable load Q_1 are calculated as

$$u_{fin.G} = u_{inst.G}(1 + k_{def}) \; [mm] \qquad 7.33$$

$$u_{fin.Q.1} = u_{inst.Q.1}(1 + \psi_{2.1} \cdot k_{def}) \; [mm] \qquad 7.34$$

Creep deformations in timber structures are influenced by moisture content and are accounted for with the creep factor k_{def}. For LVL in climate class 3, the creep factor is set to 2.0. The resulting infinite and final deformations for permanent and variable load are presented in Table 7.19.

Table 7.19 Infinite and final deformations.

Deformations		**Value** [mm]
Infinite deformation, permanent load	$u_{inst.G}$	-12.5
Infinite deformation, variable load	$u_{inst.Q}$	-5.27
Final deformation	u_{fin}	28.3

Instantaneous and final deformations of a pedestrian bridge are limited according to Chapter 7 in EC5-2:

$$\delta_{lim} = \frac{1}{200} \qquad 7.35$$

The largest deformation is found in the span across the road, and is verified accordingly:

$$u_{fin} \leq \delta_{lim} \cdot L_3 \; [mm] \tag{7.36}$$

Deflection due to shear is neglected as the deck is assumed to interact like a horizontal truss.

7.3.3 Support in ULS

The following subchapter presents the final design of the support columns and the required capacity of the support foundation. The capacity of the columns is verified for ULS load combinations.

Maximum load effects on the columns

The reaction force from vertical load on the bridge is divided by the number of columns at the support. The horizontal reaction force is translated to a bending moment at the foundation and a resulting vertical force in the support column. As the columns are inclined in longitudinal direction, the vertical load on one column is divided into axial and perpendicular components. The load response in the columns are illustrated in Figure 7.13.

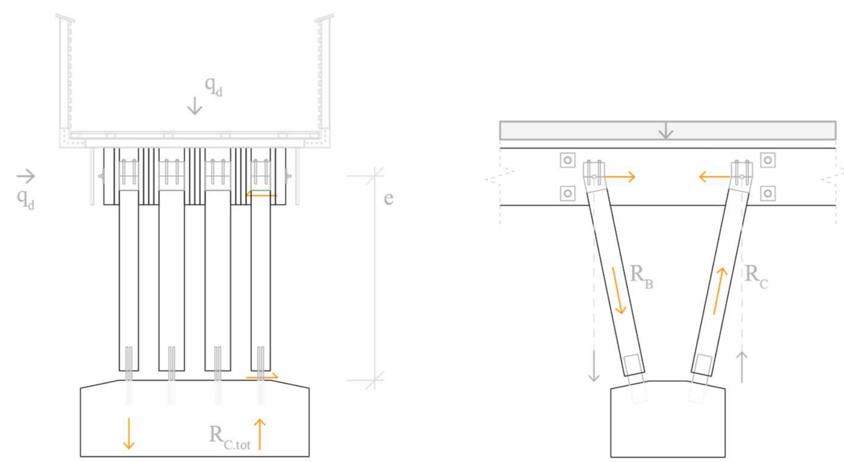

Figure 7.13 Load response in the supports due to load on the bridge.

The reaction force from horizontal load on the bridge is translated by shear through the column to the foundation.

The columns are tested for the axial load component combined with bending due to wind load, in addition to shear stresses in the top and bottom. The design of the bridge deck enables the perpendicular load component to be taken by the LVL panels between the inclined columns according to the principles of strut and tie.

Furthermore, the support columns under the viewing platform are tested for an additional vertical load from the staircase. Table 7.20 summarises the load effects on the support columns in the intermediate support and platform support respectively.

Table 7.20 Load effects on columns at the supports

Load effects		**Value**
Intermediate support		
Axial load	$N_{0.B}$	-92.7 [kN]
	$N_{0.C}$	163 [kN]
Bending moment from wind load	M_x	0.96 [kNm]
Deflection from wind load	$\delta_{w.x}$	0.14 [mm]
Shear force	V_B	-11.2 [kN]
	V_C	19.6 [kN]
Deflection from accidental load	$\delta_{w.x}$	77.9 [mm]
	$\delta_{w.y}$	136 [mm]
Platform support		
Axial load	$N_{0.D}$	200 [kN]
	$N_{0.E}$	-30.5 [kN]
Bending moment from wind load	M_x	11.3 [kNm]
Deflection from wind load	$\delta_{w.x}$	12.2 [mm]
Shear force	V_D	17.9 [kN]
	V_E	-3.95 [kN]
Deflection from accidental load	$\delta_{w.x}$	172 [mm]
	$\delta_{w.y}$	154 [mm]
Staircase load	P_k	0.64 [kN]

Capacity verification

The compression capacity of the columns is verified according to Chapter 6.3.2 in EC5. The columns are designed as pinned-pinned with an effective buckling length l_{ef} equal to the column length. The design compression stresses are verified according to EC5:

$$\sigma_{c.0.d} \leq N_{cr} \tag{7.37}$$

The critical buckling load of the column is calculated for the respective direction as

$$N_{cr.x} = k_{c.x} \cdot f_{c.0.d} \; [kN] \tag{7.38}$$

$$N_{cr.y} = k_{c.y} \cdot f_{c.0.d} \; [kN] \tag{7.39}$$

Combined transverse and axial load in the columns are verified according to EC5:

$$\frac{\sigma_{c.0.d}}{k_{c.y} \cdot f_{c.0.d}} + \frac{\sigma_{m.y.d}}{f_{m.y.d}} + k_m \frac{\sigma_{m.x.d}}{f_{m.x.d}} \leq 1 \tag{7.40}$$

$$\frac{\sigma_{c.0.d}}{k_{c.x} \cdot f_{c.0.d}} + k_m \frac{\sigma_{m.y.d}}{f_{m.y.d}} + \frac{\sigma_{m.x.d}}{f_{m.x.d}} \leq 1 \tag{7.41}$$

The bending stresses are due to initial deformation in the columns, combined with transverse load from wind or accidental load:

$$M_{Ed} = N_0(\Delta_0 + \delta_x) + M_x \; [kNm] \tag{7.42}$$

The initial out of straightness is applied on the LVL columns is conservatively assumed as the value for glulam (Swedish Wood, 2016):

$$\Delta_0 = \frac{L}{300}\ [mm] \tag{7.43}$$

Tension stresses in the columns are verified according to EC5, where the size effect is accounted for in the design capacity of the column:

$$\sigma_{t.d} \leq f_{t.0.d} \tag{7.44}$$

The effect of combined transverse load and tension is verified according to EC5:

$$\frac{\sigma_{t.d}}{f_{t.o.d}} + \frac{\sigma_{m.y.d}}{f_{m.y.d}} + k_m \frac{\sigma_{m.x.d}}{f_{m.x.d}} \leq 1 \tag{7.45}$$

$$\frac{\sigma_{t.d}}{f_{t.o.d}} + k_m \frac{\sigma_{m.y.d}}{f_{m.y.d}} + \frac{\sigma_{m.x.d}}{f_{m.x.d}} \leq 1 \tag{7.46}$$

Shear stresses in the top and bottom part of the column are verified according to EC5:

$$\tau_d \leq f_{v.0.edge.d} \tag{7.47}$$

The applied vertical load on the platform columns lead to an additional moment in the column, which is calculated as:

$$M_{Ed} = N_0(\Delta_0 + \delta_x) + M_x + P \cdot \mathrm{e}_p\ [kNm] \tag{7.48}$$

With P being the point load from the staircase and e_p the eccentricity of the load in relation to the column end. The resulting bending stresses combined with an axial load are verified in the same manner.

The resulting utilisation ratios in of the support columns are presented in Table 7.21. These are due to permanent and variable load on the superstructure combined with specific loads on the columns.

Table 7.21 Support column utilisation ratios

Design stress	**Utilisation** [%]
Intermediate columns	
Axial compression	19.1
Axial compression and bending, wind load	27.0
Axial compression and bending, accidental load	62.6
Shear	30.6
Tension	10.4
Tension and bending	18.2
Platform columns	
Axial compression	53.6
Axial compression and bending, wind load	90.3
Axial compression and bending, wind load + staircase	88.1

Axial compression and bending, accidental load x-dir	95.5
Axial compression and bending, accidental load + staircase	**130**
Shear	14.9
Tension	3.1
Tension and bending	39.8

Note that the accidental loads require much larger capacity of the column elements than variable and permanent loads combined. The columns close to the road that also supports the staircase requires larger dimension than the rest, preferably with a width of 324 mm instead of 270 mm. This results in a utilisation ratio of 89%.

Loads on abutments
Summary of the load on the abutments is presented in Table 7.22.

Table 7.22 Required capacity of the abutments.

Load response	**Load** [kN]
Hill-side support	
Vertical	54.7
Transverse	9.28
Intermediate support	
Vertical	216
Transverse	364
Horizontal	438
Shear	78.4
Platform support	
Vertical	305
Transverse	455
Horizontal	365
Shear	71.6

7.3.4 Dynamic analysis

In addition to capacity and deformation analysis, the dynamic response of the main bridge structure must be verified. An exact response of the structure will not be carried out, but an estimation of the response based on predicted periodic forces for similar load situations is considered sufficient.

Resonance may occur if one of the natural frequencies of the bridge is equal to the frequency from an imposed force. If the imposed frequency is larger than the natural frequency of the bridge, vibrations may also occur. The natural frequency depends on the stiffness, mass, and span length of the structure. In EC5-1, the natural frequency for a simply supported, rectangular floor structure is calculated as

$$f_1 = \frac{\pi}{2l^2}\sqrt{\frac{(EI)_l}{m}} \qquad 7.49$$

For a bridge deck with several spans and varying stiffness along the length, this equation is too conservative. Instead, a FE model is built to simulate a more accurate dynamic response of the main structure of the bridge deck. In addition to the natural frequency, the corresponding deformation mode is of interest. This indicates what type of induced force that will cause resonance.

Finite Element model

Abaqus is used to simulate the dynamic response of the main structure of the bridge deck. As laminated veneer lumber is the main material of the load-bearing elements, the model must consider the orthotropy of the material. This is ensured by using plane stress elements to build up the section. The bridge deck is modelled as a shell element with length corresponding to the total length of the bridge and width set to the distance between the outer straight beams.

To simulate the behaviour of the real bridge structure, the stiffness must be accounted for. As the model computes the stiffness based on the dimensions of the element combined with material properties, the real stiffness can be accounted for by adjusting the geometry of the FE model. An effective height is calculated from the moment of inertia in the real bridge deck while the width is kept equal to bridge dimensions. As the stiffness of the bridge deck varies in the span and over the support, two separate models are built.

$$h_{ef.span} = \sqrt[3]{\frac{12 \cdot I_{span}}{W}} \; [mm] \qquad 7.50$$

$$h_{ef.support} = \sqrt[3]{\frac{12 \cdot I_{support}}{W}} \; [mm] \qquad 7.51$$

Material properties are assigned according to the mean values for Kerto-S beams for elastic behaviour and material type lamina. As the producer does not state the shear modulus in transverse direction, this can be estimated to one tenth of the longitudinal direction. In the model, the property of Kerto-Q is conservatively chosen. Material orientation is assigned to the model according to the bridge design. Table 7.23 present the chosen material properties used in the FE model.

Table 7.23 Material properties in FE model.

Mean values		Value
Density	ρ_m	5.10e-10 [ton/mm^3]
Modulus of elasticity, parallel to grain, along	$E_{0.m}$	13800 [MPa]
Modulus of elasticity, perpendicular to grain, edgewise	$E_{90.edge.m}$	430 [Mpa]
Shear modulus, edgewise	$G_{0.edge.m}$	600 [Mpa]
Shear modulus, parallel to grain, flatwise	$G_{0.flat.m}$	600 [Mpa]
Shear modulus, perpendicular to grain, flatwise	$G_{90.flat.m}$	22 [Mpa]

The shell element is partitioned at the support locations and assigned with corresponding boundary conditions, according to Figure 7.14.

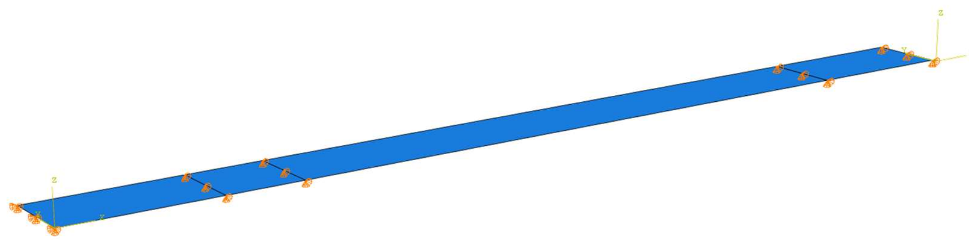

Figure 7.14 Boundary conditions assigned to the FE model.

The frequency analysis is performed with linear perturbation and limited for a maximum frequency of 50 Hz. A structural, quadratic mesh is chosen with element size of 10 mm.

Limitations of the model

The purpose of the FE model is to estimate the dynamic response of the bridge deck, to exclude the risk of resonance due to an induced force. Therefore, the complexity of the bridge deck is disregarded in the model, as an estimation of the natural frequency can be determined for an adjusted stiffness. These are performed conservatively and does not represent the accurate response of the structure. However, if the estimated natural frequency of the structure is smaller than or close to the predicted vibrations from pedestrians or wind, the model would need to be refined to exclude the risk of resonance. Otherwise, adjustments to the structure is necessary with the aim of increasing the structural stiffness. As a result of this, the FE model cannot be used to simulate the torsional stiffness, as this largely depend on the geometry of the deck.

Result of frequency analysis

The first natural frequency is found for vertical vibration in the span-model and support-model at 7 Hz and 8 Hz respectively. The two models show similar response in the following modes for type of vibration but the intervals between each mode are larger for the support-model, which is associated with the larger stiffness of the model.

Owing to this, only the results of the span-model are presented and verified, as these are the more critical and more representative. The first eight modes are presented in Table 7.24. The modes indicate which direction the deck will deform for different frequencies. This behaviour is relevant to identify to predict what type of external forces that can cause resonance in the structure.

Table 7.24 Eigenmodes, model of span.

Increment	**Frequency** [Hz]	**Type**
Mode 1	7	Vertical
Mode 2	14	Torsional
Mode 3	19	Vertical
Mode 4	20	Horizontal
Mode 5	30	Torsional
Mode 6	36	Vertical
Mode 7	47	Base state
Mode 8	48	Horizontal

However, a comparison of the results of the two models reveal that a shared natural frequency is found for 20 Hz. Both models experience horizontal deformation, but for different mode numbers (Mode 4 and 3). It is also observed that the two models deform in the opposite direction for the second and third vertical vibration modes, and for the horizontal vibration modes. However, this is assumed to be a feature in Abaqus as the models are symmetric.

Figure 7.15 to Figure 7.17 illustrate the vertical, torsional, and horizontal vibration modes for the span-model.

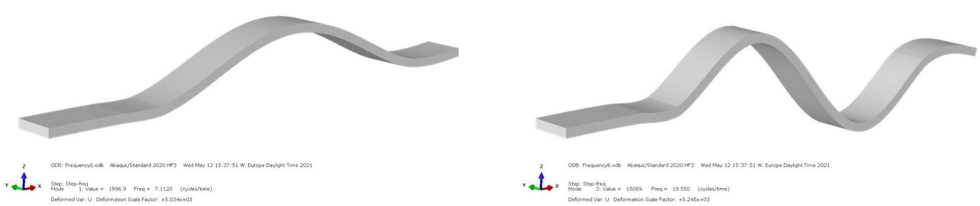

Figure 7.15 Vertical deformation for eigenmode 1 and 3.

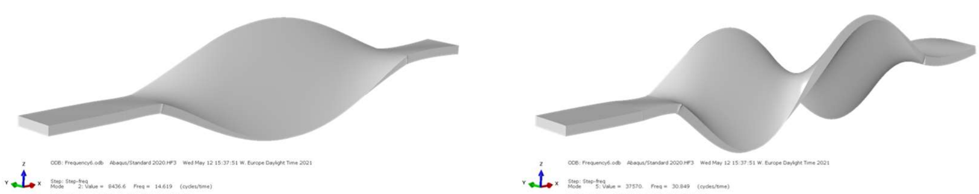

Figure 7.16 Torsional deformation for eigenmode 2 and 5.

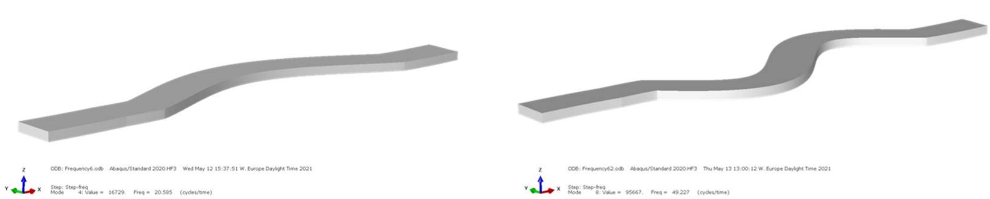

Figure 7.17 Horizontal deformation for eigenmode 4 and 8.

Verification of dynamic response

Vertical accelerations of a timber bridge caused by one pedestrian depends on the first natural frequency for vertical deformation of the bridge (EC5-2):

$$a_{vert.1} = \begin{cases} \dfrac{200}{M \cdot \xi}, & f_{vert} < 2.5\ Hz \\ \dfrac{200}{M \cdot \xi}, & 2.5\ Hz < f_{vert} < 5.0\ Hz \end{cases} \qquad 7.52$$

For a group of joggers crossing the bridge, the vertical vibration is expected at 3 Hz (Chapter 5.7, EC1-2). As the natural frequency for vertical deformation is larger than 5 Hz for both stiffness-models, the bridge deck structure will not resonate for pedestrian induced acceleration in vertical direction.

Horizontal accelerations of a timber bridge caused by one pedestrian is calculated as (EC5-2):

$$a_{hor.1} = \frac{50}{M \cdot \xi}, \qquad 0.5\ Hz < f_{hor} < 2.5\ Hz \qquad 7.53$$

As the frequency for horizontal deformation is larger than 2.5 Hz, the bridge deck structure will not resonate for pedestrian induced acceleration in horizontal direction. Limitations on transverse wind-induced vibrations are not considered in EC5-2 and are also disregarded in these verifications.

7.3.5 Torsional stiffness

When looking at torsional stiffness, there are two aspects to consider. The first aspect is whether the cross-section has a closed or open force path, and the second aspect is how the force is transported in the lengthwise direction towards the supports. For closed domains, the torsional stresses all go in the same direction and the rotational stability is determined by the length of the lever arm from the rotation centre. For an open domain, the torsional stresses reverse and go in both directions in the cross-section, and the rotational stability is more dependent of the material. As a result, a closed cross-section has a higher torsional stiffness compared to an open domain. The difference of the force paths in an open and closed cross-section is illustrated in Figure 7.18.

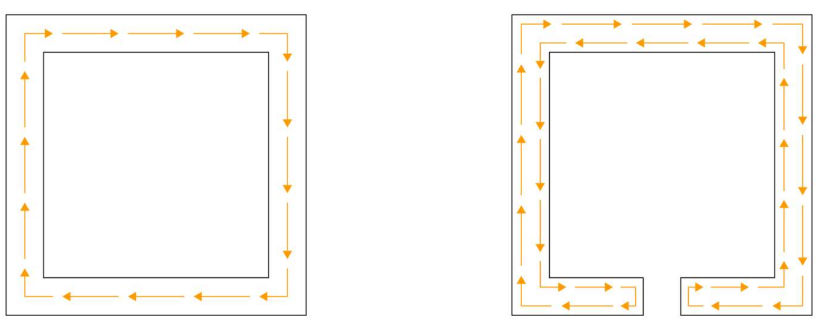

Figure 7.18 Torsional stress flow of a closed versus open cross-section.

For the second aspect of torsional stiffness, the force should also be able to travel in a helix-pattern in the lengthwise direction to the supports. The schematically force path is illustrated in Figure 7.19.

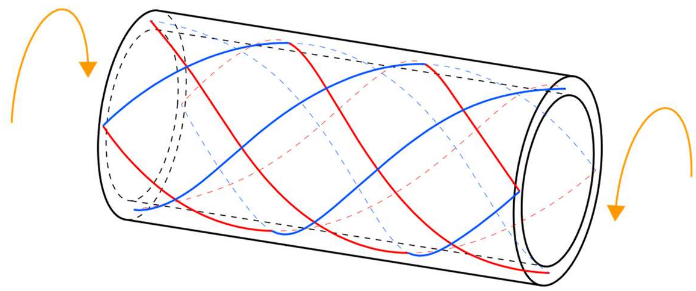

Figure 7.19 Lengthwise force flow of a tube.

The torsional stiffness of the proposed bridge design is achieved by the closed force path created by the two layers of tension bars as well as the straight LVL beams. A principle force flow is presented in Figure 7.20.

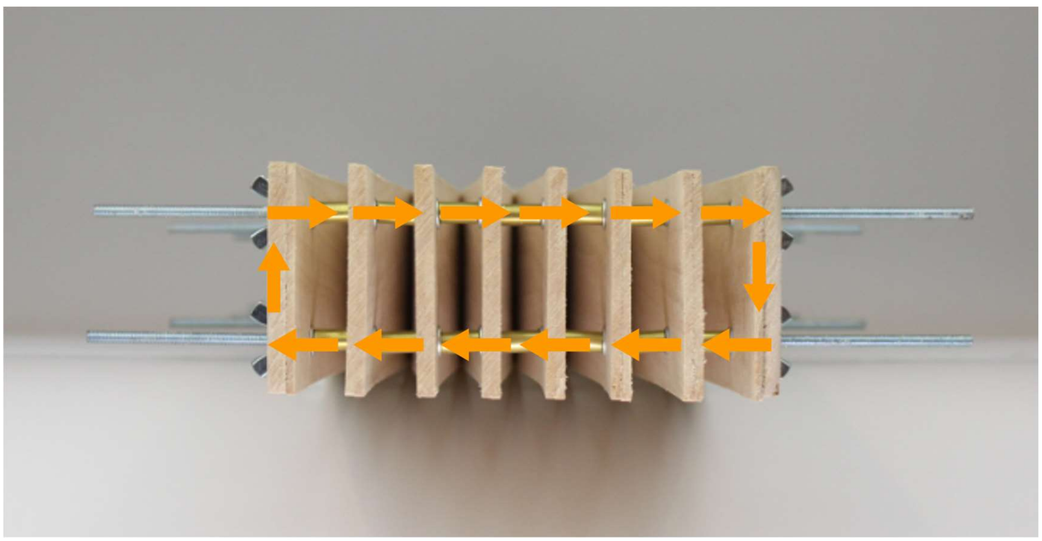

Figure 7.20 Principle torsional stress flow of the superstructure.

When looking at the lengthwise force flow, the torsional stiffness is mainly achieved by the outer straight beams, which carries the torsion with help of shear forces. It is also possible to see a helically force path through the superstructure. If only looking at the superstructure from above, the top part of the bent panels carries the forces in tension and compression through the diagonals in the built-up truss to the opposite straight beam. Then the forces diagonally go down vertically in the straight beams, and then horizontally again through the truss diagonals. This force flow is not as governing as the forces carried through shear in the straight beams, resulting in quite a poor torsional stiffness of the whole superstructure. A schematically lengthwise force flow through the diagonals of the superstructure is shown in Figure 7.21.

The truss system of the actively bent beams is statically determined when the edges are transversely fixed at the boundaries. In this case, a transverse beam secures the rotation at the edges of the outer straight beams and curved panels. At the supports, the columns are integrated into the deck. By this, the deck is fixed in each end of every span, and consequently rotationally secured.

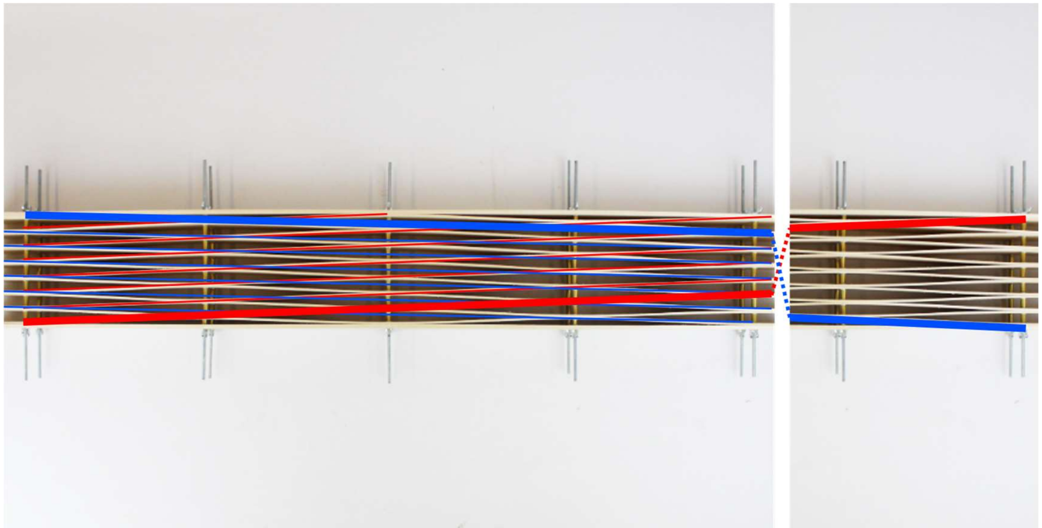

Figure 7.21 Helically force flow through the superstructure. The bent panels create a truss system enabling forces in the horizontal as well as the vertical plane.

The exact torsional stiffness of the cross-section is not calculated but is instead tested in a physical model in scale 1:10. Induced rotations on the bridge deck prove a weaker torsional stiffness compared to vertical and horizontal bending stiffness, which indicate that the governing failure mode of the superstructure will be torsion. If required, the torsional stiffness of the superstructure can be increased by inserting a third layer of tension bars, creating additional path for the stresses. Another possibility would be to make the connection between the superstructure and the supporting beams for the bridge deck more rigid. This will also create a new force path for the stresses. A larger lever arm will result in larger torsional stiffness, so the tension bars should be as close to the upper and lower edges as possible. As a general comment, the capacity of the drilled holes for the tension bars needs to be checked.

7.3.6 Moisture induced deformation

Moisture dependent deformations must be considered if the moisture content in the entire bridge increase from factory to site climate. According to manufacturer, the LVL products are delivered with a moisture content of 8-10%. As the bridge is designed for service class 3, with assumed moisture content of 10-16%, moisture dependent deformations must be considered (Eurofins Expert Services Oy, 2020).

The capacity of the bridge is verified for larger moisture content by the factor k_{mod}. The dimensional changes due to moisture change with resulting stresses are calculated below. According to the manufacturer, the moisture induced dimensional change ΔL is calculated as

$$\Delta L = \Delta\omega \cdot \alpha_H \cdot L \qquad 7.54$$

Where $\Delta\omega$ is the change of moisture content, α_H is the dimensional variation coefficient for each direction, provided by the manufacturer, and L is the dimensional length in the respective direction.

The total dimensional change in the transverse direction is the sum of the dimensional change of each panel. The resulting compression stresses due to dimensional change in transverse direction are taken by the compression steel tubes and tension bar. Change in vertical and lengthwise direction will lead to shear stresses in the connection between panel and steel element. Resulting stresses due to dimensional change are calculated for each direction respectively

$$\sigma = \mathrm{E} \cdot \varepsilon = \mathrm{E}\frac{\Delta L}{L} \qquad 7.55$$

The resulting dimensional change and corresponding stresses in the respective direction are listed below. As the moisture induced stresses are small related to stresses due to applied load, these are not considered in further detail design. The moisture induced stresses are presented in Table 7.25.

Table 7.25 Resulting dimensional change and stresses due to moisture change

Direction	**Length change** [mm]	**Stresses** [MPa]
Transverse	0.19	0.08
Vertical	0.15	0.03
Lengthwise	0.22	0.11

7.3.7 Floating structure

The floating pier is built up by transverse panel deck of solid timber and longitudinal IPE-beams with diagonal bracing. The beams are simply supported by pontoon elements with a spacing of 5 m, see Figure 7.22.

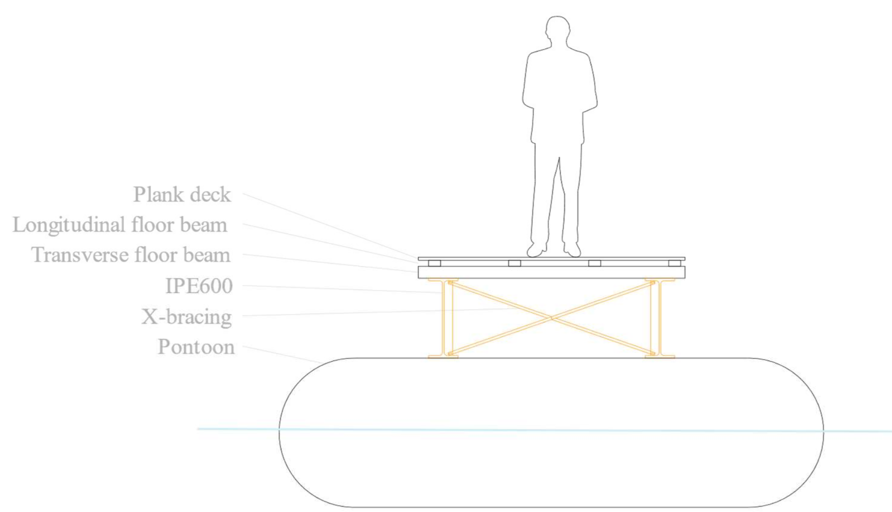

Figure 7.22 Cross-section of the floating platform structure.

The dimensions of the pontoons are governed by the load on the deck, which is the self-weight of the deck elements combined with pedestrian load. The principles of the partial factor method are not used to determine the design load as only an estimated dimension of the pontoons is searched for.

$$q_d = G_k + Q_{fk} \ [kN/m] \qquad 7.56$$

The total load on each pontoon is calculated accordingly, where C_m is the mean circumference of the deck and n is the number of pontoons:

$$q_{d.n} = q_d \frac{C_m}{n} \ [kN/m] \qquad 7.57$$

Archimedes principle of uplift force in water is used to determine the required volume of the pontoons, where the uplift force F_L must be equal to the total load on each pontoon:

$$F_L = V \cdot \rho \cdot g \ [kN] \qquad 7.58$$

The required dimension of one pontoon is 2 x 3.5 x 5 m (h x w x L).

7.4 Local design

7.4.1 Prestressed connections

The prestressing between the lamellas should be sufficient to compensate for the bending stresses due to transverse bending and prevent slip due to transverse shear. The required compression force is calculated for the Service Limit State.

A steel bar is threaded through the cross-section to enable pre-tensioning of the cross-section. Compression steel tubes secure the forced curvature of the LVL panels, and steel plates distribute the compression force to the panels.

Curvature force
The force required to create the sinusoidal shape is calculated as a point load on a continuous beam to the desired deflection. The load-situation can be translated into a simply supported beam with counteracting bending moments at the supports, as illustrated in Figure 7.23.

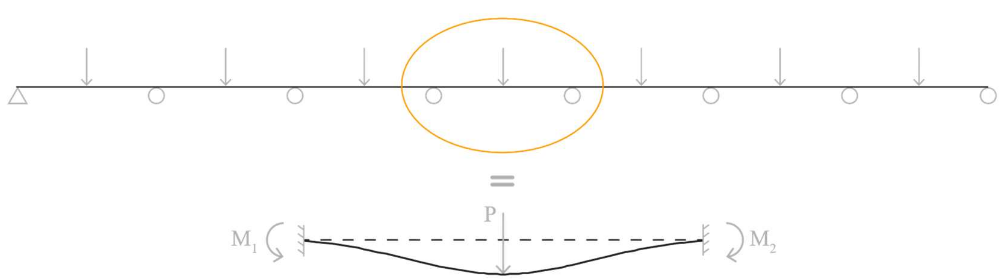

Figure 7.23 Load model of the curved panels.

To achieve a sinusoidal pattern, a certain deflection p is required and is defined in Chapter 7.3.1 about induced bending. The corresponding point load P to achieve this deflection can be solved from the equation for a fixed beam with midspan deflection *p* and bending moment M_1 and M_2

$$p = \frac{M_1 L^2}{16EI} + \frac{M_2 L^2}{16EI} + \frac{PL^3}{48EI} \ [mm] \qquad 7.59$$

The flexural rigidity *EI* is modulus of elasticity for flatwise bending times the modulus of elasticity of one LVL panel. The span length is equal to the frequency of the sinus-curves. The required compression on the LVL-panels must be larger than the required point load *P*.

Required compression on the pre-tensioned lamellas

The friction between the LVL panels must be larger than the transverse load effect. This is secured by a threaded prestress bar. Dywidag prestress bars are usually used in stress-laminated decks in Sweden. In this case, a threaded bar of diameter 26.5 mm is chosen (OIB, 2018).

The minimum prestressing force is the largest value of transverse bending stress or transverse shear stress on the bridge deck. This is illustrated in Figure 7.24 and stated in the following equation.

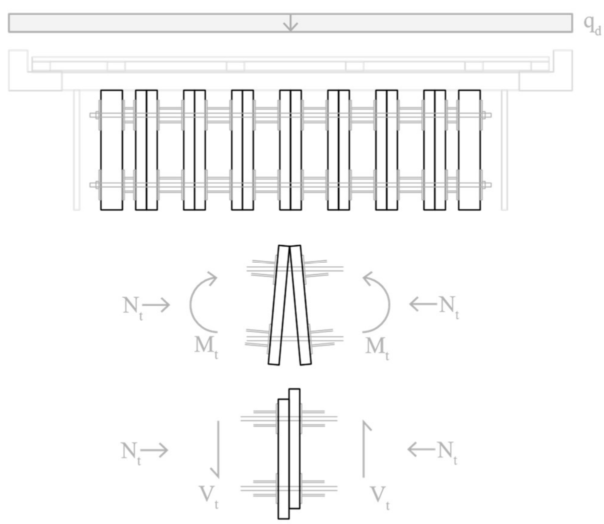

Figure 7.24 Minimum prestress force on the lamellas.

$$N_t = max\left(\frac{1.5V_t}{h \cdot \mu}, \frac{6M_t}{h^2}\right) \ [kN/m] \qquad 7.60$$

The transverse load effects due to uniformly distributed load across the deck, which is in this case is traffic load, are calculated as:

$$M_t = \frac{q_d L^2}{8} \ [kNm] \qquad 7.61$$

$$V_t = \frac{q_d L}{2} \ [kN] \qquad 7.62$$

For planed wood to planed wood, moisture content > 16% and load perpendicular to the grain, the friction coefficient μ is set to 0.40 according to table 6.1 in EC5-2. The area of the shear stress is taken as the effective area of the steel plate, where the forces are assumed to be distributed in a 45° angle from the edge of the plate. The bending stresses are calculated over the height over the panels times the effective width of the panels. In this case, the bending stresses are dimensioning for the required friction force. The corresponding compression force on the contact area between the LVL-panels are calculated as following, σ_c being the resulting bending stresses and w_{ef} times h_{ef} the effective height and width:

$$N_{c.panel} = \sigma_c \cdot w_{ef} \cdot h_{ef}\ [kN] \quad 7.63$$

The required tension force in the steel bars is calculated as:

$$N_{t.bar} = \sigma_c \cdot A_{bar}\ [kN] \quad 7.64$$

The spacing between the contact points in the bridge deck are not considered in these calculations, which therefore leaves a rather conservative result. If the holes for the bar is 20 percent less than the height of the lamellas, or if the hole size is less than 50 mm (EC5-2) the holes can be disregarded from capacity calculations. For the chosen dimension of prestress bar, these calculations can be disregarded.

Verifications

The corresponding compression stress from the steel bars must be larger than the required curvature point load P on the panels:

$$2N_t \geq P\ [kN] \quad 7.65$$

Furthermore, the LVL panels must have sufficient capacity to withstand the compression forces. The required compression stresses on the panels are distributed from the steel plates to the panels and are verified for the design compression capacity perpendicular to the grain, h being the height of the panels:

$$\sigma_c \frac{h_{ef}}{h} \leq f_{c.0.d}\ [MPa] \quad 7.66$$

The required tension force $N_{c.bar}$ must be smaller than the maximum initial stressing force of the bars, $P_{m.0.max}$. In addition, maximum allowed pretension of the bar is 70% of the ultimate tension capacity:

$$\frac{N_{c.bar}}{2} \leq P_{m0.max}\ [kN] \quad 7.67$$

$$N_{c.bar} \leq 0.7 f_u \cdot 2A_{bar}\ [MPa] \quad 7.68$$

Finally, the compression tubes must have sufficient capacity to withstand the compression forces. The compression tubes must be checked for buckling if the slenderness ratio λ is larger than 0.2. The minimum compression stresses distributed by the steel tubes is verified as:

$$\sigma_{c.tube} = \frac{N_{c.bar}}{2 \cdot A_{tube}} \; [MPa] \tag{7.69}$$

$$\sigma_{c.tube} \leq f_y \tag{7.70}$$

The required forces on the cross-section are summarised in Table 7.26, with resulting utilisation ratios of the compressed cross-section in Table 7.27.

Table 7.26 Required prestress forces

Force		**Value** [kN]
Point load for deflection	P	186
Compression force on the panels	N_t	880
Tension force in the steel rods	$N_{c.bar}$	6.3
Compression force in the steel tubes	$N_{c.tube}$	3.1

Table 7.27 Resulting utilisation ratios of the prestressed connection

Stresses	**Utilisation** [%]
Compression stress on the panel	16.8
Max initial tension in the prestress bar	1.0
Utilised tension capacity	0.54
Compression of the steel tubes	0.7

7.4.2 Lamella joints

As the superstructure is designed to be continuous, the LVL straight beams and the bent panels need to be joined into separate pieces before assembled to the whole superstructure. For the straight beams, slotted-in steel plates are used and located where the bending moment is as small as possible. For the total superstructure length 27.3 m joints are required, and the joint design is illustrated in Figure 7.25.

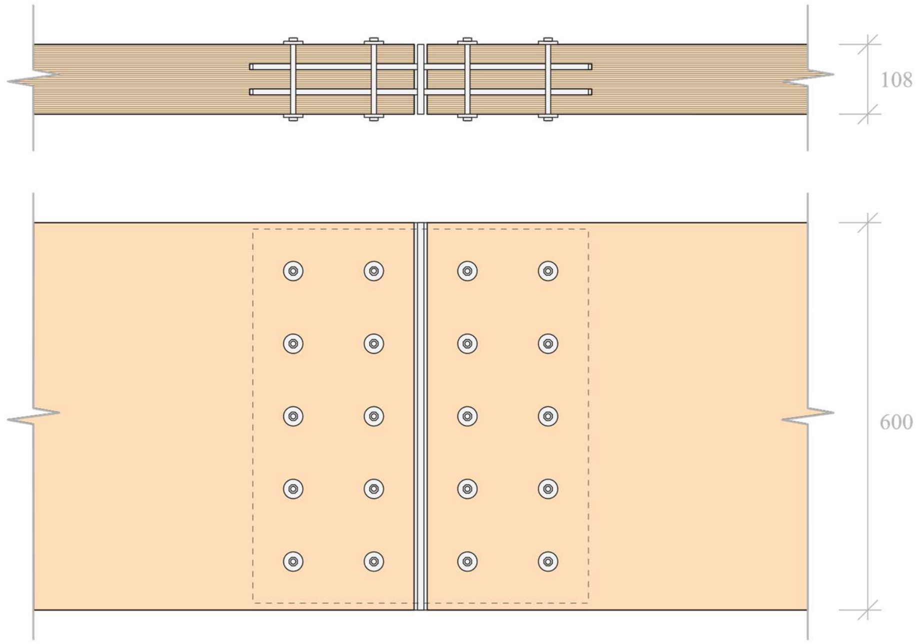

Figure 7.25   Detail of joint for the straight LVL beams.

For the bent panels, the same principle with slotted in steel is used, but here steel hooked plate strips are used instead to increase the shear friction between the elements. To assure that there is enough capacity for the bent panels the joint of two LVL panels is placed at the connection to another continuous panel, see Figure 7.26. Another steel hooked plate strip is inserted between the two panels to achieve even more friction between two bent panels. This extra shear friction results in less required prestressing force in the threaded bars.

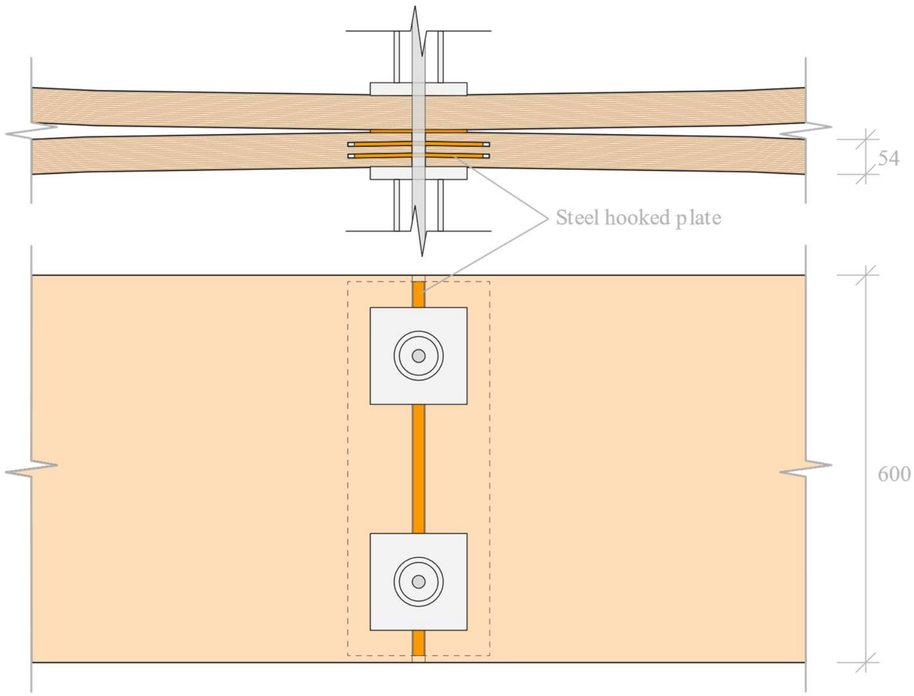

Figure 7.26 Detail of joint for the bent LVL panel as well as the connection to an adjacent panel.

To make sure that the superstructure does not have a local weakness, the joint of a bent panel is never at the same location as the joint of the adjacent panel. Consequently, the joints are phase shifted to distribute the weakness of a joint. Figure 7.27 shows in an illustrative way the phase shifting of the bent panel joints and the location of the joints of the straight beams.

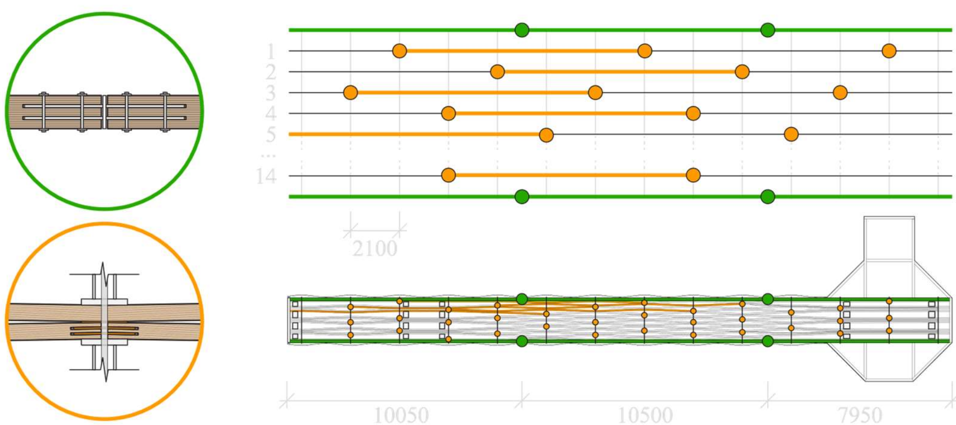

Figure 7.27 Phase shifted joints for the bent LVL panels as well as the joint locations for the straight LVL beams.

7.4.3 Column to superstructure connection

The support columns are connected to the inside of the LVL panels with the use of a steel cap and bolts. The steel cap is integrated in the superstructure during the assembly and connected to the columns when the structure is lifted into place. A detail of the connection is illustrated in Figure 7.28.

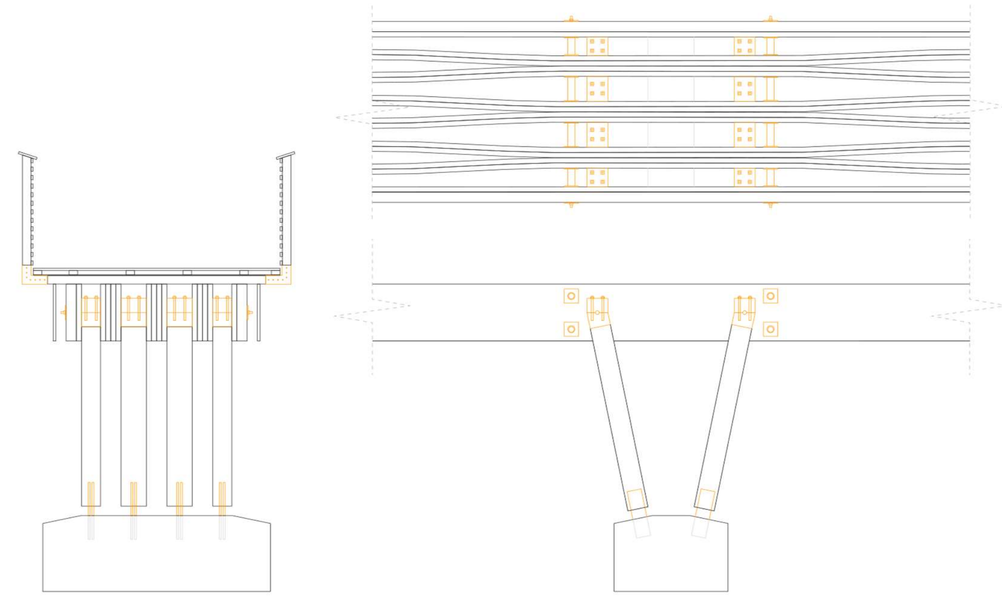

Figure 7.28 Connection between superstructure and support.

7.5 Production

To produce the bridge, prefabricated parts are transported to the site where they then are assembled on ground before lifted to their final positions. The schematical plan for the production on site is as following. First ground preparation is done before concrete foundations are casted on their locations. The two column supports on each side of the road are built, with temporary supporting scaffolding. Elements of the superstructure are preassembled into longer pieces before being bent and prestressed in the assembling of the continuous superstructure. This also applies for the straight staircase. The straight staircase is lifted to its position and attached to the platform support, providing horizontal support to the platform and bridge superstructure. Then the bridge superstructure is lifted by cranes onto the supports and connected to the pinned connections. After that, the curved steel stair is lifted to its position and connected to the cantilevering parts of the platform tower as well as supported from underneath. At last the railing and decking is built on top of the superstructure as well as the platform and stairs.

For the superstructure, prefabricated beams and panels shorter than 12 m are transported to the site. As a result, no specific allowance for transport must be applied for. On site the straight lamella beams and the bent lamella panels are joined into one long continuous piece. A schematic sketch of the joint positions is shown in Figure 7.27 as previously described.

The beams and panels are pre-drilled for better precision in addition to a simplified assembly process. One straight beam is used as a reference position with threaded bars put through. Thereafter each lamella panel is mounted one by one onto the threaded bars with distancing pieces in specific positions. Figure 7.29 shows the assembly method of the superstructure in a schematic way. When all panels and distances are at the right positions, prestressing of the threaded bars is done by fastening the nuts. This will reduce the distance between lamella panels, and the distancing pieces will prevent shrinking which creates bending of the lamella panels. The nuts are fastened until the gap between the panels is closed and the required prestressing force is achieved.

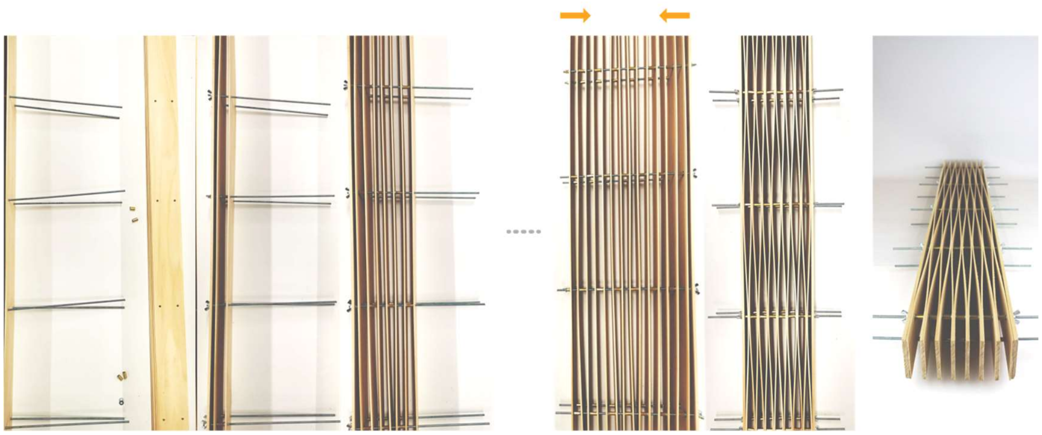

Figure 7.29 Schematic assembly method of the superstructure.

When executing the assembly method in a model in scale 1:10, it was found important to screw the nuts in the same pace along the whole superstructure to avoid that one end shrinks faster than the other end. An uneven tensioning caused deformation on some of the tension bars. The curved lamella panels are held together by friction created by the prestressing force in the threaded bars. Worth of noting is that a bent lamella with a radius of 14 m and a threaded bar centre-to-centre distance of 2.1 m the offset of drilled hole between the straight beam and the lamella is only 1.4 mm!

8 Discussion

The aim of the thesis can be summarised in the following two research questions: *"In what way can a bridge proposal be achieved that meets the requirements and ideas of the client Next Step Group for the planned residential area Wendelstrand?"* and *"In what way can an iterative design method be used to develop a structural concept that enhances both engineering solutions and architectural qualities?"*.

The challenge was to design a bridge that meets the ideas of Next Step Group, that corresponds with the profile of Wendelstrand and has a customised design for the actual site. The design proposals were developed according to a set of design criteria and evaluated for specified demands. The intention of integrating architectural qualities with engineering solutions was specified as a governing design criterion to secure a development of the design proposals within the specified framework of contextual criteria and requirements.

8.1 The proposed bridge

The bridge design answers to the request of the client Next Step Group on several levels. Firstly, the straight path establishes both the physical and visual connection from Wendelstrand to Landvettersjön. Secondly, the strong wood-profile is recognised through the materiality of the structural concept and is included in the detailing. An example is how the columns stretch up into the superstructure, where the wave-pattern is straightened out to provide enough space for the connection. Lastly, the bridge has additional qualities, rather than just being a connection between point A and B. The viewing platform enables pedestrians to pause and look out over Landvettersjön. In addition, the circular floating pier enables a variety of possible activities in the lake such as the possibility to swing, attach floating restaurants, sauna boats and add a canoe rental. This will be available for the public as well as residents in Wendelstrand. In addition, pedestrians can experience the bridge structure from underneath as both the stairs and accessible ramp are led underneath the platform structure. Attention for architectural qualities are reflected in the design choices regarding the visual expression of the bridge.

A challenge with the design proposal was to solve the connection between the viewing platform and the lake, which has a height difference of approximately 8 m. An idea was to lead the staircase out in the lake and connect it to the pier. Since only floating structures could be used in the water, it would be difficult to provide horizontal stability to the viewing platform without creating a large anchoring to the land. Therefore, the rational decision was to lead the staircase directly down on the shore strip. In that way, the shore protection is respected and permanent impact in the lake is limited.

The requirements from the Swedish Transport Administration are met in the final bridge design, in terms of clearance as well as general detailing and dimensioning of the bridge structure. However, only the main connection between the superstructure and columns are thoroughly designed, in addition to the connection between the bent LVL panels. As many connections are yet to be solved, the bridge design must be further investigated before construction is possible. For sustainability aspects, the structural height of the superstructure is strived for to be as small as possible, to reduce the amount of structural material. Further optimisation of reducing the amount of timber can be done in the rest of the bridge structure, for example in the viewing platform or staircase.

Moreover, a strong integration between architectural and engineering qualities are found in the bridge proposal, where the structural concept is a big part of the visual appearance. Curved beams in a sinusoidal pattern mimic the behaviour of a horizontal truss, which is determined by the geometry of the beams. Active bending and pre-tensioning of the deck provides required horizontal and vertical stiffness. Consequently, a characteristic visual appearance is assigned to the bridge structure.

8.2 The design process

No examination of different design methods was performed in the beginning of the thesis, but the chosen method was adapted without any further ado. The purpose of the iterative design method was to investigate, develop and evaluate to result in the most suitable bridge design for the current site. Relating to the stated research questions, the iterative process aimed to include expectations of the client combined with efficient engineering solutions and architectural qualities. A spatial investigation was concentrated on possible paths, affected by aspects concerning topography conditions and contextual requirements, in addition to the visual and conceptual relation to Wendelstrand. Structural concepts were then applied to these paths. An examination of how or if these structures affected the above-mentioned aspects was then iteratively performed. Furthermore, the possibilities of including other functions in the bridge design were investigated in relation to the structural concept and contextual limitations.

Qualities of the intentional concepts were combined and developed into more refined designs, which in turn were evaluated and compared to each other. To evaluate the different aspects separately and in relation to each other, and ensure a broad investigation of possible qualities, every contextual demand was, intentionally, not followed strictly in each phase. By doing so, the design task was looked at from different angles and a large and thorough variety in the design concepts were achieved. The different perspectives resulted in a conscious development of the final design proposal. Lastly, the final bridge proposal aimed to meet every defined contextual requirement, as well as fulfilling the intention of the design criteria.

Hand calculations were used to obtain the dimensioning forces and bending moments in the structure, which in turn determined the dimensions of the load-bearing parts. Accurate simplifications were used to determine the effect of active bending of the LVL panels. The bending was integrated in the calculations by applying initial deformations in combination with requirements for stressed skin panels. As a limitation, only the most important connections for the structural concept were calculated and designed. That is, the connection between the LVL panels and required friction force obtained from the prestress bar. Consequently, several details were not validated or optimised, but preliminary designed based on reference projects.

By building physical model an understanding of the consequences and possibilities of active bending of the LVL panels were achieved. It was a quick and easy way to understand how the built-in forces and stresses behave. There was no time for an extra literature study of active bending, so physical models were a great tool. The insight of achieving the same deformed shape by either longitudinally push the lamella together or by pressing it outwards using transversal spacers was useful when developing the design and the detailing of the lamellas. As a result, a feasible assembly method was developed and proven in scaled physical models. Time was spent on building physical models to verify the structural stability and assembly method. Consequently, less time was given to create a detailed FE-model to analyse the accurate structural response.

The general limitation of the thesis was determined with the chosen site, and the intention of designing a site-specific bridge for a real client. Clear boundary conditions and specific requirements were defined, which established a limitation for the bridge design. Following, as the scope concerned the conceptual design of the bridge structure, less time was given to design the floating pier structure in the lake. A suggestion for cross-section and load-bearing concept was given, in addition to a proposal for different activities on the pier.

8.3 Suggestions for future work

As a result of the limitations of the thesis, and the obtained answers to the research questions, new questions arose. The following listed topics would contribute to developing the final design proposal into a more feasible bridge design.

Torsional stability
Physical models proved that the bridge structure was likely to fail due to lack of torsional stability above other structural responses. As accurate simulations of the rotational capacity were excluded from the design verifications, this would be prioritised in further development of the design. If the torsional stability proved to be insufficient, it would be suggested to add another pair of prestressing bars adjacent to the existing ones. This would create a squared geometry, which would allow for an additional horizontal path for the helicoidal load transportation in lengthwise direction. Another solution would be to secure a stiffer connection between the superstructure and the transverse beams on the bridge deck, as well as adding cross-bracings underneath.

Active bending
Active bending in the bridge design needs further research. As the solution is based on understanding from physical experiments, a thorough literature study on the topic would be beneficial for the development of the bridge proposal. A simulation using Finite Element tools could also contribute for further development of the concept. This would allow for a quick comparison between actively bent beams with built-in stresses and pre-bent elements. As the geometry would still mimic a horizontal truss, could the same element dimensions be used, how would the vertical capacity be affected, and how would the required friction force from the prestress bar be affected? With the use of computer simulations, an investigation and optimisation of the relation between wave amplitude and frequency, number of elements and element dimensions could be performed. In addition to this, the torsional behaviour could be monitored for the solutions presented above. It would also be easier to obtain quick results when comparing the structural solution for different timber materials, or a combination of several.

In addition to this, a couple of interesting aspects concerning the combination of active bending, LVL and bridge structures is proposed for further research:

- Consequences of applying the method concerning material and connections. How are actively bent LVL beams affected and what are the long-term effects?
- What are the exact structural benefits, and do they exceed the complexity of assembly and construction?

Connections

The superstructure is designed as a continuous element. Consequently, the joints of the curved LVL panels must enable continuous behaviour. A design for these joints and their locations are proposed, but should ultimately be further investigated, optimised, and verified before being applied to a real bridge structure. It should also be mentioned that the thinness of the LVL panels may complicate such a solution, as the amount of effective material in the connection is small.

Floating structure and foundation elements

To achieve a complete bridge design proposal, the floating structure must be solved. Firstly, the design of the pontoons should be further developed to obtain a structure with small visual and physical impact on the lake. Different load cases resulting from the various activities proposed for the client must be considered. Secondly, as the floating structure is suggested to be anchored to the staircase abutment, this foundation element requires careful detailing. Following from this, a design solution for the bridge foundation elements is outside of the thesis scope, which should be prioritised in further development of this design proposal.

Horizontal stability

The global horizontal stability of the platform support was secured with the use of the staircase as a structural member. Future work should include further investigation into other solutions to the stability challenge, preferably with the aim of reducing the amount of structural material.

9 Conclusion

When designing and building a timber bridge many and various aspects must be considered. Common for all bridges, structural aspects must be included when developing the bridge design. The bridge is in turn defined by site-specific conditions, which in this case is Wendelstrand in Mölnlycke. Unique preconditions and limitations require unique solutions, which are developed through thorough investigations and identification of design possibilities. As a result, a site-specific bridge proposal can be developed to fulfil the identified contextual requirements.

The iterative design process generated a large variation of possible solutions and provided a wide perspective for the design proposals. It was a very useful tool to see the task from different perspectives and to move forward in the design process. Clearly stated boundary conditions and design requirements define the framework for the design development, and a direction for the evaluation of the proposals. Governing design factors, contextual requirements, and site limitations were prioritised in relation to the research question. This proved to be helpful when comparing different proposals or evaluating conflicting designs choices. Simultaneously, challenging the weight of the defined evaluation criteria proved to be necessary to broaden the perspective on possible solutions. As a result, the final design proposals were developed consciously, where every possible aspect was considered.

At last, the outcome of the whole thesis could be summarised in the following: A specific site implies unique preconditions and requires a unique solution.

10 References

Boverket. (2016). *Boverkets konstruktionsregler, EKS 10*. Boverket.

Boverket. (2019a). *Karta med snölastzoner*. https://www.boverket.se/sv/byggande/regler-for-byggande/om-boverkets-konstruktionsregler-eks/sa-har-anvander-du-eks/karta-med-snolastzoner/ Hämtad 2021-06-16

Boverket. (2019b). *Karta med vindlastzoner*. https://www.boverket.se/sv/byggande/regler-for-byggande/om-boverkets-konstruktionsregler-eks/sa-har-anvander-du-eks/karta-med-vindlastzoner/

Brandt, K. (2018). 96 metre long wooden bridge designed for the river. *Wood Magazine*, *3*. https://www.swedishwood.com/publications/wood-magazine/2018-3/s-shaped-bridge/

Burkhard, W. (2017). *02_Neckartenzlingen_012*. https://hochbau-fotografie.de/

Camathias SA. (2015a). *Staderas-7-1030x552*. https://www.camathias-sa.ch/referenzen/

Camathias SA. (2015b). *Staderas-8-1030x674*. https://www.camathias-sa.ch/referenzen/

Dodoo, A., Gustavsson, L., & Sathre, R. (2016). *Climate impacts of wood vs . non-wood buildings*. https://skr.se/tjanster/merfranskr/rapporterochskrifter/publikationer/climateimpactsofwoodvsnonwoodbuildings.28751.html

Ekwall, T. (2017). *Ein regionales Wahrzeichen Schweizer Ingenieurbaukunst | Espazium*. Espazium. https://www.espazium.ch/de/aktuelles/ein-regionales-wahrzeichen

Eurofins Expert Services Oy. (2020). *Product Certificate No. EUFI29-20000676-C/EN*. https://www.metsawood.com/global/Tools/MaterialArchive/MaterialArchive/Eurofins-certificate-Kerto-LVL-S-beam-Q-panel.pdf

Garfvé, J. (n.d.). *Kvalitetsbok Wendelstrand* (p. 68).

González, M. F. (n.d.). *Curved Girder Bridge Neckartenzlingen / Ingenieurbüro Miebach*. Retrieved March 18, 2021, from https://www.archdaily.com/894350/curved-girder-bridge-neckartenzlingen-ingenieurburo-miebach

Google maps. (2021). *Google maps statelite view of Mölnlycke, Gothenburg*. https://www.google.com/maps/@57.6692944,12.1473151,3573m/data=!3m1!1e3

Göteborgs Stad Trafikkontoret. (2017). *Lutningar - Gång- och cykelbana*. https://tekniskhandbok.goteborg.se/Arkiv/2017-1/__site/__planering__utformning__lutningar__gångochcykelbana.html

Guetg, M. (n.d.). *EINE BRÜCKE ALS VISITENKARTE*. Retrieved March 17, 2021, from http://www.cubatura.swiss/de/article/eine-bruecke-als-visitenkarte--76

Gustafsson, M., Lipkin, Y., & Bergkvist, P. (1996). *Träbroar*. Träinformation AB.

Härryda Kommun. (2019). *Samrådsredogörelse*. https://www.harryda.se/byggaboochmiljo/planarbete/detaljplaner/molnlycke/bostaderochverksamheteriwendelstrand.4.5c50ed73160e02f941a5b4.html

Härryda Kommun. (2020). *Planbeskrivning*. https://www.harryda.se/byggaboochmiljo/planarbete/detaljplaner/molnlycke/bostaderochverksamheteriwendelstrand.4.5c50ed73160e02f941a5b4.html

Holzindustrie, S. (n.d.). *Neckartenzlingen, DE*. Retrieved March 18, 2021, from https://www.schaffitzel.de/en/bridge-construction/references/343-neckartenzlingen-de

Ingenieurbüro Miebach. (2017). *neckartenzlingen-abschnitt-geschichtet02*. https://www.ib-miebach.de/en/

International Federation for Structural Concrete. (2013). Fib Model Code for Concrete Structures 2010. In *Wilhelm Ernst & Sohn* (pp. 191–194).

Krona, K.-M. (2019). *Krav Brobyggande* (Issue 3.0). https://trvdokument.trafikverket.se/

Makiol Wiederkehr. (2014a). *Fussgängersteg Geheidgraben*. http://www.holzbauing.ch/index.php?id=400

Makiol Wiederkehr. (2014b). *Konstruktiv mit Holz 1992-2018*. https://issuu.com/lignum/docs/mw2018

Miebach, I. (n.d.). *Wide Span Girder Bridge*. Retrieved March 18, 2021, from https://www.ib-miebach.de/en/projects/timber-bridges/girder-bridges-made-from-timber/curved-girder-bridge-neckartenzlingen-de493.html

Norconsult. (2018). *Geoteknik PM : Geotekniska förhållanden*. https://www.harryda.se/byggaboochmiljo/planarbete/detaljplaner/molnlycke/bostaderochverksamheteriwendelstrand.4.5c50ed73160e02f941a5b4.html

Oertli, H. (2018). *Tor ins Tal Surselva: Holzbau Schweiz*. First Magazine. https://www.holzbau-schweiz.ch/de/first/magazine-online/detail/magazin-artikel/tor-ins-tal-surselva/magazin-backlink/58/

OIB. (2018). *European Technical Assessment ETA-05/0123* (pp. 10–10). https://www.dywidag-systems.com/fileadmin/downloads/global/construction/approvals/en/dsi-dywidag-eta-05-0123-post-tensioning-system-using-bars-en.pdf

Pousette, A., & Fjellström, P.-A. (2004). *Broinspektion - träbroar*.

Proposition 2016/17:146 Ett klimatpolitiskt ramverk för Sverige, Pub. L. No. 2016/17:146, 2016/17:146 70 (2017). https://www.regeringen.se/rattsliga-dokument/proposition/2017/03/prop.-201617146/

Ronnebrant, R. (2020). *Bärighetsberäkning av broar TDOK 2013:0267* (Issue 7.0). https://trvdokument.trafikverket.se/

Sektorn för samhällsbyggnad. (2020). *Antagandehandling för detaljplan för Bråta 2:139 m.fl.* https://www.harryda.se/download/18.5482c6b117220add0ca30153/1589869056051/Planbeskrivning.pdf

Standardname. (2015). *Staderas Brücke*. Www.Camathias-Sa.Ch.

https://www.youtube.com/watch?v=4W845TKMWBg

Svenskt Trä. (n.d.). *Brotyper - översikt*. Retrieved February 17, 2021, from https://www.traguiden.se/planering/planera-ett-trabygge/trabroar/trabroar/brotyper/?previousState=1

Svenskt Trä. (2009). *Större bärverk av trä*. https://www.svenskttra.se/bygg-med-tra/byggande/olika-trakonstruktioner/storre-barverk-av-tra/

Swedish Wood. (2016). Design of Timber Structures v.1. In E. Borgström (Ed.), *IABSE reports = Rapports AIPC = IVBH Berichte* (2nd ed., Vol. 1). Swedish Forest Industries Federation. www.swedishwood.com

Trafikverket. (2021). Krav - VGU, Vägars och gators utformning. In *2021:001* (p. 369). Trafikverket. http://trafikverket.diva-portal.org/smash/get/diva2:1511818/FULLTEXT01.pdf

von Büren, C. (2016). *Über die Brücke und in die Natur*. Lignum. https://www.lignum.ch/auf_einen_klick/news/lignum_journal_holz_news_schweiz/news_detail/ueber-die-bruecke-und-in-die-natur/

Wendelstrand. (n.d.-a). *02-from-water-final-1300x1100*. https://www.wendelstrand.se/om-wendelstrand/

Wendelstrand. (n.d.-b). *Rendering-Lakehouse-1000x800*. https://www.wendelstrand.se/om-wendelstrand/

Wendelstrand. (2018). *STUDIE AV STRANDOMRÅDET* (p. 13).

Wickersheimer, D. J. (1976). The Vierendeel. *Journal of the Society of Architectural Historians*, *35*(1), 54–60. https://doi.org/10.2307/988971

Appendix

A. Bridge database

B. Calculations – Global dimensioning and Detailed design

APPENDIX A - Bridge database

DESCRIPTION	STRUCTURAL CONCEPT	VERTICAL LOAD	HORIZONTAL LOAD	POINT LOAD	ROTATIONAL STABILITY	FOUNDATION	PRINCIPLE CONNECTIONS	PRODUCTION	ASSEMBLY	MATERIAL	DURABILITY
Slab bridge											
Beam bridge											
Pedestrian Bridge Crossing the Neckar River Location: Neckartenzlingen, Germany Designer: Ingenieurbüro Miebach Engineer: Engineering office Blankenhorn, Gottlob Brodbeck GmbH & Co. KG Completed: 2017 Length: 96 m Width: 3 m	Main structure consisting of trepped block laminated glulam beams that follow a gentle S-shape. For an efficient utilization of material the cross-section is graded according to the stress usage.	Design load of 5 kN/m² Bending of beams to compression of pylons	Due to its S-shape, extra help against horisontal forces is gained. The horisontal force is taken by the glulam blocks as well as the transversal smaller beams.	Point load is transferred down to the foundation by bending in the beam.	The bridge gets rotational stability due to its S-shape	The bridge stands simply supported at two concrete columns in the middle. The ends are also considered pinned with rotational allowance.	Gerber hinge between beam parts. The beams have hinged connections at the support.	Local wood engineering firm manufactured the bridge components. The cantilever bridge timber parts was prefabricated and transported to the site in three parts. Prefabricated concrete slab with anti-slip surface	The continuous beam creates moment diagram with zero crossings in the main span, which are designed as so-called Gerber hinge. In this way the design achieves sensible transport dimensions and a simplified assembly.	Laminated glulam beam Railing including horizontal stainless steel wires and handrail of acetylated timber. Decking made of pre-cast concrete slabs with anti-slip surface.	The prefabricated concrete slabs has an overhang of 30 cm, which works as a roof for the structure. The glulam beams gradually angling 30 degrees in beneath the bridge helps to keep rain from reaching the structure itself. In addition, there are steel drainage channels fitted below the joints between the concrete slabs. As an extra precaution, the wood is also treated with a thin glaze to protect it against damp and air pollution. The cable railing is made from steel and stainless steel,
Bow River Pedestrian Bridge Location: Banff, Canada Designer: StructureCraft Engineer: Fast + Epp Completed: 2013 Length: 113 m Width: 4 m	The primary structural system is simple: Propped by drilled piers located just outside the normal river channel, 40m haunched glulam girders cantilever from either side to support a 34m suspended span. The bridge cross section comprises twinned sets of glulam girders stepped to follow the flow of forces, which range in depth from 2.6m at the piers to 0.9m at the suspended span. The 4m wide deck is made of pre-stressed solid timber panels, removable to provide access to the service pipes hidden below, and to allow for simple replacement, if required.	Uniformly load distribution transferred down to the foundation through bending.	Horisontal steel bracing handles horisontal load.	40-50 pedestrians would cause lateral "lock-in" and increase the resonant accelerations. Two mass-dampers placed under the deck (visually exposed) were tuned to address footstep and jogging excitation	The horizontal steel trussing provides both the diaphragm and support for the service pipes concealed just below the bridge deck. The bracing is configured such that only the timber chords are continuous, resulting in very little length expansion, one of the bonus features of wood.	Tension rods tie the propped cantilevers down to Rundlestone-faced concrete abutments at either end of the bridge. Control of vibration due to small width: two uniquely-tuned mass dampers were suspended beneath the bridge to reduce dynamic forces.	The central drop span sits on neoprene bearing pads on notches in the receiving ends of the cantilevered glulam girders. The neoprene pads transfer the compression across the halving joint. Long timber screws either side of the connection reinforce the joint to prevent splitting perpendicular to grain, and a steel drag strap atop the beams connect them and transfer axial loads.	3 segments: two haunch glulam girders on either side and a removable, modular timber deck (allowing for ease of replacement and access to the service pipes running beneath)	Extensive prefabrication allowed the pices to be shipped to site and assembled on the shoreline. All cutting, drilling, sanding and finishing was performed indoors under controlled conditions so that members were protected from the elements both in transit and on site. Jigs were built to ensure accurate assembly of the main bridge components in the field. Erected in three lifts over two days.	Glulam girder and timber deck, horisontal steel truss, concrete foundation. A visually minimal stainless cable guardrail system involving 135m long continuous cables, required fine-tuned pretension analysis to ensure adequate tension in the summer, and avoid overtension in the winter.	75 year design life

Stuttgart Wooden Bridge Location: Remstal, Germany Designer: Knippers Helbig + Cheret Bozic Engineer: - Completed: 2019 Length: 30 m Width: 3.2 m	This family of mass timber bridges are the world's first integral wooden bridges and have therefore no joints and bearings. The bridge superstructure, a block-glued laminated spruce timber beam is connected rigidly to the reinforced concrete abutments. The stepped, laminated timber beam is formed corresponding to the moment force diagram.	Load is carried through bending moment, cross-section also varies in line with the moment distribution.	The load is transferred in shear by the stiff cross-section of the girder. It seems that there are transversal steel bars for the hand rails which could aslo contribute to the horisontal capacity. Use shear locks at the abutments? Looks like so.	Extra thick in mid span (at largest bending moment) due to point load?	The rigid intregral joint provides rotational stability due to the extensive distribution of the long rebars.	Reinforced concrete abutments which takes up the shape from the girder. The rebars frin the girder is casted to the abutments.	The superstructure is monolithically integrated into the reinforced concrete abutmends. There is no expansion joint at the transition to the abutment.	The block glued laminated timber beam is connected into one big piece. Then 78 rebars with a length of 2.3-3m were pressed into the girder. 1.2 m of the rebars are glued in the girder. After rebar connection, and installation of sensors, it is transported to construction site.	The girder is lifted to its final location. Very important that there is the exact right angle and location at the abutments since the concrete is going to be casted on site and that there should be a tight connection.	Spruce block-glued laminated timber beam. Decking of 8 cm thick precast carbon fiber reinforcement concrete.	The superstructure is protected against direct weathering by the bridge deck and a diffusion barrier cover on top of the timber deck. Sensors for permanent moisture monitoring are installed in the solid wood structure at relevant points. The end faces of the girder is protected with a special end-grain seal to permanently revent poisture from beign transported over the end-grain surfaces into the girder. "The carbon fiber reinforcement is extremely durable, which promises a significantly longer life span compared to conventional solutions of the highly stressed bridge deck."
Castle Moat Bridge Location: Darmstadt, Germany Designer: TU Darmstadt, FB Architektur und FB Statik Engineer: Fast + Epp Completed: 2007 Length: 26 m Width: 4 m	The world's first composite bridge made of wood and plexiglas. It is a temporary model structure for research purposes. Composite-beam bridge. To maintain the cultural and historical apsects of the castle surrounding, the bridge stands on two supports in the moat and is cantilevering the last part to the pavement.	The plexiglas-wood structure on each side of the walkway functions as beams where the lower timber handles tension and compression in the upper one, while the plexiglas transfers shear.	Steel frames in the bottom distributes the horisontal forces.	Point loads from pedestrians are led directly through the steel frame to the two composite girders as well as it also is distributed longitudinally by the steel frames.	The high composite girders provides rotational stability due to shear. The bridge is 4m wide and the supports are placed as wide as possible. This gives better rotational stability than if the composite-beams would be as narrow as the walkway. Due to the cantilevering at both ends of the bridge, the span shortens which also increase rotational stability.	The forces goes down to vertically into the ground, through two I-beams and then into concrete foundations at each end. No horisontal force goes into the wall to protect the castle's historical aspect.	The PMMA is mounted with several bolts(?) to the upper and lower glulam girders. The composite structure is fastened to I-beams over both supports.	The whole superstructure is prefabricated in one piece.	First the foundation is casted on site. The bridge is then transported to the site in one piece, and lifted to its final position.	Glued laminated timber Thermoplastic PMMA Steel covering as well as steel frame	The wooden parts are protected with steel sheets that cantilevers over the beams. The bolt/screw holes are covered as well. The PMMA is completely recycable and could be dismantled into smaller parts and used again in other projects when the research phase is finished.
Aurland Lookout, Aurland, Norway Location: Aurland, Norway Designer: Saunders arkitektur, Wilhelmsen arkitektur Engineer: Node Rådgivende Ingeniører AS Completed: 2005 Length: 30 m Width: 4 m	Bending. Load bearing steel frames of rectangular section covered with pressurised pine wood.	Vertical support of the deck in inclined steel "legs", connected to the lower foundation element on the mountain side. Tension in the curve of the ramp	Horisontal stiffness of the bridge is provided by the upper foundation.	Point load is transferred to the edge beams through the transversal framework, to the foundation elements.	Rotational/lateral stability in the bridge deck is provided by transversal steel framework in the deck	Two concrete foundations; upper foundation deals with horisontal wind forces (shaped as a lying U, fastened to the rock with tension bolds. Lower foundation supports the two steel legs, bolted to the mountain-side. Cross-section of the steel legs: 0.3x0.5 m	Wooden joints on the side of the rail: semi-circle joints (invisible from a distance)	Prefabricated and customised steel beams (walkway). Prefabricated and bent massive wood panels ("railing")	Cast-in-situ foundation. Framework and on-site assembly of the deck (crane). Steel beams lifted on place by cranes, framework welded on site. Covered with wood panels and massive wood.	Load bearing galvanised steel, covered with pressure treated pine. Two parallell frames with a rectangular section; 0.3m wide, 1.1m high cross section. Floor: steel trusses with c-c 1 m covered with 0.65 m massive wood, connected with screws from the underside of the steel frame.	Pressure treated pine makes the wood more rot resistance (needs continuous maintenance to avoid degradation). Will show signs of weathering over time.
Fussgängersteg Gheidgraben Location: Gheidgraben, Schweiz Designer: Werk1 Architekten und Planer AG Engineer: Makiol Wiederkehr AG Completed: 2013 Length: 7.45 m Width: 1.97 m	Simple supported beam bridge.	The pavement beam (also wavy) takes care of the vertical load.	Threaded rods in a grid of 600mm handles the horisontal forces.	A point load is firstly distributed transversally through the rods to the two outer beams, and secondly longitudinally through the wavy beam elements.	The hand rails also gives stability for bending in longitudinal way. Relatively short span and wide bridge, so that helps with the rotational stability.	Concrete foundation. There are elongated holes at one of the support, to allow shrinkage and swelling. LNP 120x120x10mm steel profiles over the supports.	Two threaded rods in the walkway wavy beam elements. The boards are spread apart or pulled together with washers and nuts as well as sleeves.	The bridge was prefabricated.	After prefabrication, the bridge was lifted to its position.	The decking, railing and handrail consists of massive rough-sawn oak boards. Steel threaded rods.	Due to the wavy shape, water can fall off the structure, and it can be dried. The intention is to let the bridge have a aged appearance with rust and wather torn wood.

The Claude Bernard Overpass Location: Paris, France Designer: DVVD Engineer: DVVD Completed: 2015 Length: 100 m Width: -	Continuous arch with metal framework. The three steel tubes in an arch shape are connected by the metal framework. Rest areas and viewpoints in the middle. In order to reduce the height of the structure and its impact upon the landscape, and in the interests of a more subtle outline, the load-bearing structure has been conceived as two variable-inertia three-dimensional arches. This solution enhances the inertia of the structural beams and reduces weight.	Consists of three variable dimensional arches. Allows for larger intertia but lesser weight of the structure; allowing the structure to be lifted by crane, as well as lowering the height of the arch.	Horisontal steel beams (with bracing) provides horisontal stability.	The load is transferred transversally to the steel frames with the help of the transversal steel beams. When the load reach one steel frame it can be transferred to the foundation through one of three longitudinal steel beams.	The bridge is curved, which provides rotational stiffnes. The perpendicular ramp also can provide rotational stability (depending on connection with the bridge)	Branch-like steel columns. Probably concrete foundation below.	Bolted connection between the lifted steel truss and the rest of the structure. The wooden parts works more like cladding.	Pile-mounted abundments and stairways. Prefabricated timber arch including cladding and deck.	Foundations and connecting stairs assembled, thereafter the prefabricated deck was lifted into place and connected to the supports in one night. Counterweights was used to increase the load-bearing capacity of the crane during assembly	Three steel tube "arches" connected by metal framework, covered by timber cladding. Timber fretwork on each side of the deck that acts as protective railing.	The two steel arches are protected by wood cladding, to prevent damage. The wood can easily be replaced. Water can easily run through the gaps between the wood. It seems a bit difficult to maintain the steel structure. Maybe it is possible to remove larger segments of the wood cladding?
Yusuhara Wooden Bridge Museum Location: Takaoka-Gun, Japan Designer: Kengo Kuma and Associates Engineer: Kengo Kuma and Associates Completed: 2012 Length: 47 m Width: 8 m	A 4.4 m wide bridge girder consisting of 11 cypress japanese laminated lumber by 180x700mm, are resting on a center pier by traditional Japanese and Chinese cantilever structure. "The overall structure is created utilizing the overlapping wood member system called 'Tokiyo' used in traditional Japanese temple architecture, creating a presence (materiality) and abstractness which should be called 'wood masonry' that cannot be obtained with a framework type of structure.	The load is transferred through steel frameworks on the sides and through the 'Tokio' structure down to the mid pillar.	The yellow marked girder is able to take the horisontal forces.	A point load is transferred through the overlapping and decreasing grid. The beams are taking the point load by bending, through compression to the next layer, bending, compression and then finnally down to the column.	The homogenuous girder (marked in yellow in picture for horisontal load distribution) also helps with the rotational stability as well as the "moment stiff" column connection at the ground. The central column is crossed shaped and has a large cross shaped foundation, to prevent so it starts to rotate.	Steel frames and steel RHS in mid column leads the forces down to concrete foundations.	There are cut-outs in the beams to make perfect fit and give stability. But on some places the beams are also connected by screws.	The cedar pieces are locally produced, and they are assembled on site. The girder might come in larger pieces.	The foundation is casted and steel frames constructed. From the center pillar (with steel core) the cantilevering 'Tokiyo' system is built up with a temporary framework. The framework is removed when the 'Tokiyo' and girder is connected to the other two steel frames.	Local Japanese laminated red cedar.	The strucutre is protected by the upper roof as well as the form of the structure narrows down the closer to the column it gets.
Strut frame bridge											
Frame bridge											
King post truss bridge											
Krúsrak bridge Location: Sneek, Netherlands Designer: OAK Architects Engineer: Lüning Completed: 2010 Length: 32 m Width: 12 m	Truss arch bridge. The two wooden trusses are linked together in the middle for stability. Optimising of the cross-section for traffic resulted in the curved shape and triangular framework. Height (clearance): 4.6 m	Distributed in the curved truss elements, through the vertcal deck to the concrete foundations	Transversal horisontal steel beams in deck transfer load to the outer longitudinal wooden beams.	Can support the heaviest load class of 60 tons. Lifts point load and transfer through truss. As well as directly through the bottom beam.	Steel ties in the upper part helps with the rotational stability.	Concrete pylons	Block-glued laminated timber from accoya	Completely prefabricated	Transported to site in one piece and lifted to its place	Accoya wood: acetylated softwood (locally produced in Arnhem). Road-surface of steel (the original design intension of wooden deck required a thickness of 2m)	Due to chemical treatment the bridge can withstand insects, fungi and weather. Life expactancy 80 yeards
King post truss bridge with struts											
Erdberger Footbridge in Vienna Location: Vienna, Austria Designer: Arch. Johannes Zeininger Engineer: Ingenieurbüro Alfred Pauser, Ziviltechnikergesellschaft für Bauwesen Completed: 2003 Length: 85.2 m Width: 3.7 m	Strutted frame and suspension structure. Two main girders in glulam (0.36 m width, cc 3.34m). Span lengths: 14.8m - 52.8m - 14.8m. Top point 6m above deck. Inclination: 6%	Bending in bridge deck. Load is transferred either to the tension cable and then down in compression through the tilted legs, or directly to a tilted leg and then down to foundation.	Bracing in the legs, takes horisontal load.	A point load in mid of the bridge is ransferred through bridge deck, through the tension cable up to the diagonal legs and then down to the foundation. More at the sides, the load goes through bending in the bridge deck, and then down by compression in the tilting legs or directly to the foundation.	Cross bracing on top to give horisontal and rotational stability.	Concrete foundation surface meets legs perpendicular.	The foundation is considered pinned. The connection between leg and bridge deck consists of steel plates through the leg and then bolts holding the wood and steel together.	Prefabricated and preassembled sections (legs)	In-situ casted concrete foundations + four pairs of supports with wind bracing. Thereafter the two prefabricated and preassembled sections (approx 45 m long) lifted into place and connected to the supports. Wind bracing above the deck installed before the middle, suspended section is lifted into place.	Main structure: glulam of domestic larch. Deck: plywood boards + 6 cm blacktop. Foundations: in-situ concrete. Steel secondary beams (galvanised), suspensions, railings and masts	A steel plate is covering the end cut (and thus fiber opening) for where the inclined legs meets the bridge deck. There is also a wider plate on the legs, making the water run off and away from structure. Bridge deck is a bit (maybe too small) cantilevering out over the structure to prevent water from rinning down the superstructure.

Arch bridge

Pedestrian Bridge in Zapallar Location: Zapallar, Chile Designer: Enrique Browne Engineer: Alfonso Larrain Completed: 2008 Length: 20 m Width: 2 m	It has the shaped section of a boat, but corresponds to a triangular inverted arch, which is longitudinally curved, which reduces distortion and enhances the structure. Main structure consists of a curved beam in the bottom. Secondary structure is two parrallel beams to the main structure located as the two vertices of an upside down triangle. The beams are joined as a frame with the boardwalk and the hand rail skeleton.	Main structure in bottom of bridge handles the bending moment.	Transverse beams in upper part of the superstructure provides horisontal stability.	The frame connecting the three beams helps to distribute point loads as well as meeting the required deflection criterias.	The curvature of the bridge together with the frame of the three beams provides rotational stability.	Concrete foundations dug deep into the clay on both sides of the road.	Bolts into metal sheets	Prefabrication of the superstructure in Santiago.	The superstructure is lifted to its final position. After that electrical equipment, and pathway and railings are added. As well as a safetynet to prevent people from throwing rocks on the cars.	Glulam beams, galvanized metal net	There is a small gap between the lower beam and the covering "råspont" to let it dry out. But other than that, no documented durability methods.
Kintai Bridge Location: Iwakuni, Japan Designer: Kikkawa Hiroie Engineer: Kikkawa Hiroie Completed: 1673 (2004) Length: 175 m Width: 5 m	Wooden arch bridge. Five spans (three arch spans, two girder birdge spans), four stone piers and two wooden piers (at endspan, on dry riverbed). The wooden deck was placed "floating" on top of the frame using mortise and tenon joints, which allowed the rising flood water to lift up the pathway and carry it off down stream while the main structure would be spared. Rebuilt locally. Three midspans: 35.1 m, endspans 34.8 m	Vertical load is transferred through the arches to the foundation elements. The girder bridge at the bridge ends work mainly in bending, and has a shorter span between the vertical supports than the arches. The timber supports at the dry riverbed are diagonally braced	The structural weight of the bridge provides horisontal stability when subjected to floods. The width of the supports provides horisontal stability.	Point loads are distributed in the grid of timber elements and transferred through the logitudinal elements of the walkway to the foundation elements.	The timber walkway consists of layers of crossed wood elements, which provides rotational stiffness to the bridge. The structural height of the arch varies accross the length (thicker at the supports, thinner in the top), making the arches as material efficient as possible.	Original stone piers was later changed to concrete foundations. On dry riverbed, the bridge is supported by braced timber columns.	The bridge was initially constructed without the use of nails (the numerous small pieces was fitted carefully together), but copper sheets were laid over the main wooden parts after construction (for protection and additional stiffness to the connection).	In the later eras of rebuilding, standard rulers were used in combination with drawings which simplified the rebuilding significantly.	-	-	-
Fussgängerbrücke im Wildpark Langenberg Location: Langnau am Albis, Schweiz Designer: Makiol Wiederkehr AG Engineer: Makiol Wiederkehr AG Completed: 2009 Length: 78 m Width: 2.6 m	Arch bridge. Two three-hinged arches made of glued laminated timber in the main structure. Arches in compression and walking area as a tension band. Arch span: 44m	This walking area is designed as a tension band and connected to the cross member in the middle of the arch.	A steel cross-bracing is used between the arches.	A point load is transferred to the arch beams through the cross bracing as well as rectangular steel profiles in the middle of the arch.	The cross bracing and the two arches gives rotational stability.	Reinforced concrete foundations where the arch meets ground as well at the two ends of the bridge. The foundation meets the arches perpendicular to the compression forces.	The arch bridge is formed from the primary structural parts of the two three-hinged arches with cross-sections of 240 x 1080-940 mm as well as the two strut rows with cross-sections of 360x120-160mm and 280x120-140mm, each consisting of glued laminated timber in spruce / fir. Ribbed panels made of laminated veneer lumber with a thickness of 69mm and ribs in glued laminated timber with a cross-section in the ramp area of 120x640mm and in the bridge center area of 120x320mm run over the steel crossbeam in the longitudinal direction.	The arches, the middle fields of the carriageway, the railing and the stiffening crosses were assembled in the factory and delivered to the construction site in five large elements.	The bridge was transported to the site in five large parts, which were assembled in one night while Albisstrasse was closed to traffic. This was followed by the final assembly of the railing, which then also served as fall protection for all subsequent work.	Main structure: glued laminated timber in spruce / fir. Pavement: stone mastic asphalt (Gussasphalt) with fine grit scattering to prevent slipping when wet Railing: untreated larch.	The pavement is sealed watertight at the sides with T-steel prifiles which protects the main structure from weather. Drainage pipes along the longitudinal slope, and then led away from the structure at the foundations. The handrail battens are screwed in from the outside so they can be easily replaced.

Kingsway Pedestrian Bridge Location: Burnaby, BC, US Designer: Busby Perkins + Will Engineer: Fast + Epp Completed: 2008 Length: 44 m Width: 3 m	Arch bridge, cable stayed deck. Simple arch with post-tensioned concrete walkway ssupended on steel tension rods. The arch is tied to the walkway itself to resist the outward forces and avoid large and costly buttresses.	The post-tensioned walkway is suspended from the arch, which distributes the load to the foundation at the edges. Uniform stress distribution in the timber elements was provided by using plocking pieces to transfer load form the edge of he arch to the more interior wood members. Projected HSS beams from the glulam arches are connected to steel rods, which support the concrete walkway. These sections, together with the internal wood blocking between the glulam beams, transfer some of the vertical loads away from the outermost arches.	As the arch is tied to the post-tensioned walkway, the outward, horisontal forces in the longitudinal direction is minimised. The pinched shape (provided by tension rods in the top) provies horisontal (transverse) stability at the edges. The glass guards connected to the steel rods result in large horisontal wind forces imparted to the tension rods, which required detailed analysis.	Point load is transferred to the edge of the walkway, through the tension rods and down through the arch to the edges of the bridge.	Tension cables on each side of the arch/walkway provies lateral stability, as well as lateral stiffening between the continuous arch elements. The bi-axial curve of the arch (wider at the edges, thinner in the middle) provies horisontal/rotational stability at the edges.	Large buttresses was intentionally avoided (due to econony) by tying the arch to the walkway. The foundation elements only take vertical loads from the bridge.	The joints and details were carefully analysed as such hybrid wood-steel arch has not been done before. Consideration: construction tolerance, difference in shrinkage, uniform stress distribution, etc. The steel haunch-to-concrete platform connection includes a sliding connection to avoid large thrust forces on the souuth concrete structure.	Six thin glulam beams (30 m long, 150 mm thick) was bi-axially curved and anchored at both edges by a steel haunch. The two outer beams (which are required to bend the furthest) was thinner (75 mm thick, 600 mm deep). The individual beams are connected and forms a double curved solid arch. Also called a timber drop-in span	The glulam arches was prefabricated in a parking ot adjacent to the site. The entire timber arch + steel roof cover was prefabricated close to the site and lifted into place using two cranes. The road was closed for only a day. The glulam elements were post-tensioned on-site using steel rods glued into the cross holes.	Timber arch, post-tensioned concrete deck, steel tension rods and steel roof cover. Glass guards connected to the tension rods (2.4 m tall)	Precasted concrete planks was chosen instead of steel plate with concrete fill, to minimise long-term maintenance. The mass of the concrete deck also mitigate vibrations.
Richmond Olympic Oval Location: Richmond, Canada Designer: Cannon Design Engineer: Fast + Epp, StructureCraft Completed: 2008 Length: 3-12.8 m Width: -	Depth of one truss: 660 mm The roof panels connect and stabilise the primary arches, which span about 100 m accross the building. 500 panel units (one unit=3 truss arches), 55 unique panels forms The transversal roof panels consist of bent and post-tensioned V-shaped timber truss arches composed of small wood elements. The main arches are composed of timber and steel, which due to the low height works as a hybrid of beam and arch (both bending and shear).	Vertical load (self weight of the roof) is distributed in the truss arches to the main timber arches on each side, and down to the foundation. The outward forces of the panels was minmised due to the tension rod tying the trusses together.	The traingular arches was hydraulically bent and tensioned with a steel rod. The end plates of the arches transfer the compression in the timber arch into tension in the tie rods.	A point load on the roof will be distributed among the three trusses of each panel (that works rigidly due to the continuous, stressed, plywood skin), down to the main arches and further to the foundation.	CNC'd lywood bulkheads hold the V-shape in place, providing rotational stability of each truss (the black sheet is a part of the fire safety and acoustic installment)	The internal tension rod of the panels are bolted to the top of the main arches in six connection points (three on each side). The foundation elements of the main arches are concrete buttresses. The triangular shape of the buttresses provides both longitudinal (outward forces) and transverse stability to the structure, where the height and selfweight of the buttresses provides the necessary vertical stability.	Every second 2x4 "strand" in the cross-section is continuous, connected with clip angles to the neighbouring strand. Additionally screwed connections.	The panels were designed parametrically, where dimensions a structral design of each unit optimised for the unique position in the global model. Several rules embedded in the vode frove the geometric layout of the openings and splice lodations (important for the acoustic performance of the panels). One panel unit consist of three trusses. The unit was post-tension and anchored by steel tension rods.	After the main arches and temporary bracing was erected, the roof panels were lifted in place and bolted to the main arches (6 connection points). Thereafter the continuous plywoodlayer was stiched to the panels. Since the panels were optimised and controlled parametrically in the digital model, the manual re-work was minimised.	Timber V-shaped roof panels made out of small pieces of pine. Covered with stressed-skin plywood creating a rigid panel. Hybrid main arch of glulam and steel. Steel tension rods, concrete buttresses.	The roof timber trusses are made out of lumber from forests killded by the mointain pine beetle. The project is said to have stored over 2500 tonnes of carbon by utilising these trees. The structure itself is protected by a continuous sheet of plywood, which again is covered by a thin metal sheet.
Underspanned bridge											
Langlaufbrücke Samedan Location: Samedan, Switzerland Designer: - Engineer: - Completed: 2005 Length: - Width: -	Compression arch with a tension cable, which gives "two extra supports" in the middle.	Compression in the arch and struts, and tension in tension cable	The pathway consisting of transversal beams (into a "slab"), leads the horisontal forces through shear to the supports.	Point load is led transversally to the two compression arches and then down to foundation.	Pretension gives rotational stability.	Concrete foundation	Steel parts distribute high compression forces at timber connections. The V-connection has a cover sheet to prevent water to weaken the structure.	The bridge is prefabricated in parts and then transported to the site.	The compression beams are lifted to their position, then the bridge deck is mounted. Lastly the railing is applied.	Superstructure: Gluelaminated timber with steel tension band.	The walkway has wear and tear planks, which can be replaced. As well as extra planks for vehicle tires. The superstructure is protected with help of that the bridge deck cantilevers out on both sides.

Pedestrian and Cycle Bridges Over the Gave d'Aspe and Gave d'Ossau Location: Oloron, France Designer: RFR Engineer: Ingenieurbüro Miebach Completed: 2009 Length: 50 m Width: 2.5 m	Timber-steel framework construction. a bottom chord in steel and a top chord of several glulam beams placed together. The glulam beams are attached to the steel cross beams. This network enables a low superstructure height with a large span of 48 meters. Due to the combination of timber and steel the bridge is very light and slender.	Tension member 350mm wide steel plate with varying thickness between 20 to 60mm according to the bending moment and thus axial force distribution. The struts join the cross-beams next to their ends and therefore transfer higher axial loads to the timber beams situated at the outer edges of the deck. The stiffer the cross-beams in horizontal direction the more even the load distribution between timber beams. The geometry of the cross-beams was therefore optimized for their horizontal inertia, to minimize their visual appearance and take advantage of the reduced total structural depth.	In the level of the glue laminated beams there is an additional round steel diagonal brace to carry the wind loads.	Top glulam chord distributes the point load down to the steel truss system. Tension in bottom steel plates, down to foundation.	The diagonals in the truss helps with the rotational stability.	The concrete abutment piers are dressed with stones from the torrents. The last two cross-beams are reinforced to carry the neoprene and steel bridge bearings that transfer the reaction loads to the abutments.	Extra bracing system for horizontal wind forces. Prestressed 30 mm diameter steel rods. Elimination of overstressed joint design by adding stiffening plates.	Superstructure prefabricated in two halves. Lower steel tension member welded on site. Decking was placed in situ after the bridge was on site.	The two superstructure parts was transported to site and then spliced together. Steel tension member welded on site (post-tensioning), before lifted to it's final position by crane. Finally decking was placed in situ due to lack of lifting capacity from cranes.	The glulam beams are made of laminated Douglas wood, which are on the upper side protected with rhepanol foil. The planks of oak timber are fluted to ensure adequate resistance for walkers. The oak decking forms the wear surface for pedestrians and cyclists. It can be easily replaced in time, along with the waterproof membrane. Each decking plank re-ceived two of anti-sliding strips, made of an epoxy resin and sand filled groove.	Douglas fir, a species that is naturally resistant to biological attacks (class 3, as per EN 355). The deck beam structure are protected by the decking. Rephanol waterproofing foil, sandwiched between the longitudinal beams and decking gives further protection against moisture.
Truss bridge											
Punt Staderas Location: Laax, Switzerland Designer: Walter Bieler AG Engineer: Walter Bieler AG, Stephan Berni Completed: 2015 Length: 115 m Width: 2.5 m	Rigid frame bridge. The brigde girder is designed as a beam grating, which acts as a Vierendeel girder in the longitudinal direction. The grating consists of two vertical layers of four longitudinal beams each, and an intermediate layer with horisontal cross beams every 1.05 m. The layered structure enables a static height of 0.64 m. Bicycle and pedestrian bridge. Different length of the nine spans. Slope: 6% (accessible)	Vertical load is distributed in the layered grating and to the bottom longitudinal beams (through distribution of bending forces), to the support elements. A Vierendeel girder is characterised by the rectangular frame (compared to triangular truss frames). Moment joints are used to resist substantial bending forces. Enables a larger span than a trangular truss structure but has a more complicated distribution of stresses.	The width of the support elements provies horisontal stability in the transverse direction of the bridge, while the fanned shape of the of the supports stabilises in the longitudinal direction.	Point loads are transferred through the layered grating to the bottom longitudinal beams, to the supports/foundation.	The structural height of the deck grider adds to the rotational stability of the deck, as well as the intermediate layer of transverse elements. The Vierendeel truss stiffenes the bridge.	Piers: 3x6 rows of inclined beams that creates a fan-shape. At the ends, the bridge stands on reinforced concrete abutments	Shear tests verified the load-bearing capacity and rigidity of the bolded connections between the side and cross-members.	Locally produced wood elements of the same dimension, except the longitudinal glulam beams in the main span across the road.	(no information)	Wood deck and piers Consists exclusively of wooden members of 160/240 mm except from the main span across the road, which consists of glulam beams, C24.	-
Thalkirchner Brücke Location: München, Germany Designer: Dietrich Ingenieur Architektur Engineer: Dietrich Ingenieur Architektur Completed: 1992 Length: 197 m Width: 13 m	Continuous space framework over 15 spans, each 13.5 m long. The bridge is carrying both cars and pedestrians. Three different cross-sections and four different lengths of the spruce bars.	The distributed load is transferred in the compression space truss arch down to the concrete foundations.	Due to the dense space truss the horisontal load can easy find its way down to the foundation through the diagonals. With the 'small' spans the buckling lengts are small which also helps with the horisontal stability.	Point load on asphalt distributed down on corrugated steel sheet. The load then goes down through one of the four longitudinal arches and then down to the concrete foundations.	Since the bridge is 13 m wide and that there is a wide contact with the concrete foundations the bridge has a good rotational capacity. Also the many spans helps with the rotational stability (compared to longer spans). (The asphalt also gives extra dead-weight.)	Concrete foundations in river as well as on land.	Casted steel nodes with one common center node for all connecting bars. Each bar head is screwed with one screw each to the node ball. High-strength screws are used with pretensioned so they could handle the absorb the dynamic loads from the road traffic.	All parts were standardised and manufactured in a large amount. They were pre-assembled in larger assembly units. At last they where assembled together on the construction site. Three different cross-sections and four different lengths of the spruce bars	Pre-assembled parts which were later assembled on site.	The framework consists of glued spruce and larch wood and is held together by cast steel knots. The railings are made of larch wood. The pavements have been renewed due to wear and tear (sidewalk in oak and asphalt on roadway).	The main structure of the bridge is well protected against weather by a complete covering from above, under the walkway and roadway. The main structure also inlines inwards under the bridge deck, so that it is even further protected. The ends of the bars are sealed with epoxy resin.
Mathematical Bridge Location: Cambridge, UK Designer: William Etheridge Engineer: William Etheridge Completed: 1649 (1905) Length: 12 m Width: -	Arch bridge, consisting of straight timbers arranged radially and tangentially.	The tangential and radial beams forms a triangulated truss. Compression in the tangential beams, and the force is lifted up through the vertical beams.	A horisontal bracing system under the walkway distributes the horisontal loads.	Poin load on deck transfers through horisontal bracing to the two side trusses. Then the short trusses through the load goes in compression in the tangents and lifted up by tension in the radials, and zigzaging down to the abutments.	The arch form gives rotational stability, as well as the rigid supports.	The stone foundation surface meets the bridge perrpendicular.	Today, there are bolted connections (former iron screws and oak pins). The picture also shows how the tangential beams goes through the radial beams with cut outs to get a better match as well as a rigid connection.	Assumption. Built on site on temporary scaffolding in the water.	Assumption. A temporary scaffold in the water, and the bridge was built on that. The two longitudinal trusses copy of each other and then added the horisontal bracing.	Original bridge: Oak superstructure, iron screws and oak pins. 1905: Rebuilt in teak, with bolted connections instead.	Due to the straight tangentials running through the radial parts, water gathered there starting to degenerate the bridge. The oak superstructure of Etheridge's bridge has had to be refurbished twice. In 1904-5, the entire timber structure was rebuilt in teak. Bolted connections replaced the original iron screws and oak pins.

La passerelle de la Paix Location: Lyon, France Designer: Dietmar Feicgtinger Architects Engineer: Schlaich Bergermann & Partner Completed: 2014 Length: 157 m Width: 5 m, 8 m	Combined truss arch and cantiveler bridge. Two cantivelers built of a 3D assymetric tube structure. Two walkways (upper and lower riverbank) join and form a large public space. Two arches formed of tube sections = bottom chord. Box-girder = top chord. Top and bottom chords are linked and stiffened by triangular steel elements and diagonals to create a truss tructure. The relative positions between the elements varied across the length of the bridge. Bicycle lane + footpath and footpath. 8 + 5 m 220 m total, 160 m span, 60m appriach bridge on the park side. Height above water: 8 m	The triangular truss transferres the vertical load from the box girder and the arch to the foundation elements.	The wide triangular shape provides horisontal stability to the bridge. Also, the cantilever box girder contributes to horisontal stability in the longitudinal direction. The "eccentricity" of the varying cross-section allows the two paths to counterweight eachother.	Point loads transferred to the triangular truss elements and longitudinally to the foundation elements.	Triangular steel elements that links and stiffenes the top and bottom chords. Damping system was subjected to dynamic testing before installment.	Soil diapgragm walls in the foundation: 10 m by 14 m, 20 m deep	Due to the efficient assembly method, the welding and coating operations were simplified	Steel elements for the superstructure fabricated in Switzerland. The two ends of the main arch were assembled and welded on site after the single tube elements, diagonals and vertical diaphragm structures and upper box girder units were brought to site by tryck. The central third of the arch was brought to site in a single piece. The three sections were assembed on site	3 stages of assembly: 1st: foundation, and production and assembly of the super-elevated geometry on temporary supports (at the side of the river bank). 2nd: installation of the temporary cable support system on top of the bridge. 3rd: placing the bridge in its final position. The whole structure of 160 m long andd 8 m tall was put to place at the same time (transported by boat). 3rd: insallation of the upper chord box girder, damping system etc. Goal: minimise the time for which the river had to be closed to shipping traffic, and best solution for achieving geometrical accuracy during assembly on the site.	Steel truss elements (S355). Light wooden deck (oak planks, 50 mm thickness) with anti-slipping (epoxy resin bands with silex). Railing: inox integrating LED lights and cable-net filling.	The epoxy rasin coat of the wooden deck increases the durability of the wood (and provies anti-slipping). The welds connecting the truss and box girder is hidden under the girder deck.
L'Estellier Footbridge Location: Aiguines, France Designer: Engineer: Completed: 2004 Length: Width:	Steel truss arch bridge. Truss elements assembles the structure. Can only take 10 people at the time	The inclined truss elements distributes the vertical load from the path to the upper and lower steel continuous chords, down to the foundation.	Horisontal stiffness is provided by the rectangular foundation elements (placed perpendicular to the bridge), and by the V-shape of the bridge.	Point load is transferred from the walkway to the transverse elements and inclined/diagonal elements, to the upper and lower chords.	The V-shape of the bridge provides the rotational stability. The walkway is placed on transverse elements on the lower chord, that are longitudinally connected to eachother on the outer side of the bridge, as well as diagonally connected to the lower chord. The upper and lower chord are stiffened with vertical and diagonal steel members. This together provides rotational stability to the bridge, athough it is said to oscillate when you walk on it.	The bridge lands on concrete foundations on each side. The rectangular shape of the foundation provides horisontal stability to the structure. As the bridge is tied in tension, outward forces are minimised.	The elements are either bolted or welded.	(no documented information was found)	(no documented information was found)	Steel	Regular maintenance of the steps, bolt tightening, anti-rust paining and guardrails.
Truss Bridge in Traunreut Location: Traunreut, Germany Designer: Dietrich Ingenieur Architektur, Traunstein Engineer: Köppl, Rosenheim Completed: 2008 Length: 50 m Width: 3 m	Truss construction with round columns and copper covering. The covered truss structure consists mostly of glulam beams of spruce that are standardized in length and cross-section.	Load is transferred through the truss system in tension and compression. The truss system itself is precambered to reduce final deflection position.	Steel cross bracing in top and bottom of the truss gives horisontal stability. The load is transferred through the horisontal bracing in roof down through the longitudinal truss, and finally to the abutments.	Point load is distributed transversally through the deck out to the two main truss frame walls. Then tansferred through the truss down to the abutments.	From the lower transverse gray steel tube, dagonals go up to the upper transverse tubes to give rotational stability?	Abutments in reinforced concrete. Connections are pinned on one side (and roller on other side?)	Centerline extension of glulam truss and horisontal steel bracing meets in one node.	Truss is most likely produced in a workshop and transported to site in pieces.	After that the truss structure is assembled into one piece, the bridge is lifted to it's final position. Then wooden decking and roof with copper plates are added. And so the steel balustrade and wooden handrail.	Truss structure mainly of glulam beams of spruce. Cross beams in steel. The longitudinal beams are also made of glue laminated wood. The decking made of larch planks and the steel railing contribute to the aesthetic appeal of the bridge. The roof construction with copper plates. Steel balustrade with wood handrail.	The roof cantilevers so the rain fall down far away from the structure. Water of rain cannot reach neither the structure nor the decking.
Rasteplass i Lillefjord Location: Lillefjord, Norway Designer: Pushak Engineer: Pushak Completed: 2006 Length: - Width: -	Steel truss frame 3D frame in the curve due to torsion forces.	Is transferred through the truss system. There is one upper and one lower truss.	Top view. Since the truss frame is U-shaped, there are horisontal diagonals underneath the bridge deck, which handles horisontal forces.	A point load is transferred transversally to the truss, down to the abutments.	The 3D truss frame is U shaped, and has a wide connection point on the shore, which contributes to the rotational stability.	Conrete foundation on both sides on the shore. On the side with the higher slope, rocks are placed to prevent soil movement.	Welded connections of RHS steel profiles. The wood plank structure is screwed to the steel frame, which makes wooden parts replaceable.	Prefabricated steel frame	Steel frame transported by truck and lifted on its place. Then the wood cladding was added together with the toilet house.	Steel truss frame. Deck and benches in wood	The wooden parts are meant to be torn from hikers. They can easily be replaced since the wood is only cladding and the main structure is in steel. Purpose to let the wood turn grey and age naturally.
Railway Crossing in Nettersheim Location: Nettersheim, Germany Designer: Wollenweber Architectur Engineer: Schaffitzel Holzindustrie Completed: 2014 Length: 29.5 m Width: 3 m	Covered truss structure of larch timber and larch glulam. Integrated steel frame at the two end points	Through tension and compression in truss. The diagonals does not have the same angles, but varying angles.	Timber bracing as well as horisontal steel beams	Transferred longitudinally through bridge deck beams, out through transversal steel beams to the two main truss walls. Then down to foundation through steel column/frame	Rigid steel frames at the two end points of the whole truss beam	Assymetrical supporting structure. Two steel support structures = staircases	Diagonals change angles (no one with the same angle) Bolted connection into steel plate.	Whole bridge prefabricated	Installed at night in 1.5 h. Lifted with crane	Larch timber and larch glulam. Deck of larch planks. Staircase and parapet of galvanized steel with anthracite coating	Covered roof to protect structure.

Bostanlı Bridge and Sunset Lounge Location: Karşiyaka, Turkey Designer: Studio Evren Başbuğ Engineer: Novawood, YDÇ Completed: 2016 Length: 35 m Width: 9.5 m	Turss girder bridge. Composite girder consisting of steel I-beams + concrete surface. Transversal steel frame; 10 girders, 4 m spacing. Assymmetric shape. Slightly bow-shaped in longitudinal direction.	Vertical load distributed by the outer steel I-beams, supported by the steel frame.	Concrete bulkheads provides horisontal stability on each end of the main beam.	Point loads are transferred through the transverse steel frame to the outer steel beams, to the concrete supports.	Secondary truss-beams adds rotational stability to the bridge. The asymmetric shape of the cross-section is handled by the bow shape in longitudinal direction. The concrete cover of the girder and transerse wood cover provides additional rotational stability to the bridge.	The bridge girder rests on concrete bulkheads that lies on an artificial hill made out of a resin-bound natural stone mixture. The material is porous, which allows for mainaing a better stormwater startegy.				Thermo ash-wood surface on a steel frame.	Thermowood (ash) has better durability compared to untreated wood.
Stressed-ribbon bridge											
Essinger Bridge Location: Essing, Germany Designer: Büro für Ingenieur-Architectur Dipl. Ing. Richard J. Dietrich Engineer: Heinz Brüninghoff Completed: 1986 Length: 190 m Width: 3.2 m	Stressed ribbon bridge The span consists of 9 parallell spruce glulam beams of 0.4 m lentgth (0.22x0.65 m) Main span 73 m. Static height: ; 7 m above water lever at lowest midpoint (3 m downwards) Live load 5 kN/m²	The parallell glulam girder beams in tension distributes the vertical loads to the triangular foundation elements.	The triangular shaped bracing connected to the bridge deck and the rail increase the horisontal stability. Horisontal stability in the longitudinal direction is provided in the triangular shaped foundation elements. The horisontal timber bracing carries load to steel tie rods, which brings the force down to the concrete footing.	A point load is distributed to the three sets of longitudinal glulam girder beams. Then down in the large triangulated frame down to the concrete foundation.	The railing design with outgoing double triangles, helps with the local rotational stability. The girder beams are tensioned, also preventing rotation.	Concrete foundation. Steel rods connected to the bridge deck for horisontal forces. At the abutments the glulam beams have bolted connections. It is allowed to rotate there as well.	The triangulated supports have pinned connection to the glulam beams	Prefabricated glulam beams, lengths of 40-45m and transported by trucks. Joined together by finger joints. Prefabricated pillars and pre-assembled. All connections, joints, drive shafts, coupling elements and nailed plates have been made in cast steel. All fasteners had the same size, so only one size was needed to create.	Cast in situ of concrete foundation. Prefabricated and pre-assembled pillars were put on the foundation. The prefabricated glulam beams were lifted by a crane and they were later on joined separately. The fingerjoints were pulled together and treated. A tent was used around the joining, to give right weathering conditions.	Spruce glulam beams Casted steel joints	On top of the bracing system zinc sheets are placed to protect the main structure from rainfall. There is a problem with brown rot, especially at the supporting frames.
Cable-stayed bridge											
Anaklia-Ganmukhuri Pedestrian Bridge Location: Anaklia, Georgia Designer: Leonhardt, Andrä und Partner Engineer: Fast + Epp GmbH Completed: 2011 Length: 506 m Width: 9 m	Cable-stayed deck (60 m , 84 m span) combined with simply supported truss deck (48 m) Spatial triangular framework.	The cables carries the bridge in tension in the larges spans. For the shorter spans, the load is transferred through tension and compression in the truss.	There are transversal beams under the bridge deck. The triangular shaped truss (with the inclination) also provides horisontal stability.	Transported to either of the three main longitudinal beams in the truss system. And then transported through the cables to the pylon, or directly to the foundation.	The pylon is standing in an upside down V, creating equilibrium. Every support is Y shaped and there is a steel profile attached at the supports preventing the wood truss to rotate.	Y-columns in concrete.	"Hess Limitless" adhesive connection: Finger joint glued on site. Scarfs in glugam top and bottom faces.	All wooden components prefabricated.	The prefabricated framework is lifted ontop of the casted concrete pillars. Pylon is built and then the bridge parts are connected from the pylon outwards and then hung by the steel cables.	Timber truss deck. Steel cables, concrete pylon	A translucent polycarbonate cladding is applied as covering, to protect the wood structure.
Suspension bridge											
Punt Ruinalta Location: Bonaduz, Switzerland Designer: Walter Bieler AG Engineer: Walter Bieler AG Completed: 2010 Length: 105 m Width: -	Suspension bridge in wood and steel, and concrete pylons/foundation.	The suspension cables bear the self weight in tension.	The walking deck consists of transversal horisontal beams, which are densely spread. This provides horisontal stability. Each beam is connected by two longer rods at each end.	A point load is transported from transversal walkway beams into the longitudinal beams, and then distributed to the cables. The longitudinal beams are relatively stiff, so the bridge deck does not deflect locally at the point load.	The suspension cables are tilted outwards, this gives extra rotational stability compared to cables perpendicular to the walking deck.	The concrete pillars are integrated in the design. They should compensate for a tensile force of 100 ton (981 kN).	There is air gaps between all elements to make sure that moist and water can dry out. The transversal pathway beams har hung in two rods going up in longitudinal beams. This longitudinal beams are lifted up by the suspension cables.	First the pylons and foundations are casted. After that the suspension cables are mounted on site. The bridge deck is prefabricated in smaller pieces and then assembled on site.	The suspension cables are mounted on site. The prefabricated bridge deck parts are then lifted on their right position with the help of a cableway and then connected to the tension cables. There is an overlay on the bridge parts so they can be connected together.	Steel cables, wood in bridge deck and reinforced concrete pylons and abutments.	There is a small airgap between all components, so rain and dirt can fall off and so that the structure is able to dry.
Iya Vine Bridge Location: Iya Valley, Japan Designer: - Engineer: - Completed: 12th Century Length: 45 m Width: -	Suspension bridge made out of mountain vine. Built from actinidia arguta vines amassing a total of 5 tons To strengthen the bridge, steel cables are hidden inside the vine. Due to safety reasons, the bridge is rebuilt every three years. "Today's bridges are more sturdy than their predecessors: steel cables are hidden beneath the vines, the gaps between planks measure seven inches, and each bridge is rebuilt every three years."	The bridge is carried by the suspension cables. As well as by the upper hand rail cables thuroughly connected to the supports at both ends.	The bridge sways a bit. The tension in the hand rails together with the suspension cables gives horisontal stability.	Point load from a human is transferred transversally through the thin "beams" to the hand rails, and then through the suspension cables. There are also longitudinal cables/vines under the thin "beams" as well (but not as high force are going through here.	The suspension cables helps with the rotational stability.	The supports are using nearby trees as further support. The hand rails are further raised by the use of lever arms.	Originally woven connections or tied connections. But since a steel cable is hidden beneath, we cannot see the steel connections. But most likely clamps.	The vines are voven around the main steel cables. As well as fastening the walk way "beams".	Assumption. The hand rail cables is straightened over the span. Then the foot platforms are added from each side and then the suspension cables added and then tensioned.	Actinidia arguta vines, harvested from the mountains during the harsh winter, were woven together to form the vine bridge.	The bridge is rebuilt every 3 year with new vines.

APPENDIX B - Global dimensioning and Detailed design

Global dimensioning

Calculate for six straight, continuous beams with an intermediate support.

The span is built up by two parallel, continuous LVL beams with curved LVL panels in between, working in active bening.
Additional bridge parts: transverse floor beams, plywood + construction board, longitudinal floor beams and transverse panel deck with epoxy resin and quartz sand cover. The outer LVL beams are protected with prebent LVL panel. The railing is fastened in steel L-profiles to the transverse floor beams with longitudinal timber panels. The detailed design of the railing connection will be performed at a later stage.

The bridge is designed for pedestrians only as any service veichle or cyclists cannot access the bridge.

The bridge is categorized for safety class 3

The bridge is calculated for load case 4 (LM4) according to EN1991-2 4.3.2 (2) (d).

Site geometry

$L_1 := 4.2\text{m}$	Length of the left span
$L_2 := 2.1\text{m}$	Length of the left support span
$L_3 := 16.8\text{m}$	Length of the right span
$L_4 := 4.2\text{m}$	Length of the right support span
$L := L_1 + L_2 + L_3 + L_4 = 27.3\,\text{m}$	Total length of the bridge
$B := 2.5\text{m}$	Width of deck

Sinus pattern geometry

$s_{sin} := \frac{4.2}{2}\text{m} = 2.1\,\text{m}$	Length of half sinus wave = cc distance threaded bar
$b_{sin} := 130\text{mm}$	Distance between sinus waves
$r_{sin} := 14.5\text{m}$	Radius of the sinus waves
$b_{sin.sup.m} := 476\text{mm}$	Mid CC distance between panels over the support
$b_{sin.sup.e} := 443\text{mm}$	Outer CC distance bt panels over the support

Permanent load - load bearing elements

Straight LVL beams

LVL dimensions

$t_{veneer} := 3\text{mm}$	Nominal thickness of veneer (Mestä Wood)
$n_{veneer.s} := 9$	Number of veneers in one lamination
$t_{lvl.s} := t_{veneer} \cdot n_{veneer.s} = 27 \cdot \text{mm}$	Lamella thickness, standrard dimension

Beam dimensions

$h_{lvl.s} := 600\text{mm}$	Height of outer beams
$b_{lvl.s} := 4 \cdot t_{lvl.s} = 108 \cdot \text{mm}$	Width of outer beams
$n_{lvl.s} := 2$	Number of straight, outer beams

Material properties, LVL S grade beams

$f_{m.0.edge.k.lvl} := 44MPa$	Bending edgewise	Eurofins certificate
$f_{m.0.flat.k.lvl} := 50MPa$	Bending flatwise	
$f_{t.0.k.lvl} := 35MPa$	Tension II to grain	
$f_{c.0.k.lvl} := 35MPa$	Compression II to grain	
$f_{c.90.edge.k.lvl} := 6MPa$	Compression edgewise, perpendicular to grain	
$f_{c.90.flat.k.lvl} := 2.2MPa$	Compression flatwise perpendicular to grain	
$f_{v.0.edge.k.lvl} := 4.1MPa$	Shear edgewise	
$f_{v.0.flat.k.lvl} := 2.3MPa$	Shear flatwise	
$E_{0.k.lvl} := 11600MPa$	Elastic modulus, II to grain	
$\rho_{k.lvl} := 480 \frac{kg}{m^3}$	Density	
$E_{0.mean.lvl} := 13800MPa$	Elastic modulus, II to grain	
$E_{90.edge.mean} := 430MPa$	Elastic modulus, perp to grain, edge	
$E_{90.flat.mean} := 130MPa$	Elastic modulus, perp to grain, flat	
$\rho_{mean.lvl} := 510 \frac{kg}{m^3}$	Mean density	
$s_k := 0.12$	Size effect parameter	

Size effect

Size effect LVL beam subjected to bending, **if the majority of the layers are oriented in the same direction**

$$k_{h.lvl} := \begin{cases} \min\left[\left(\frac{300mm}{h_{lvl.s}}\right)^{s_k}, 1.2\right] & \text{if } h_{lvl.s} \neq 300mm \\ 1 & \text{otherwise} \end{cases} = 0.92$$

EN1995-1-1 eq. 3.3

Size effect LVL beam subjected to tension, assume that the LVL beam is continuous

$$k_{l.lvl.s} := \begin{cases} \min\left[\left(\frac{3000mm}{L}\right)^{\frac{s_k}{2}}, 1.1\right] & \text{if } L \neq 3000mm \\ 1 & \text{otherwise} \end{cases} = 0.876$$

EN1995-1-1 eq. 3.4

Partial factors

$k_{mod.p} := 0.5$	Permanent load, service class 3	EN1995-1-1 tab. 3.1
$k_{mod.s} := 0.7$	Short term load, service class 3	
$\gamma_{M.lvl} := 1.2$	LVL	

Design strength

$$f_{m.0.edge.d.lvl} := k_{mod.p} \cdot k_{h.lvl} \cdot \frac{f_{m.0.edge.k.lvl}}{\gamma_{M.lvl}} = 16.87 \cdot MPa$$

EN1995-1-1 eq. 2-14

$$f_{m.0.flat.d.lvl} := k_{mod.p} \cdot \frac{f_{m.0.flat.k.lvl}}{\gamma_{M.lvl}} = 20.833 \cdot MPa$$

$$f_{t.0.d.lvl.s} := k_{mod.p} \cdot k_{l.lvl.s} \cdot \frac{f_{t.0.k.lvl}}{\gamma_{M.lvl}} = 12.774 \cdot MPa$$

$$f_{c.0.d.lvl} := k_{mod.p} \cdot \frac{f_{c.0.k.lvl}}{\gamma_{M.lvl}} = 14.583 \cdot MPa$$

$$f_{c.90.edge.d.lvl} := k_{mod.p} \cdot \frac{f_{c.90.edge.k.lvl}}{\gamma_{M.lvl}} = 2.5 \cdot MPa$$

$$f_{c.90.flat.d.lvl} := k_{mod.p} \cdot \frac{f_{c.90.flat.k.lvl}}{\gamma_{M.lvl}} = 0.917 \cdot MPa$$

$$f_{v.0.edge.d.lvl} := k_{mod.p} \cdot \frac{f_{v.0.edge.k.lvl}}{\gamma_{M.lvl}} = 1.708 \cdot MPa$$

$$f_{v.0.flat.d.lvl} := k_{mod.p} \cdot \frac{f_{v.0.flat.k.lvl}}{\gamma_{M.lvl}} = 0.958 \cdot MPa$$

Self-weight of all straight beams

$$G_{k.lvl.s} := \rho_{k.lvl} \cdot g \cdot n_{lvl.s} b_{lvl.s} \cdot h_{lvl.s} = 0.61 \cdot \frac{kN}{m}$$

Curved LVL panels

LVL dimensions

$n_{veneer} := 9$	Number of veneers in one lamination
$t_{lvl} := t_{veneer} \cdot n_{veneer} = 27 \cdot mm$	Standard dimension Stora Enso S grade

Panel dimensions

$h_{lvl} := h_{lvl.s} = 600 \cdot mm$	Height of panels
$b_{lvl} := 2t_{lvl} = 54 \cdot mm$	Width oh panels
$l_{lvl} := 12000mm$	Length of LVL panel elements, not relevant for calculations
$n_{lvl} := 14$	Number of LVL panels
$L_{lvl} := L$	Total length of the LVL panels

Size effect

As the height of the curved panels are the same as the straight beams, k.h is the same. Check size effect in tension for the total length of the continuous, curved panels.

$$k_{l.lvl.curve} := \begin{cases} \min\left[\left(\frac{3000mm}{L_{lvl}}\right)^{\frac{s_k}{2}}, 1.1\right] & \text{if } L_{lvl} \neq 3000mm \\ 1 & \text{otherwise} \end{cases} = 0.876$$

EN1995-1-1 eq. 3.4

Design strength

$$f_{t.0.d.lvl.curve} := k_{mod.p} \cdot k_{l.lvl.curve} \cdot \frac{f_{t.0.k.lvl}}{\gamma_{M.lvl}} = 12.774 \cdot MPa$$

EN1995-1-1 eq. 2-14

Self-weight of all curved panels

$$G_{k.lvl.curve} := \rho_{k.lvl} \cdot g \cdot n_{lvl} b_{lvl} \cdot h_{lvl} \cdot \frac{L_{lvl}}{L} = 2.135 \cdot \frac{kN}{m}$$

Distancers

The distancers are steel tubes in compression, threaded with a steel rod in tension. A steel plate distributes the compression forces from the steel tube to the LVL panel. Two levels

Steel quality: S275, structural hollow sections

Dimensions steel plates

$t_{plate} := 20mm$ Thickness of the steel plate

$b_{plate} := 150mm$ Width of the steel plate

$h_{plate} := 150mm$ Height of the steel plate

$A_{plate} := h_{plate} \cdot t_{plate}$ Cross-sectional area

Dimensions steel tubes

$d_{tube} := 76.1mm$ Diameter, outer

$t_{tube} := 8mm$ Thickness of the steel tube

$D_1 := d_{tube}$ Outer diameter

$d_1 := d_{tube} - 2t_{tube} = 60.1 \cdot mm$ Inner diameter

Number of elements, one layer

$L_{tube} := b_{sin} - 2 \cdot t_{plate} = 90 \cdot mm$ Length of steel tubes

$n_{tube.x} := \frac{n_{lvl}}{2} = 7$ Number of steel tubes across

$s_{tube} := s_{sin} = 2.1\,m$ Spacing tubes = distance between half amplitudes

$n_{tube.y} := \mathrm{floor}\left(\frac{L - D_1}{s_{tube}}\right) = 12$ Number of tubes along the bridge

$$A_{tube} := \frac{\pi \cdot \left(D_1^{\ 2} - d_1^{\ 2}\right)}{4} = 1.712 \times 10^{-3}\,m^2$$

$n_{plate.x} := 2 \cdot n_{tube.x}$ Number of steel plates across

$n_{plate.y} := n_{tube.y}$ Number of steel plates along the bridge

Total number of elements, n layers

$n_{layer} := 2$ Number of layers

Material properties of the steel

$f_y := 275MPa$ For t < 40 mm EN1993-1-1:2005 tab. 3.1

$f_u := 430MPa$

$E_{steel} := 210GPa$

$\rho_{k.steel} := 7850 \frac{kg}{m^3}$ EN1993-1-1

The tube is considered as very stocky/intermediate slender column, i.e. buckling capacity is not considered.

Self-weight

Self-weight of the steel tubes, total

$$G_{k.tube} := \rho_{k.steel} \cdot g \cdot n_{tube.x} \cdot A_{tube} \cdot \frac{L_{tube} \cdot n_{tube.y}}{L} \cdot n_{layer} = 0.073 \cdot \frac{kN}{m}$$

Self-weight of the steel plates, total

$$G_{k.plate} := \rho_{k.steel} \cdot g \cdot n_{plate.x} \cdot A_{plate} \cdot \frac{b_{plate} \cdot n_{plate.y}}{L} \cdot n_{layer} = 0.426 \cdot \frac{kN}{m}$$

Total self-weight of the load-bearing elements, on the length of the beams

$$G_{k.bridge} := G_{k.lvl.s} + G_{k.lvl.curve} + G_{k.tube} + G_{k.plate} = 3.245 \cdot \frac{kN}{m}$$

Permanent load - non-load bearing elements

Transverse floor beams

Material properties, C24

$\rho_{k.c24} := 420 \frac{kg}{m^3}$ Mean density DOTS2 tab. 3.3

Dimensions

$s_{tfl} := 600mm$ Spacing

$L_{tfl} := B = 2.5\,m$ Length

$t_{tfl} := 70mm$ Assumed width and thickness based on similar designs

$b_{tfl} := 90mm$

$n_{tfl} := \text{floor}\left(\frac{L - b_{tfl}}{s_{tfl}}\right) = 45$ Number of transverse floor beams along the length of the bridge

Self-weight of the floor beams on the length of the bridge

$$G_{k.tfl} := \rho_{k.c24} \cdot g \cdot L_{tfl} \cdot t_{tfl} \cdot \frac{b_{tfl} \cdot n_{tfl}}{L} = 0.107 \cdot \frac{kN}{m}$$

Plywood board

The plywood and construction board protects the load-bearing structure from moisture and dirt accumulation. The board is continuous over the whole area of the bridge deck.

Material properties, plywood K20/70

$\rho_{k.pl} := 420 \frac{kg}{m^3}$ Mean density "Tillhörande handling BKR Vänderply" tab. 2

Dimensions

$t_{pl} := 9mm$ Thickness

$b_{pl} := B = 2.5\,m$

$L_{pl} := L = 27.3\,m$

Self-weight of the panel board

$$G_{k.pl} := \rho_{k.pl} \cdot g \cdot b_{pl} \cdot t_{pl} \cdot \frac{L_{pl}}{L} = 0.093 \cdot \frac{kN}{m}$$

Longitudinal floor beams

Solid timber, C24

Dimensions

$L_{lfl} := 2 \cdot s_{tfl} = 1.2 \cdot m$ — The plank deck spans over two floor beams

$t_{lfl} := 45mm$

$b_{lfl} := 90mm$

$s_{lfl} := 120mm$ — Spacing longitudinal floor beams

$n_{lfl} := \text{floor}\left(\frac{B - b_{tfl}}{s_{tfl}}\right) = 4$ — Number of longitudinal floor beams over the width of the bridge

Self-weight of longitudinal floor beams along the bridge

$$G_{k.lfl} := \rho_{k.c24} \cdot g \cdot n_{lfl} \cdot b_{lfl} \cdot t_{lfl} = 0.067 \cdot \frac{kN}{m}$$

Transverse plank deck

Solid timber, C24

Dimensions

$L_{pd} := B = 2.5\,m$

$t_{pd} := 70mm$ — Assumed dimensions based on similar bridge designs

$b_{pd} := 195mm$

$s_{pd} := b_{pd} + 15mm = 210 \cdot mm$ — Recommended spacing between planks

$n_{pd} := \text{floor}\left(\frac{L - b_{pd}}{s_{pd}}\right) = 129$ — Number of transverse floor beams along the length of the bridge

Self-weight of the floor beams on the length of the bridge

$$G_{k.pd} := \rho_{k.c24} \cdot g \cdot L_{pd} \cdot t_{pd} \cdot \frac{b_{pd} \cdot n_{pd}}{L} = 0.664 \cdot \frac{kN}{m}$$

Railing

Solid timber, C24

Total height of railing pole, fastened to the floor beams. Required height over bridge deck: 1.2 m

Dimensions

$L_{ra} := 1.2m + t_{pl} + t_{lfl} + t_{pl} + t_{tfl} = 1.333\,m$

$s_{ra} := 2 \cdot s_{tfl} = 1.2 \times 10^{3} \cdot mm$ — Center-to-center distance railing poles

$h_{ra} := 120mm$ — Assumed dimensions based on similar bridge designs

$b_{ra} := 70mm$

$n_{ra} := 2 \cdot n_{tfl} = 90$ — Total number of railing poles

Horizontal railing planks

$h_{ra.pl} := 45mm$

$t_{ra.pl} := 22.5mm$

$n_{ra.pl} := 13$ — Number of planks on the height of the railing

$s_{ra.pl} := 92mm$

Self-weight of two rail poles

$$G_{k.ra} := \rho_{k.c24} \cdot g \cdot h_{ra} \cdot L_{ra} \cdot \frac{b_{ra} \cdot n_{ra}}{L} = 0.152 \cdot \frac{kN}{m}$$

Total weight from non-load bearing elements, on the main beams

Add weight from epoxy resin + sand

$$G_{k.cover} := 0.06 \frac{kN}{m}$$

Total weight from non-load bearing elements

$$G_{k.deck} := G_{k.tfl} + G_{k.pl} + G_{k.lfl} + G_{k.pd} + G_{k.ra} + G_{k.cover} = 1.143 \cdot \frac{kN}{m}$$

Sectional constants

$c_{lvl.s} := 200mm$ Distance from deck edge to outer beam edge

$s_{lvl} := b_{sin} + 2 \cdot b_{lvl} = 238 \cdot mm$ Center-to-center distance between the panels

Cross-sectional area

$A_{lvl.s} := b_{lvl.s} \cdot h_{lvl.s} = 0.065 \cdot m^2$ One beam

$A_{lvl} := b_{lvl} \cdot h_{lvl} = 0.032\,m^2$ One panel

$$A_{tot} := n_{lvl.s} \cdot A_{lvl.s} + n_{lvl} \cdot A_{lvl} = 5.832 \times 10^5 \cdot mm^2$$

Point of gravity

Simplified calculations without the steel plates and tubes

Point of gravity from the top of the load-bearing beams, z-direction

$$z_{tp} := \frac{n_{lvl.s} \cdot A_{lvl.s} \cdot \left(\frac{h_{lvl.s}}{2}\right) + n_{lvl} \cdot A_{lvl} \cdot \left(\frac{h_{lvl}}{2}\right)}{n_{lvl.s} A_{lvl.s} + n_{lvl} \cdot A_{lvl}} = 0.3\,m$$

Symmetry as the height of the glulam beams and LVL-panels are the same

Point of gravity from the outer edge of the outer straight beam, x-direction

Midpoint distance between the outer beams

$$l_e := \frac{B - 2 \cdot c_{lvl.s} - 2 \cdot b_{lvl.s}}{2} = 0.942\,m$$

$n_{span} := \frac{n_{lvl}}{2} = 7$ Number of openings

$$n_{s.half} := \left(\mathrm{floor}\left(\frac{n_{span}}{2}\right)\right) - 1 = 2$$

$x_{tp} := l_e + b_{lvl.s} = 1.05\,m$ x.tp is in the middle of the deck due to symmetry

Moment of interia in the span

$$I_{x.lvl.s} := \frac{b_{lvl.s} \cdot h_{lvl.s}^{3}}{12} \qquad I_{z.lvl.s} := \frac{h_{lvl.s} \cdot b_{lvl.s}^{3}}{12}$$ Straight beams

$$I_{x.lvl} := \frac{b_{lvl} \cdot h_{lvl}^{3}}{12} \qquad I_{z.lvl} := \frac{h_{lvl} \cdot b_{lvl}^{3}}{12}$$ Curved panels

$$I_{x.tot} := n_{lvl.s} \cdot \left[I_{x.lvl.s} + A_{lvl.s} \cdot \left(\frac{h_{lvl.s}}{2} - z_{tp} \right)^2 \right] + n_{lvl} \cdot \left[I_{x.lvl} + A_{lvl} \cdot \left(\frac{h_{lvl}}{2} - z_{tp} \right)^2 \right] = 0.017 \cdot m^4$$

$$I_{z.tot} := n_{lvl} I_{z.lvl} + 2 \cdot 2A_{lvl} \cdot \left[\sum_{i=1}^{n_{s.half}+1} \left(x_{tp} - b_{lvl.s} - s_{lvl} \cdot i \right) \right]^2 + 2A_{lvl} \cdot \left(x_{tp} - b_{lvl.s} - \frac{b_{lvl}}{2} \right)^2 \; ... = 0.436 m^4$$
$$+ n_{lvl.s} \cdot \left[I_{z.lvl.s} + A_{lvl.s} \cdot \left(x_{tp} - \frac{b_{lvl.s}}{2} \right)^2 \right]$$

$$W_z := \frac{I_{z.tot}}{x_{tp}} = 0.416 \cdot m^3 \qquad W_x := \frac{I_{x.tot}}{z_{tp}} = 0.058 \cdot m^3$$

Variable load

1. Traffic load

Pedestrian trafic is considered as short term actions according to EN 1995-2 2.3.1.2 (1)

$q_{fk} := 5 \frac{kN}{m^2}$ Recommended, characteristic load EN1991-2 5.3.2.1 (1)

Vertical load on the bridge surface for LM4 (EN1991-2 4.3.2 (2) (d))

$$Q_{fk} := \left(2.0 + \frac{120}{\frac{L}{m} + 30}\right) \cdot \frac{kN}{m^2} = 4.094 \cdot \frac{kN}{m^2}$$ EN1991-2 eq. 5.1

$$\text{Control}_{q.fk} := \begin{cases} \text{"OK"} & \text{if } 2.5 \frac{kN}{m^2} < Q_{fk} < 5 \frac{kN}{m^2} \\ \text{"Not OK"} & \text{otherwise} \end{cases} = \text{"OK"}$$

Vertical load on all beams

$$Q_{fk.z} := Q_{fk} \cdot B = 10.236 \cdot \frac{kN}{m}$$

Vertical load on each beam

$$Q_{fk.n.z} := Q_{fk} \cdot \frac{B}{n_{lvl.s} + n_{lvl}} = 0.64 \cdot \frac{kN}{m}$$

Horizontal load along the bridge

Horizontal load acting along the bridge in level with the upper surface of the decking.

The characteristic load is set to 10% of the vertical traffic load (EN1991-2 chp. 5.4 (2))

Horizontal load along all beams

$Q_{fk.y} := 0.10 \cdot B \cdot L \cdot Q_{fk} = 27.943 \cdot kN$ Point load

Horizontal load along each beam

$Q_{fk.n.y} := \frac{Q_{fk.y}}{n_{lvl.s} + n_{lvl}} = 1.746 \cdot kN$ Point load

This load work together with the vertical load

2. Wind load

EN1991-1-4 chp. 8 Wind actions on bridges

Design dimenisons

$d_{tot} := h_{lvl.s} + t_{pl} + t_{lfl} + t_{pl} + t_{tfl} = 0.733\, m$ EN1991-1-4 fig. 8.2

$b := B = 2.5\, m$

$L = 27.3\, m$

Force coefficient for bridges

$$\frac{b}{d_{tot}} = 3.411$$

$a_x := \frac{1.3 - 2.4}{4 - 0} = -0.275$ EN1991-1-4 fig. 8.3

$c_{fx.0} := 2.4 + a_x \frac{b}{d_{tot}} = 1.462$ Force coefficient

Horizontal wind load

For an open parapet and open safety barrier

$d := d_{tot} + 0.6m = 1.333\,m$ Reference area EN1991-1-4 tab. 8.1

For load combinations without traffic load, plain (web) beams

$A_{ref.x} := L \cdot d = 36.391\,m^2$ EN1991-1-4 8.3.1 (4)(a)

$v_{b.0} := 25.0 \frac{m}{s}$ Fundamental value for Wendelstrand (Boverket)

$c_{dir} := 1.0$ Directional factor EN1991-1-4 4.2 (2) N2

$c_{season} := 1.0$ Season factor EN1991-1-4 4.2 (2) N3

$v_b := c_{dir} \cdot c_{season} \cdot v_{b.0} = 25 \frac{m}{s}$ Basic wind velocity EN1991-1-4 eq. 4.1

$\rho := 1.25 \frac{kg}{m^3}$ Air density

$q_b := \frac{1}{2} \cdot \rho \cdot v_b^{\,2} = 0.391 \cdot \frac{kN}{m^2}$ Basic velocity pressure EN1991-1-4 4.10

<u>Terrain parameters</u>

Terrain category II EN1991-1-4 tab. 4.1

$c_0 := 1.0$ Orography factor EN1991-1-4 4.3.1 (1)

$k_l := 1.0$ Turbulence factor EN1991-1-4 4.4 (1)

$z := 58m + 5.3m$ Altitude at site + bridge height

$k_r := 0.24$ National annex tab. D2

$z_0 := 0.05m$ Roughness length EN1991-1-4 tab. 4.1

$z_{min} := 2m$ Minimum height

$z_{max} := 200m$ Maximum height EN1991-1-4 4.3.2 (1)

Exposure factor

$$c_{e.z} := \left(k_r \cdot \ln\left(\frac{z}{z_0}\right)\right)^2 \cdot \left(1 + \frac{7}{\ln\left(\frac{z}{z_0}\right)}\right) = 5.82$$ National annex tab. D2

Peak velocity pressure

$q_{p.z} := c_{e.z} \cdot q_b = 2.273 \times 10^3\,Pa$ EN1991-1-4 eq. 4.8

Reference height from lowest ground level to the centre of the bridge structure

$$z_e := 5.3m + \frac{\left(h_{lvl.s} + t_{pl} + t_{lfl} + t_{pl} + t_{tfl}\right)}{2} = 5.667\,m$$ EN1991-1-4 8.3.1 (6))

$0.5 < \frac{b}{d_{tot}} < 4 = 1$

$z_e \le 20m = 1$

Force factor

$$C_x := 6.7 + \left(\frac{b}{d_{tot}} - 0.5\right)\cdot\frac{3.6 - 6.7}{4 - 0.5} = 4.122$$ EN1991-1-4 tab. 8.2

Force in x-direction, Simplified method (EN1994-1-4 8.3.2)

$$F_{w.x} := \frac{1}{2}\cdot\rho\cdot v_b^{\,2}\cdot C_x\cdot A_{ref.x} = 58.595\cdot kN$$ EN1991-1-4 eq. 8.2

Total horizontal wind load on the long side of the bridge, on all beams

$$Q_{w.x} := \frac{F_{w.x}}{L} = 2.146\cdot\frac{kN}{m}$$

Total horizontal wind load on the long side of the bridge, on one beam

$$Q_{w.n.x} := \frac{F_{w.x}}{L\cdot\left(n_{lvl.s} + n_{lvl}\right)} = 0.134\cdot\frac{kN}{m}$$

Horizontal wind load, along the bridge

$$F_{w.y} := 0.25\cdot F_{w.x} = 14.649\cdot kN$$ EN1991-1.4 8.3.4 (1)

Total horizontal wind load along each beam

$$Q_{w.y} := \frac{F_{w.y}}{n_{lvl.s} + n_{lvl}} = 0.916\cdot kN$$ Point load

3. Snow load

EN 1991-1-3 chp. 5.1

$\mu_i := 0.8$ Flat "roof"

$C_e := 1.0$

$C_t := 1.0$

$s_{k.swe} := 1.5\,\frac{kN}{m^2}$ Boverket EKS

$$s_{snow} := \mu_i\cdot C_e\cdot C_t\cdot s_{k.swe} = 1.2\cdot\frac{kN}{m^2}$$

Total snow load on the bridge

$$q_{snow} := s_{snow}\cdot B = 3\cdot\frac{kN}{m}$$

The snow load is considered in the load combinations if it exceeds the permanent loads

$$Control_{snow} := \left|\begin{array}{l} \text{"Consider snow"} \quad \text{if } q_{snow} > G_{k.bridge} + G_{k.deck} \\ \text{"Don't consider snow"} \quad \text{otherwise} \end{array}\right. = \text{"Don't consider snow"}$$

ULS Load combinations

Risk class 3 — EKS10 13§

$\gamma_d := 1.0$ — EKS10 14§

Vertical loads (x)

Total permanent load on all beams, vertical (z)

$G_k := G_{k.bridge} + G_{k.deck} = 4.387 \cdot \frac{kN}{m}$ — EN1990 eq. 6.10

Total variable load on all beams, vertical (z)

$Q_{fk.z} = 10.236 \cdot \frac{kN}{m}$

Total variable load on one beam, vertical

$Q_{fk.n.z} = 0.64 \cdot \frac{kN}{m}$

Partial factors

Traffic load are considered short term load duration.

$k_{mod.s} = 0.7$

Partial factors for load combinations according to STR-2

$\gamma_G := 1.2$

$\gamma_Q := 1.5$

Load factors for load combinations

$\psi_{0.fk} := 0.4$ — Traffic load — EN1990 tab. A2.2

Load cases

$LC1_z := \gamma_G \cdot G_k = 5.265 \cdot \frac{kN}{m}$ — Load case 1: self-weight

$LC2_z := \gamma_G \cdot G_k + \gamma_Q \cdot Q_{fk.z} = 20.618 \cdot \frac{kN}{m}$ — Load case 2: self-weight + traffic load

$LC3_z := \gamma_G \cdot G_k + \gamma_Q \cdot \psi_{0.fk} \cdot Q_{fk.z} = 11.406 \cdot \frac{kN}{m}$ — Load case 2: self-weight + characteristic traffic load

Critical load case, vertical direction

$q_{d.z} := \max\left(LC1_z, LC2_z, LC3_z\right) = 20.618 \cdot \frac{kN}{m}$

Transverse loads (x)

Total variable load on all beams, transverse (x)

$Q_{w.x} = 2.146 \cdot \frac{kN}{m}$

Partial factors for load combination

Load combination factors for variable loads on bridges

$\psi_{0.w} := 0.3$ Wind load main load EN1990 tab. A2.2

Load combinations, x-direction

Wind load is the only load in x-direction

$LC1_x := \gamma_Q \cdot Q_{w.x} = 3.22 \cdot \frac{kN}{m}$

$LC2_x := \gamma_Q \cdot \psi_{0.w} \cdot Q_{w.x} = 0.966 \cdot \frac{kN}{m}$

$q_{d.x} := \max\left(LC1_x, LC2_x\right) = 3.22 \cdot \frac{kN}{m}$

Longitudinal loads (y)

Total variable load on one beam, longitudinal (y)

$Q_{k.n.y} := Q_{fk.n.y} + Q_{w.y} = 2.662 \cdot kN$

Partial factors for load combination

Load combination factors for variable loads on bridges

$\psi_{0.w} = 0.3$ Wind load main load

$\psi_{0.fk} = 0.4$ Traffic load main load

Load combinations, y-direction

$LC1_y := \gamma_Q \cdot \left(Q_{w.y} + Q_{fk.n.y}\right) = 3.993 \cdot kN$

$LC2_y := \gamma_Q \cdot \left(Q_{w.y} + \psi_{0.w} \cdot Q_{fk.n.y}\right) = 2.159 \cdot kN$ Wind main load

$LC3_y := \gamma_Q \cdot \left(\psi_{0.fk} \cdot Q_{w.y} + Q_{fk.n.y}\right) = 3.169 \cdot kN$ Traffic main load

Critical load case, y-direction

$q_{d.y} := \max\left(LC1_y, LC2_y, LC3_y\right) = 3.993 \cdot kN$ Point load on **one** beam

Load case 2, traffic main load is the critical load case.

Load response - vertical load in ULS

Span lengths

$L_{tot} := L_1 + L_2 + L_3 + L_4 = 27.3\,m$

Critical load cases

$q_{d.ULS.z} := q_{d.z} = 20.618 \cdot \frac{kN}{m}$ Design load (traffic load + self-weight)

$G_{d.ULS.z} := \gamma_G \cdot G_k = 5.265 \cdot \frac{kN}{m}$ Self-weight only

Distributed loads, vertical load

Distributed load in four, unequal spans. Vertical load working on all beams in the cs.

Load in each span:

$q_{1.ULS} := q_{d.ULS.z} = 20.618 \cdot \frac{kN}{m}$ $q_{3.ULS} := q_{d.ULS.z} = 20.618 \cdot \frac{kN}{m}$

$q_{2.ULS} := q_{d.ULS.z} = 20.618 \cdot \frac{kN}{m}$ $q_{4.ULS} := q_{d.ULS.z} = 20.618 \cdot \frac{kN}{m}$

Support rotation

$$\theta_A = \frac{M_A \cdot L_1}{3 \cdot E \cdot I} + \frac{M_B \cdot L_1}{6 \cdot E \cdot I} + \frac{q_1 \cdot L_1^3}{24 \cdot E \cdot I} \qquad \theta_{C2} = \frac{M_C \cdot L_3}{3 \cdot E \cdot I} + \frac{M_D \cdot L_3}{6 \cdot E \cdot I} + \frac{q_3 \cdot L_3^3}{24 \cdot E \cdot I}$$

$$\theta_{B1} = \frac{M_A \cdot L_1}{6 \cdot E \cdot I} + \frac{M_B \cdot L_1}{3 \cdot E \cdot I} + \frac{q_1 \cdot L_1^3}{24 \cdot E \cdot I} \qquad \theta_{D1} = \frac{M_C \cdot L_3}{6 \cdot E \cdot I} + \frac{M_D \cdot L_3}{3 \cdot E \cdot I} + \frac{q_3 \cdot L_3^3}{24 \cdot E \cdot I}$$

$$\theta_{B2} = \frac{M_B \cdot L_2}{3 \cdot E \cdot I} + \frac{M_C \cdot L_2}{6 \cdot E \cdot I} + \frac{q_2 \cdot L_2^3}{24 \cdot E \cdot I} \qquad \theta_{D2} = \frac{M_D \cdot L_4}{3 \cdot E \cdot I} + \frac{M_E \cdot L_4}{6 \cdot E \cdot I} + \frac{q_4 \cdot L_4^3}{24 \cdot E \cdot I}$$

$$\theta_{C1} = \frac{M_B \cdot L_2}{6 \cdot E \cdot I} + \frac{M_C \cdot L_2}{3 \cdot E \cdot I} + \frac{q_2 \cdot L_2^3}{24 \cdot E \cdot I} \qquad \theta_E = \frac{M_D \cdot L_4}{6 \cdot E \cdot I} + \frac{M_E \cdot L_4}{3 \cdot E \cdot I} + \frac{q_2 \cdot L_4^3}{24 \cdot E \cdot I}$$

Continuum condition gives:

$\theta_{B1} = -\theta_{B2}$

$-\theta_{C1} = \theta_{C2}$

$\theta_{D1} = -\theta_{D2}$

Support moment

$M_{A.ULS} := 0kN \cdot m$ End support hill-side

$M_{E.ULS} := 0 \cdot kN \cdot m$ End support lake-side

$M_{C.guess} := 1000kN \cdot m$ Initial guess

$$M_{B.ULS}(M_{C.ULS}) := \frac{-\left(\frac{M_{A.ULS} \cdot L_1}{6} + \frac{q_{1.ULS} \cdot L_1^3}{24} + \frac{M_{C.ULS} \cdot L_2}{6} + \frac{q_{2.ULS} \cdot L_2^3}{24}\right)}{\left(\frac{L_1 + L_2}{3}\right)}$$

$$M_C = \frac{-\left(\frac{M_B \cdot L_2}{6} + \frac{q_2 \cdot L_2^{\ 3}}{24} + \frac{M_D \cdot L_3}{6} + \frac{q_3 \cdot L_3^{\ 3}}{24}\right)}{\left(\frac{L_2 + L_3}{3}\right)}$$

$$M_{D.ULS}(M_{C.ULS}) := \frac{-\left(\frac{M_{C.ULS} \cdot L_3}{6} + \frac{q_{3.ULS} \cdot L_3^{\ 3}}{24} + \frac{M_{E.ULS} \cdot L_4}{6} + \frac{q_{4.ULS} \cdot L_4^{\ 3}}{24}\right)}{\left(\frac{L_3 + L_4}{3}\right)}$$

$$M_{C.ULS} := \mathrm{root}\left[M_{C.guess} + \frac{\left(\begin{array}{l}\frac{M_{B.ULS}(M_{C.guess}) \cdot L_2}{6} + \frac{q_{2.ULS} \cdot L_2^{\ 3}}{24} \ \ldots \\ + \frac{M_{D.ULS}(M_{C.guess}) \cdot L_3}{6} + \frac{q_{3.ULS} \cdot L_3^{\ 3}}{24}\end{array}\right)}{\left(\frac{L_2 + L_3}{3}\right)}, M_{C.guess}\right] = -471.453 \cdot kN \cdot m$$

$$M_{B.ULS} := M_{B.ULS}(M_{C.ULS}) = 44.479 \cdot kN \cdot m$$

$$M_{D.ULS} := M_{D.ULS}(M_{C.ULS}) = -402.431 \cdot kN \cdot m$$

$$M_{max.s.ULS} := \min(M_{A.ULS}, M_{B.ULS}, M_{C.ULS}, M_{D.ULS}, M_{E.ULS}) = -471.453 \cdot kN \cdot m$$

Reaction forces

$$R_{A.ULS} := \frac{-M_{A.ULS}}{L_1} + \frac{M_{B.ULS}}{L_1} + \frac{q_{1.ULS} \cdot L_1}{2} = 53.888 \cdot kN$$

$$R_{B1.ULS} := \frac{M_{A.ULS}}{L_1} + \frac{-M_{B.ULS}}{L_1} + \frac{q_{1.ULS} \cdot L_1}{2} = 32.707 \cdot kN$$

$$R_{B2.ULS} := \frac{-M_{B.ULS}}{L_2} + \frac{M_{C.ULS}}{L_2} + \frac{q_{2.ULS} \cdot L_2}{2} = -224.033 \cdot kN$$

$$R_{B.ULS} := R_{B1.ULS} + R_{B2.ULS} = -191.326 \cdot kN$$

$$R_{C1.ULS} := \frac{M_{B.ULS}}{L_2} + \frac{-M_{C.ULS}}{L_2} + \frac{q_{2.ULS} \cdot L_2}{2} = 267.331 \cdot kN$$

$$R_{C2.ULS} := \frac{-M_{C.ULS}}{L_3} + \frac{M_{D.ULS}}{L_3} + \frac{q_{3.ULS} \cdot L_3}{2} = 177.299 \cdot kN$$

$$R_{C.ULS} := R_{C1.ULS} + R_{C2.ULS} = 444.63 \cdot kN$$

$$R_{D1.ULS} := \frac{M_{C.ULS}}{L_3} + \frac{-M_{D.ULS}}{L_3} + \frac{q_{3.ULS} \cdot L_3}{2} = 169.082 \cdot kN$$

$$R_{D2.ULS} := \frac{-M_{D.ULS}}{L_4} + \frac{M_{E.ULS}}{L_4} + \frac{q_{4.ULS} \cdot L_4}{2} = 139.115 \cdot kN$$

$$R_{D.ULS} := R_{D1.ULS} + R_{D2.ULS} = 308.197 \cdot kN$$

$$R_{E.ULS} := \frac{M_{D.ULS}}{L_4} + \frac{-M_{E.ULS}}{L_4} + \frac{q_{4.ULS} \cdot L_4}{2} = -52.519 \cdot kN$$

$$R_{tot.ULS} := q_{1.ULS} \cdot L_1 + q_{2.ULS} \cdot L_2 + q_{3.ULS} \cdot L_3 + q_{4.ULS} \cdot L_4 = 562.869 \cdot kN$$

$$R_{check.ULS} := R_{A.ULS} + R_{B.ULS} + R_{C.ULS} + R_{D.ULS} + R_{E.ULS} - R_{tot.ULS} = 0 \cdot kN$$

$$R_{max.c.ULS} := \max\left(R_{A.ULS}, R_{B.ULS}, R_{C.ULS}, R_{D.ULS}, R_{E.ULS}\right) = 444.63 \cdot kN$$

$$R_{max.t.ULS} := \min\left(R_{A.ULS}, R_{B.ULS}, R_{C.ULS}, R_{D.ULS}, R_{E.ULS}\right) = -191.326 \cdot kN$$

Shear force distribution

$$V_{1.ULS}(x) := R_{A.ULS} - q_{1.ULS} \cdot x$$

$$V_{2.ULS}(x) := R_{A.ULS} + R_{B.ULS} - q_{1.ULS} \cdot L_1 - q_{2.ULS} \cdot \left(x - L_1\right)$$

$$V_{3.ULS}(x) := R_{A.ULS} + R_{B.ULS} + R_{C.ULS} - q_{1.ULS} \cdot L_1 - q_{2.ULS} \cdot L_2 - q_{3.ULS} \cdot \left[x - \left(L_1 + L_2\right)\right]$$

$$V_{4.ULS}(x) := R_{A.ULS} + R_{B.ULS} + R_{C.ULS} + R_{D.ULS} \cdots \\ + -q_{1.ULS} \cdot L_1 - q_{2.ULS} \cdot L_2 - q_{3.ULS} \cdot L_3 - q_{4.ULS} \cdot \left[x - \left(L_1 + L_2 + L_3\right)\right]$$

$$V_{ULS}(x) := \begin{array}{|l} V_{1.ULS}(x) \ \text{ if } x \le L_1 \\ V_{2.ULS}(x) \ \text{ if } L_1 < x \le L_1 + L_2 \\ V_{3.ULS}(x) \ \text{ if } L_1 + L_2 < x \le L_1 + L_2 + L_3 \\ V_{4.ULS}(x) \ \text{ if } L_1 + L_2 + L_3 < x \le L_1 + L_2 + L_3 + L_4 \end{array}$$

$$V_{A.x.ULS} := \begin{pmatrix} 0m \\ 0m \end{pmatrix} \qquad V_{A.y.ULS} := \begin{pmatrix} 0 \\ R_{A.ULS} \end{pmatrix} = \begin{pmatrix} 0 \\ 53.888 \end{pmatrix} \cdot kN$$

$$V_{B.x.ULS} := \begin{pmatrix} L_1 \\ L_1 \end{pmatrix} = \begin{pmatrix} 4.2 \\ 4.2 \end{pmatrix} m \qquad V_{B.y.ULS} := \begin{pmatrix} R_{B2.ULS} \\ -R_{B1.ULS} \end{pmatrix} = \begin{pmatrix} -224.033 \\ -32.707 \end{pmatrix} \cdot kN$$

$$V_{C.x.ULS} := \begin{pmatrix} L_1 + L_2 \\ L_1 + L_2 \end{pmatrix} = \begin{pmatrix} 6.3 \\ 6.3 \end{pmatrix} m \qquad V_{C.y.ULS} := \begin{pmatrix} R_{C2.ULS} \\ -R_{C1.ULS} \end{pmatrix} = \begin{pmatrix} 177.299 \\ -267.331 \end{pmatrix} \cdot kN$$

$$V_{D.x.ULS} := \begin{pmatrix} L_1 + L_2 + L_3 \\ L_1 + L_2 + L_3 \end{pmatrix} = \begin{pmatrix} 23.1 \\ 23.1 \end{pmatrix} m \qquad V_{D.y.ULS} := \begin{pmatrix} R_{D2.ULS} \\ -R_{D1.ULS} \end{pmatrix} = \begin{pmatrix} 139.115 \\ -169.082 \end{pmatrix} \cdot kN$$

$$V_{E.x.ULS} := \begin{pmatrix} L_1 + L_2 + L_3 + L_4 \\ L_1 + L_2 + L_3 + L_4 \end{pmatrix} = \begin{pmatrix} 27.3 \\ 27.3 \end{pmatrix} m \qquad V_{E.y.ULS} := \begin{pmatrix} -R_{E.ULS} \\ 0 \end{pmatrix} = \begin{pmatrix} 52.519 \\ 0 \end{pmatrix} \cdot kN$$

$$V_{max.ULS} := \max\left(V_{A.y.ULS}, V_{B.y.ULS}, V_{C.y.ULS}, V_{D.y.ULS}, V_{E.y.ULS}\right) = 177.299 \cdot kN$$

$$V_{min.ULS} := \min\left(V_{A.y.ULS}, V_{B.y.ULS}, V_{C.y.ULS}, V_{D.y.ULS}, V_{E.y.ULS}\right) = -267.331 \cdot kN$$

Moment distribution

$$M_{1.ULS}(x) := R_{A.ULS} \cdot x - q_{1.ULS} \cdot x \cdot \frac{x}{2}$$

$$M_{2.ULS}(x) := R_{A.ULS} \cdot x + R_{B.ULS} \cdot (x - L_1) - q_{1.ULS} \cdot L_1 \cdot \left(x - \frac{L_1}{2}\right) - q_{2.ULS} \cdot (x - L_1) \cdot \left(\frac{x - L_1}{2}\right)$$

$$M_{3.ULS}(x) := R_{A.ULS} \cdot x + R_{B.ULS} \cdot (x - L_1) + R_{C.ULS} \cdot [x - (L_1 + L_2)] \ldots$$
$$+ -q_{1.ULS} \cdot L_1 \cdot \left(x - \frac{L_1}{2}\right) - q_{2.ULS} \cdot L_2 \cdot \left[x - \left(L_1 + \frac{L_2}{2}\right)\right] - q_{3.ULS} \cdot [x - (L_1 + L_2)] \cdot \left[\frac{x - (L_1 + L_2)}{2}\right]$$

$$M_{4.ULS}(x) := R_{A.ULS} \cdot x + R_{B.ULS} \cdot (x - L_1) + R_{C.ULS} \cdot [x - (L_1 + L_2)] + R_{D.ULS} \cdot [x - (L_1 + L_2 + L_3)] \ldots$$
$$+ -q_{1.ULS} \cdot L_1 \cdot \left(x - \frac{L_1}{2}\right) - q_{2.ULS} \cdot L_2 \cdot \left[x - \left(L_1 + \frac{L_2}{2}\right)\right] - q_{3.ULS} \cdot L_3 \cdot \left[x - \left(L_1 + L_2 + \frac{L_3}{2}\right)\right] \ldots$$
$$+ -q_{4.ULS} \cdot [x - (L_1 + L_2 + L_3)] \cdot \left[\frac{x - (L_1 + L_2 + L_3)}{2}\right]$$

$$M_{ULS}(x) := \begin{cases} M_{1.ULS}(x) & \text{if } x \le L_1 \\ M_{2.ULS}(x) & \text{if } L_1 < x \le L_1 + L_2 \\ M_{3.ULS}(x) & \text{if } L_1 + L_2 < x \le L_1 + L_2 + L_3 \\ M_{4.ULS}(x) & \text{if } L_1 + L_2 + L_3 < x \le L_1 + L_2 + L_3 + L_4 \end{cases}$$

Field moment

$$x_{00} := 0$$

$$x_{0.1.ULS} := \text{Maximize}(M_{1.ULS}, x_{00}) = 2.614\,m$$

Point where shear force is zero

$$x_{0.2.ULS} := \text{Maximize}(M_{2.ULS}, x_{00}) = -6.666\,m$$

$$x_{0.3.ULS} := \text{Maximize}(M_{3.ULS}, x_{00}) = 14.899\,m$$

$$x_{0.4.ULS} := \text{Maximize}(M_{4.ULS}, x_{00}) = 29.847\,m$$

$$x_{0.1.ULS} := \begin{cases} x_{0.1.ULS} & \text{if } 0m \le x_{0.1.ULS} \le L_1 \\ 0m & \text{otherwise} \end{cases}$$

Check if zero shear force point is within the span, otherwise it is replaced with a dummy number.

$$x_{0.2.ULS} := \begin{cases} x_{0.2.ULS} & \text{if } L_1 \le x_{0.2.ULS} \le L_1 + L_2 \\ L_1 & \text{otherwise} \end{cases}$$

$$x_{0.3.ULS} := \begin{cases} x_{0.3.ULS} & \text{if } L_1 + L_2 \le x_{0.3.ULS} \le L_1 + L_2 + L_3 \\ L_1 + L_2 & \text{otherwise} \end{cases}$$

$$x_{0.4.ULS} := \begin{cases} x_{0.4.ULS} & \text{if } L_1 + L_2 + L_3 \le x_{0.4.ULS} \le L_1 + L_2 + L_3 + L_4 \\ L_{tot} & \text{otherwise} \end{cases}$$

$$M_{f1.ULS} := M_{1.ULS}(x_{0.1.ULS}) = 70.422 \cdot kN \cdot m$$

$$M_{f2.ULS} := M_{2.ULS}(x_{0.2.ULS}) = 44.479 \cdot kN \cdot m$$

$$M_{f3.ULS} := M_{3.ULS}(x_{0.3.ULS}) = 290.867 \cdot kN \cdot m$$

$$M_{f4.ULS} := M_{4.ULS}(x_{0.4.ULS}) = -1.63 \times 10^{-12} \cdot kN \cdot m$$

$$M_{max.f.ULS} := \max(M_{f1.ULS}, M_{f2.ULS}, M_{f3.ULS}, M_{f4.ULS}) = 290.867 \cdot kN \cdot m$$

Maximum field moment

Zero moment positions

$$x_{M0.1.ULS} := \mathrm{root}\left(M_{ULS}(x), x, 0, \frac{L_1}{2}\right) = 0\,\mathrm{m}$$

$$x_{M0.2.ULS} := \mathrm{root}\left(M_{ULS}(x), x, \frac{L_1}{2}, L_1 + \frac{L_2}{2}\right) = 4.397\,\mathrm{m}$$

$$x_{M0.3.ULS} := \mathrm{root}\left(M_{ULS}(x), x, L_1 + \frac{L_2}{2}, L_1 + L_2 + \frac{L_3}{2}\right) = 9.587\,\mathrm{m}$$

$$x_{M0.4.ULS} := \mathrm{root}\left(M_{ULS}(x), x, L_1 + L_2 + \frac{L_3}{2}, L_1 + L_2 + L_3 + \frac{L_4}{2}\right) = 20.211\,\mathrm{m}$$

$$x_{M0.5.ULS} := \mathrm{root}\left(M_{ULS}(x), x, L_1 + L_2 + L_3 + \frac{L_4}{2}, L_{tot}\right) = \blacksquare$$

Deflection

$$EI := E_{0.mean.lvl} \cdot I_{x.tot} = 241.445 \cdot \mathrm{MPa} \cdot \mathrm{m}^4$$ Flexural Rigidity

$$\kappa_{ULS}(x) := \frac{M_{ULS}(x)}{EI}$$ Curvature

$$\theta_{A.ULS} := \frac{\int_0^{L_1} \kappa_{ULS}(x) \cdot (L_1 - x)\,dx}{L_1} = 3.926 \times 10^{-4}$$

$$\theta_{B1.ULS} := \frac{\int_0^{L_1} \kappa_{ULS}(x) \cdot x\,dx}{L_1} = 5.215 \times 10^{-4}$$

$$\theta_{B2.ULS} := \frac{\int_{L_1}^{L_1+L_2} \kappa_{ULS}(x) \cdot (L_1 + L_2 - x)\,dx}{L_2} = -5.215 \times 10^{-4}$$

$$\theta_{C1.ULS} := \frac{\int_{L_1}^{L_1+L_2} \kappa_{ULS}(x) \cdot (x - L_1)\,dx}{L_2} = -1.269 \times 10^{-3}$$

$$\theta_{C2.ULS} := \frac{\int_{L_1+L_2}^{L_1+L_2+L_3} \kappa_{ULS}(x) \cdot (L_1 + L_2 + L_3 - x)\,dx}{L_3} = 1.269 \times 10^{-3}$$

$$\theta_{D1.ULS} := \frac{\int_{L_1+L_2}^{L_1+L_2+L_3} \kappa_{ULS}(x) \cdot (x - L_1 - L_2)\,dx}{L_3} = 2.07 \times 10^{-3}$$

$$\theta_{D2.ULS} := \frac{\displaystyle\int_{L_1+L_2+L_3}^{L_1+L_2+L_3+L_4} \kappa_{ULS}(x)\cdot\left(L_1 + L_2 + L_3 + L_4 - x\right) dx}{L_4} = -2.07 \times 10^{-3}$$

$$\theta_{E.ULS} := \frac{\displaystyle\int_{L_1+L_2+L_3}^{L_1+L_2+L_3+L_4} \kappa_{ULS}(x)\cdot\left(x - L_1 - L_2 - L_3\right) dx}{L_4} = -9.031 \times 10^{-4}$$

$$f_{1.ULS}(x) := \theta_{A.ULS}\cdot x - \int_0^x \int_0^x \kappa_{ULS}(x)\, dx\, dx$$

$$f_{2.ULS}(x) := \theta_{B2.ULS}\cdot\left(x - L_1\right) - \int_{L_1}^x \int_{L_1}^x \kappa_{ULS}(x)\, dx\, dx$$

$$f_{3.ULS}(x) := \theta_{C2.ULS}\cdot\left(x - L_1 - L_2\right) - \int_{L_1+L_2}^x \int_{L_1+L_2}^x \kappa_{ULS}(x)\, dx\, dx$$

$$f_{4.ULS}(x) := \theta_{D2.ULS}\cdot\left(x - L_1 - L_2 - L_3\right) - \int_{L_1+L_2+L_3}^x \int_{L_1+L_2+L_3}^x \kappa_{ULS}(x)\, dx\, dx$$

$$f_{ULS}(x) := \left| \begin{array}{ll} f_{1.ULS}(x) & \text{if } x \le L_1 \\ f_{2.ULS}(x) & \text{if } L_1 < x \le L_1 + L_2 \\ f_{3.ULS}(x) & \text{if } L_1 + L_2 < x \le L_1 + L_2 + L_3 \\ f_{4.ULS}(x) & \text{if } L_1 + L_2 + L_3 < x \le L_1 + L_2 + L_3 + L_4 \end{array} \right.$$

Maximum deflection

$$x_{\theta 0.1.guess} := \frac{L_1}{2} = 2.1\,\text{m}$$ Guess of where curvature is zero

$$x_{\theta 0.2.guess} := L_1 + \frac{L_2}{2} = 5.25\,\text{m}$$

$$x_{\theta 0.3.guess} := L_1 + L_2 + \frac{L_3}{2} = 14.7\,\text{m}$$

$$x_{\theta 0.4.guess} := L_1 + L_2 + L_3 + \frac{L_4}{2} = 25.2\,\text{m}$$

$$x_{\theta 0.1.ULS} := \text{root}\left(\int_0^{x_{\theta 0.1.guess}} \kappa_{ULS}(x)\, dx - \theta_{A.ULS}, x_{\theta 0.1.guess}\right) = 2.214\,\text{m}$$ Position where curvature is zero

$$x_{\theta 0.2.ULS} := \text{root}\left(\int_{L_1}^{x_{\theta 0.2.guess}} \kappa_{ULS}(x)\, dx - \theta_{B2.ULS}, x_{\theta 0.2.guess}\right) = 5.449\,\text{m}$$

$$x_{\theta 0.3.ULS} := \text{root}\left(\int_{L_1+L_2}^{x_{\theta 0.3.guess}} \kappa_{ULS}(x)\, dx - \theta_{C2.ULS}, x_{\theta 0.3.guess}\right) = 14.866\,\text{m}$$

$$x_{\theta0.4.ULS} := \mathrm{root}\left(\int_{L_1+L_2+L_3}^{x_{\theta0.4.guess}} \kappa_{ULS}(x)\,dx - \theta_{D2.ULS}, x_{\theta0.4.guess}\right) = 24.799\,m$$

Maximum field deflection

$$f_{max.1.ULS} := -f_{1.ULS}\left(x_{\theta0.1.ULS}\right) = -0.551 \cdot mm$$
$$f_{max.2.ULS} := -f_{2.ULS}\left(x_{\theta0.2.ULS}\right) = 0.485 \cdot mm$$
$$f_{max.3.ULS} := -f_{3.ULS}\left(x_{\theta0.3.ULS}\right) = -24.744 \cdot mm$$
$$f_{max.4.ULS} := -f_{4.ULS}\left(x_{\theta0.4.ULS}\right) = 1.552 \cdot mm$$
$$f_{max.up.ULS} := \max\left(f_{max.1.ULS}, f_{max.2.ULS}, f_{max.3.ULS}, f_{max.4.ULS}\right) = 1.552 \cdot mm$$
$$f_{max.down.ULS} := \min\left(f_{max.1.ULS}, f_{max.2.ULS}, f_{max.3.ULS}, f_{max.4.ULS}\right) = -24.744 \cdot mm$$

Summary of design load response - vertical load in ULS

Maximum support moment in support C
Maximum field moment in field 3

$$M_{max.z} := \max\left(\left|M_{max.s.ULS}\right|, \left|M_{max.f.ULS}\right|\right) = 471.453 \cdot kN \cdot m$$

Maximum reaction force (compression) in support C
Maximum reaction force (tension) in support B

$$R_{max.c.z} := R_{max.c.ULS} = 444.63 \cdot kN$$

$$R_{max.t.z} := R_{max.t.ULS} = -191.326 \cdot kN$$

Maximum shear force in support C
Design shear force = negative shear

$$V_{max.z} := \max\left(\left|V_{max.ULS}\right|, \left|V_{min.ULS}\right|\right) = 267.331 \cdot kN$$

Maximum deflection in span 3

$$\delta_{max.uls} := f_{max.down.ULS} = -24.744 \cdot mm$$

Load response - transverse load in ULS

Distributed loads, transverse load

$q_{1.ULS.x} := q_{d.x} = 3.22 \cdot \frac{kN}{m}$

$q_{3.ULS.x} := q_{d.x} = 3.22 \cdot \frac{kN}{m}$

$q_{2.ULS.x} := q_{d.x} = 3.22 \cdot \frac{kN}{m}$

$q_{4.ULS.x} := q_{d.x} = 3.22 \cdot \frac{kN}{m}$

Support rotation

Continuum condition gives:

$\theta_{B1} = -\theta_{B2}$

$-\theta_{C1} = \theta_{C2}$

$\theta_{D1} = -\theta_{D2}$

Support moment

$M_{A.ULS.x} := 0kN \cdot m$ End support hill-side

$M_{E.ULS.x} := 0 \cdot kN \cdot m$ End support lake-side

$M_{C.guess} := 1000kN \cdot m$ Initial guess

$$M_{B.ULS.x}(M_{C.ULS.x}) := \frac{-\left(\frac{M_{A.ULS.x} \cdot L_1}{6} + \frac{q_{1.ULS.x} \cdot L_1^3}{24} + \frac{M_{C.ULS.x} \cdot L_2}{6} + \frac{q_{2.ULS.x} \cdot L_2^3}{24}\right)}{\left(\frac{L_1 + L_2}{3}\right)}$$

$$M_C = \frac{-\left(\frac{M_B \cdot L_2}{6} + \frac{q_2 \cdot L_2^3}{24} + \frac{M_D \cdot L_3}{6} + \frac{q_3 \cdot L_3^3}{24}\right)}{\left(\frac{L_2 + L_3}{3}\right)}$$

$$M_{D.ULS.x}(M_{C.ULS.x}) := \frac{-\left(\frac{M_{C.ULS.x} \cdot L_3}{6} + \frac{q_{3.ULS.x} \cdot L_3^3}{24} + \frac{M_{E.ULS.x} \cdot L_4}{6} + \frac{q_{4.ULS.x} \cdot L_4^3}{24}\right)}{\left(\frac{L_3 + L_4}{3}\right)}$$

$$M_{C.ULS.x} := \operatorname{root}\left[M_{C.guess} + \frac{\left(\frac{M_{B.ULS.x}(M_{C.guess}) \cdot L_2}{6} + \frac{q_{2.ULS.x} \cdot L_2^3}{24} \ldots + \frac{M_{D.ULS.x}(M_{C.guess}) \cdot L_3}{6} + \frac{q_{3.ULS.x} \cdot L_3^3}{24}\right)}{\left(\frac{L_2 + L_3}{3}\right)}, M_{C.guess}\right] = -73.618 \cdot kN \cdot m$$

$M_{B.ULS.x} := M_{B.ULS.x}(M_{C.ULS.x}) = 6.945 \cdot kN \cdot m$

$M_{D.ULS.x} := M_{D.ULS.x}(M_{C.ULS.x}) = -62.84 \cdot kN \cdot m$

$M_{max.s.ULS.x} := \min(M_{A.ULS.x}, M_{B.ULS.x}, M_{C.ULS.x}, M_{D.ULS.x}, M_{E.ULS.x}) = -73.618 \cdot kN \cdot m$

Reaction forces

$$R_{A.ULS.x} := \frac{-M_{A.ULS.x}}{L_1} + \frac{M_{B.ULS.x}}{L_1} + \frac{q_{1.ULS.x} \cdot L_1}{2} = 8.415 \cdot kN$$

$$R_{B1.ULS.x} := \frac{M_{A.ULS.x}}{L_1} + \frac{-M_{B.ULS.x}}{L_1} + \frac{q_{1.ULS.x} \cdot L_1}{2} = 5.107 \cdot kN$$

$$R_{B2.ULS.x} := \frac{-M_{B.ULS.x}}{L_2} + \frac{M_{C.ULS.x}}{L_2} + \frac{q_{2.ULS.x} \cdot L_2}{2} = -34.983 \cdot kN$$

$$R_{B.ULS.x} := R_{B1.ULS.x} + R_{B2.ULS.x} = -29.876 \cdot kN$$

$$R_{C1.ULS.x} := \frac{M_{B.ULS.x}}{L_2} + \frac{-M_{C.ULS.x}}{L_2} + \frac{q_{2.ULS.x} \cdot L_2}{2} = 41.744 \cdot kN$$

$$R_{C2.ULS.x} := \frac{-M_{C.ULS.x}}{L_3} + \frac{M_{D.ULS.x}}{L_3} + \frac{q_{3.ULS.x} \cdot L_3}{2} = 27.685 \cdot kN$$

$$R_{C.ULS.x} := R_{C1.ULS.x} + R_{C2.ULS.x} = 69.429 \cdot kN$$

$$R_{D1.ULS.x} := \frac{M_{C.ULS.x}}{L_3} + \frac{-M_{D.ULS.x}}{L_3} + \frac{q_{3.ULS.x} \cdot L_3}{2} = 26.402 \cdot kN$$

$$R_{D2.ULS.x} := \frac{-M_{D.ULS.x}}{L_4} + \frac{M_{E.ULS.x}}{L_4} + \frac{q_{4.ULS.x} \cdot L_4}{2} = 21.723 \cdot kN$$

$$R_{D.ULS.x} := R_{D1.ULS.x} + R_{D2.ULS.x} = 48.125 \cdot kN$$

$$R_{E.ULS.x} := \frac{M_{D.ULS.x}}{L_4} + \frac{-M_{E.ULS.x}}{L_4} + \frac{q_{4.ULS.x} \cdot L_4}{2} = -8.201 \cdot kN$$

$$R_{tot.ULS.x} := q_{1.ULS.x} \cdot L_1 + q_{2.ULS.x} \cdot L_2 + q_{3.ULS.x} \cdot L_3 + q_{4.ULS.x} \cdot L_4 = 87.893 \cdot kN$$ Total reaction force

$$R_{check.ULS.x} := R_{A.ULS.x} + R_{B.ULS.x} + R_{C.ULS.x} + R_{D.ULS.x} + R_{E.ULS.x} - R_{tot.ULS.x} = 1.455 \times 10^{-14} \cdot kN$$

$$R_{max.c.ULS.x} := \max\left(R_{A.ULS.x}, R_{B.ULS.x}, R_{C.ULS.x}, R_{D.ULS.x}, R_{E.ULS.x}\right) = 69.429 \cdot kN$$

$$R_{max.t.ULS.x} := \min\left(R_{A.ULS.x}, R_{B.ULS.x}, R_{C.ULS.x}, R_{D.ULS.x}, R_{E.ULS.x}\right) = -29.876 \cdot kN$$

Shear force distribution

$$V_{1.ULS.x}(x) := R_{A.ULS.x} - q_{1.ULS.x} \cdot x$$
$$V_{2.ULS.x}(x) := R_{A.ULS.x} + R_{B.ULS.x} - q_{1.ULS.x} \cdot L_1 - q_{2.ULS.x} \cdot \left(x - L_1\right)$$
$$V_{3.ULS.x}(x) := R_{A.ULS.x} + R_{B.ULS.x} + R_{C.ULS.x} - q_{1.ULS.x} \cdot L_1 - q_{2.ULS.x} \cdot L_2 - q_{3.ULS.x} \cdot \left[x - \left(L_1 + L_2\right)\right]$$
$$V_{4.ULS.x}(x) := R_{A.ULS.x} + R_{B.ULS.x} + R_{C.ULS.x} + R_{D.ULS.x} \cdots$$
$$+ -q_{1.ULS.x} \cdot L_1 - q_{2.ULS.x} \cdot L_2 - q_{3.ULS.x} \cdot L_3 - q_{4.ULS.x} \cdot \left[x - \left(L_1 + L_2 + L_3\right)\right]$$

$$V_{ULS.x}(x) := \left| \begin{array}{l} V_{1.ULS.x}(x) \ \text{ if } \ x \le L_1 \\ V_{2.ULS.x}(x) \ \text{ if } \ L_1 < x \le L_1 + L_2 \\ V_{3.ULS.x}(x) \ \text{ if } \ L_1 + L_2 < x \le L_1 + L_2 + L_3 \\ V_{4.ULS.x}(x) \ \text{ if } \ L_1 + L_2 + L_3 < x \le L_1 + L_2 + L_3 + L_4 \end{array} \right.$$

$$V_{A.x.ULS.x} := \begin{pmatrix} 0m \\ 0m \end{pmatrix} \qquad V_{A.y.ULS.x} := \begin{pmatrix} 0 \\ R_{A.ULS.x} \end{pmatrix} = \begin{pmatrix} 0 \\ 8.415 \end{pmatrix} \cdot kN$$

$$V_{B.x.ULS.x} := \begin{pmatrix} L_1 \\ L_1 \end{pmatrix} = \begin{pmatrix} 4.2 \\ 4.2 \end{pmatrix} m \qquad V_{B.y.ULS.x} := \begin{pmatrix} R_{B2.ULS.x} \\ -R_{B1.ULS.x} \end{pmatrix} = \begin{pmatrix} -34.983 \\ -5.107 \end{pmatrix} \cdot kN$$

$$V_{C.x.ULS.x} := \begin{pmatrix} L_1 + L_2 \\ L_1 + L_2 \end{pmatrix} = \begin{pmatrix} 6.3 \\ 6.3 \end{pmatrix} m \qquad V_{C.y.ULS.x} := \begin{pmatrix} R_{C2.ULS.x} \\ -R_{C1.ULS.x} \end{pmatrix} = \begin{pmatrix} 27.685 \\ -41.744 \end{pmatrix} \cdot kN$$

$$V_{D.x.ULS.x} := \begin{pmatrix} L_1 + L_2 + L_3 \\ L_1 + L_2 + L_3 \end{pmatrix} = \begin{pmatrix} 23.1 \\ 23.1 \end{pmatrix} m \qquad V_{D.y.ULS.x} := \begin{pmatrix} R_{D2.ULS.x} \\ -R_{D1.ULS.x} \end{pmatrix} = \begin{pmatrix} 21.723 \\ -26.402 \end{pmatrix} \cdot kN$$

$$V_{E.x.ULS.x} := \begin{pmatrix} L_1 + L_2 + L_3 + L_4 \\ L_1 + L_2 + L_3 + L_4 \end{pmatrix} = \begin{pmatrix} 27.3 \\ 27.3 \end{pmatrix} m \qquad V_{E.y.ULS.x} := \begin{pmatrix} -R_{E.ULS.x} \\ 0 \end{pmatrix} = \begin{pmatrix} 8.201 \\ 0 \end{pmatrix} \cdot kN$$

$$V_{max.ULS.x} := \max\left(V_{A.y.ULS.x}, V_{B.y.ULS.x}, V_{C.y.ULS.x}, V_{D.y.ULS.x}, V_{E.y.ULS.x}\right) = 27.685 \cdot kN$$
$$V_{min.ULS.x} := \min\left(V_{A.y.ULS.x}, V_{B.y.ULS.x}, V_{C.y.ULS.x}, V_{D.y.ULS.x}, V_{E.y.ULS.x}\right) = -41.744 \cdot kN$$

Moment distribution

$$M_{1.ULS.x}(x) := R_{A.ULS.x} \cdot x - q_{1.ULS.x} \cdot x \cdot \frac{x}{2}$$

$$M_{2.ULS.x}(x) := R_{A.ULS.x} \cdot x + R_{B.ULS.x} \cdot \left(x - L_1\right) - q_{1.ULS.x} \cdot L_1 \cdot \left(x - \frac{L_1}{2}\right) - q_{2.ULS.x} \cdot \left(x - L_1\right) \cdot \left(\frac{x - L_1}{2}\right)$$

$$M_{3.ULS.x}(x) := R_{A.ULS.x} \cdot x + R_{B.ULS.x} \cdot \left(x - L_1\right) + R_{C.ULS.x} \cdot \left[x - \left(L_1 + L_2\right)\right] - q_{1.ULS.x} \cdot L_1 \cdot \left(x - \frac{L_1}{2}\right) \ldots$$
$$+ -q_{2.ULS.x} \cdot L_2 \cdot \left[x - \left(L_1 + \frac{L_2}{2}\right)\right] - q_{3.ULS.x} \cdot \left[x - \left(L_1 + L_2\right)\right] \cdot \left[\frac{x - \left(L_1 + L_2\right)}{2}\right]$$

$$M_{4.ULS.x}(x) := R_{A.ULS.x} \cdot x + R_{B.ULS.x} \cdot \left(x - L_1\right) + R_{C.ULS.x} \cdot \left[x - \left(L_1 + L_2\right)\right] + R_{D.ULS.x} \cdot \left[x - \left(L_1 + L_2 + L_3\right)\right]$$
$$+ -q_{1.ULS.x} \cdot L_1 \cdot \left(x - \frac{L_1}{2}\right) - q_{2.ULS.x} \cdot L_2 \cdot \left[x - \left(L_1 + \frac{L_2}{2}\right)\right] - q_{3.ULS.x} \cdot L_3 \cdot \left[x - \left(L_1 + L_2 + \frac{L_3}{2}\right)\right]$$
$$+ -q_{4.ULS.x} \cdot \left[x - \left(L_1 + L_2 + L_3\right)\right] \cdot \left[\frac{x - \left(L_1 + L_2 + L_3\right)}{2}\right]$$

$$M_{ULS.x}(x) := \begin{cases} M_{1.ULS.x}(x) & \text{if } x \le L_1 \\ M_{2.ULS.x}(x) & \text{if } L_1 < x \le L_1 + L_2 \\ M_{3.ULS.x}(x) & \text{if } L_1 + L_2 < x \le L_1 + L_2 + L_3 \\ M_{4.ULS.x}(x) & \text{if } L_1 + L_2 + L_3 < x \le L_1 + L_2 + L_3 + L_4 \end{cases}$$

Field moment

$$x_{00} := 0$$

$$x_{0.1.ULS.x} := \text{Maximize}\left(M_{1.ULS.x}, x_{00}\right) = 2.614\,m$$

Point where shear force is zero

$$x_{0.2.ULS.x} := \text{Maximize}\left(M_{2.ULS.x}, x_{00}\right) = -6.666\,m$$
$$x_{0.3.ULS.x} := \text{Maximize}\left(M_{3.ULS.x}, x_{00}\right) = 14.899\,m$$
$$x_{0.4.ULS.x} := \text{Maximize}\left(M_{4.ULS.x}, x_{00}\right) = 29.847\,m$$

$$x_{0.1.ULS.x} := \begin{cases} x_{0.1.ULS.x} & \text{if } 0m \le x_{0.1.ULS.x} \le L_1 \\ 0m & \text{otherwise} \end{cases}$$

Check if zero shear force point is within the span, otherwise it is replaced with a dummy number.

$$x_{0.2.ULS.x} := \begin{cases} x_{0.2.ULS.x} & \text{if } L_1 \le x_{0.2.ULS.x} \le L_1 + L_2 \\ L_1 & \text{otherwise} \end{cases}$$

$$x_{0.3.ULS.x} := \begin{cases} x_{0.3.ULS.x} & \text{if } L_1 + L_2 \le x_{0.3.ULS.x} \le L_1 + L_2 + L_3 \\ L_1 + L_2 & \text{otherwise} \end{cases}$$

$$x_{0.4.ULS.x} := \begin{cases} x_{0.4.ULS.x} & \text{if } L_1 + L_2 + L_3 \le x_{0.4.ULS.x} \le L_1 + L_2 + L_3 + L_4 \\ L_{tot} & \text{otherwise} \end{cases}$$

$$M_{f1.ULS.x} := M_{1.ULS.x}\left(x_{0.1.ULS.x}\right) = 10.996 \cdot kN \cdot m$$

$$M_{f2.ULS.x} := M_{2.ULS.x}\left(x_{0.2.ULS.x}\right) = 6.945 \cdot kN \cdot m$$

$$M_{f3.ULS.x} := M_{3.ULS.x}\left(x_{0.3.ULS.x}\right) = 45.419 \cdot kN \cdot m$$

$$M_{f4.ULS.x} := M_{4.ULS.x}\left(x_{0.4.ULS.x}\right) = 0 \cdot kN \cdot m$$

$$M_{max.f.ULS.x} := \max\left(M_{f1.ULS.x}, M_{f2.ULS.x}, M_{f3.ULS.x}, M_{f4.ULS.x}\right) = 45.419 \cdot kN \cdot m$$ Maximum field moment

Zero moment positions

$$x_{M0.1.ULS.x} := \text{root}\left(M_{ULS.x}(x), x, 0, \frac{L_1}{2}\right) = 0\,m$$

$$x_{M0.2.ULS.x} := \text{root}\left(M_{ULS.x}(x), x, \frac{L_1}{2}, L_1 + \frac{L_2}{2}\right) = 4.397\,m$$

$$x_{M0.3.ULS.x} := \text{root}\left(M_{ULS.x}(x), x, L_1 + \frac{L_2}{2}, L_1 + L_2 + \frac{L_3}{2}\right) = 9.587\,m$$

$$x_{M0.4.ULS.x} := \text{root}\left(M_{ULS.x}(x), x, L_1 + L_2 + \frac{L_3}{2}, L_1 + L_2 + L_3 + \frac{L_4}{2}\right) = 20.211\,m$$

$$x_{M0.5.ULS.x} := \text{root}\left(M_{ULS.x}(x), x, L_1 + L_2 + L_3 + \frac{L_4}{2}, L_{tot}\right) = 27.3\,m$$

Summary of design load response - transverse load in ULS

Maximum support moment in support C
Maximum field moment in field 3

$$M_{max.x} := \max\left(\left|M_{max.s.ULS.x}\right|, \left|M_{max.f.ULS.x}\right|\right) = 73.618 \cdot kN \cdot m$$

Maximum reaction force (compression) in support C
Maximum reaction force (tension) in support B

$$R_{max.c.x} := R_{max.c.ULS.x} = 69.429 \cdot kN$$

$$R_{max.t.x} := R_{max.t.ULS.x} = -29.876 \cdot kN$$

Maximum shear force in support C
Design shear force = negative shear

$$V_{max.x} := \max\left(\left|V_{max.ULS.x}\right|, \left|V_{min.ULS.x}\right|\right) = 41.744 \cdot kN$$

Load response - longitudinal load in ULS

Distributed axial load on all beams in the cross-section

$$q_{d.y} = 3.993 \cdot kN$$

$$q_{d.y.beams} := \frac{q_{d.y}}{B - 2 \cdot c_{lvl.s}} = 1.901 \cdot \frac{kN}{m}$$ Design load

Design stresses - ULS

Bending stress calculated in the center of gravity of the beams over the third support

$$\sigma_{m.d.z} := \frac{M_{max.z}}{W_x} = 8.084 \cdot MPa$$ Vertical laod

$$\sigma_{m.d.x} := \frac{M_{max.x}}{W_z} = 0.177 \cdot MPa$$ Transverse load

$k_m := 0.7$ LVL

Edgewise bending in z-direction

Verify according to EN 1995-1-1 eq. 6.11, 6.12.

$$\eta_{m.zx} := \frac{\sigma_{m.d.z}}{f_{m.0.edge.d.lvl}} + k_m \cdot \frac{\sigma_{m.d.x}}{f_{m.0.flat.d.lvl}} = 0.485$$

$$\eta_{m.xz} := k_m \cdot \frac{\sigma_{m.d.z}}{f_{m.0.edge.d.lvl}} + \frac{\sigma_{m.d.x}}{f_{m.0.flat.d.lvl}} = 0.344$$

Moment capacity of the straight LVL beam

$$W_{lvl.s.x} := \frac{b_{lvl.s} \cdot h_{lvl.s}^{2}}{6} = 6.48 \times 10^{-3} \cdot m^3 \qquad W_{lvl.s.z} := \frac{h_{lvl.s} \cdot b_{lvl.s}^{2}}{6} = 1.166 \times 10^{-3} \cdot m^3$$

$$M_{Rd.lvl.s.z} := W_{lvl.s.x} \cdot f_{m.0.edge.d.lvl} = 109.318 \cdot kN \cdot m$$

$$M_{Rd.lvl.s.x} := W_{lvl.s.z} \cdot f_{m.0.edge.d.lvl} = 19.677 \cdot kN \cdot m$$

Utilisation of the bending capacity of the straight beams

$$M_{Ed.z} := \frac{M_{max.z}}{n_{lvl.s} + n_{lvl}} = 29.466 \cdot kN \cdot m \qquad M_{Ed.x} := \frac{M_{max.x}}{n_{lvl.s} + n_{lvl}} = 4.601 \cdot kN \cdot m$$

$$\eta_{M.s.z} := \frac{M_{Ed.z}}{M_{Rd.lvl.s.z}} = 0.27 \qquad \eta_{M.s.x} := \frac{M_{Ed.x}}{M_{Rd.lvl.s.x}} = 0.234$$

Design bending stresses in one straight LVL beam

$$\sigma_{m.d.s.z} := \frac{M_{Ed.z}}{W_{lvl.s.x}} = 4.547 \cdot MPa$$

$$\sigma_{m.d.s.x} := \frac{M_{Ed.x}}{W_{lvl.s.z}} = 3.945 \cdot MPa$$

<u>Moment capacity of the curved LVL panel</u>

$$W_{lvl.x} := \frac{b_{lvl} \cdot h_{lvl}^{2}}{6} = 3.24 \times 10^{-3} \cdot m^{3} \qquad W_{lvl.z} := \frac{h_{lvl} \cdot b_{lvl}^{2}}{6} = 2.916 \times 10^{-4} \cdot m^{3}$$

$$M_{Rd.lvl.z} := W_{lvl.x} \cdot f_{m.0.edge.d.lvl} = 54.659 \cdot kN \cdot m$$

$$M_{Rd.lvl.x} := W_{lvl.z} \cdot f_{m.0.edge.d.lvl} = 4.919 \cdot kN \cdot m$$

Utilisation of the bending capacity of the straight beams

$$\eta_{M.curve.z} := \frac{M_{Ed.z}}{M_{Rd.lvl.z}} = 0.539 \qquad \eta_{M.curve.x} := \frac{M_{Ed.x}}{M_{Rd.lvl.x}} = 93.532 \cdot \%$$

Design bending stresses in one curved LVL panel

$$\sigma_{m.d.curve.z} := \frac{M_{Ed.z}}{W_{lvl.x}} = 9.094 \cdot MPa$$

Still assuming that the panels are straight

$$\sigma_{m.d.curve.x} := \frac{M_{Ed.x}}{W_{lvl.z}} = 15.779 \cdot MPa$$

Check bending stresses due to induced deformation

According to EN1995-1-1 chp. 6.4.3 (for glulam and LVL)

$$\sigma_{m.90.d} \le k_r \cdot f_{m.d}$$

EN 1995-1-1 eq. 6.41

$t_{lvl} = 0.027\,m$ Thickness one lamella

$r_{sin} = 14.5\,m$ Radius of the curved panels

Stresses in the curved zone of the bent panels, between the lamellas

$$\sigma_{m.90.d} := \frac{E_{0.k.lvl} \cdot t_{lvl}}{2 \cdot r_{sin}} = 10.8 \cdot MPa$$

$$k_{r.lvl} := \left| \begin{array}{l} 0.76 + 0.001 \cdot \frac{r_{sin}}{b_{lvl}} \ \text{ if } \ \frac{r_{sin}}{b_{lvl}} < 240 \\ 1 \ \text{ otherwise} \end{array} \right. = 1$$

EN 1995-1-1 eq 6.41

Verify

$$\eta_{m.90.d} := \frac{\sigma_{m.90.d}}{k_{r.lvl} \cdot f_{m.0.flat.d.lvl}} = 0.518$$

Combine the induced bending stresses with stresses from applied load and axial compression forces

Design compression stresses

$$F_{c.0.d} := q_{d.y} \cdot \left(n_{lvl} + n_{lvl.s}\right) = 63.888 \cdot kN$$ Compression force in all elements

$$F_{c.0.n.d} := q_{d.y} = 3.993 \cdot kN$$ Compression force in one element

$$\sigma_{c.y} := \frac{F_{c.0.d}}{A_{tot}} = 0.11 \cdot MPa$$ Design compression stress, all elements

$$\sigma_{c.y.s} := \frac{F_{c.0.n.d}}{A_{lvl.s}} = 0.062 \cdot MPa$$ Design compression stress, one straight LVL beam

$$\sigma_{c.y.curve} := \frac{F_{c.0.n.d}}{A_{lvl}} = 0.123 \cdot MPa$$ Design compression stress, one LVL panel

Utilisation in compression only

Verify according to EN 1995-1-1 eq. 6.2

$$\eta_{c.y} := \frac{\left|\sigma_{c.y}\right|}{f_{c.0.d.lvl}} = 7.512 \times 10^{-3}$$

$$\eta_{c.y.s} := \frac{\left|\sigma_{c.y.s}\right|}{f_{c.0.d.lvl}} = 4.225 \times 10^{-3}$$

$$\eta_{c.y.curve} := \frac{\left|\sigma_{c.y.curve}\right|}{f_{c.0.d.lvl}} = 8.451 \times 10^{-3}$$

Control of bending in two directions and axial compression - straight LVL beam

The straight LVL beam is subjected to bending and axial compression and should be verified according to EN1995-1-1 6.2.4 (combined bending and axial compression).

Check interaction according to EN1995-1-1 6.2.4

Edgewise orientation in z-direction

$$k_m = 0.7$$ EN1995-1-1 6.1.6 (2)

$$\eta_{m.d.s.xz} := \left(\frac{\sigma_{c.y.s}}{f_{c.0.d.lvl}}\right)^2 + k_m \cdot \frac{\sigma_{m.d.s.z}}{f_{m.0.edge.d.lvl}} + \frac{\sigma_{m.d.s.x}}{f_{m.0.flat.d.lvl}}$$ EN1995-1-1 eq. 6.19

$$\eta_{m.d.s.zx} := \left(\frac{\sigma_{c.y.s}}{f_{c.0.d.lvl}}\right)^2 + \frac{\sigma_{m.d.s.z}}{f_{m.0.edge.d.lvl}} + k_m \cdot \frac{\sigma_{m.d.s.x}}{f_{m.0.flat.d.lvl}}$$ EN1995-1-1 eq. 6.20

Control of bending and axial compression - curved LVL panels

The LVL panels are initially deformed and subjected to bending and axial compression, and should be verified according to EN1995-1-1 6.3.3 (stability).

As the LVL panels are designed to work as a horizontal truss, the bending in x-direction will not be checked for one panel only. Bending in z-direction + compression + induced deformation will be checked for one panel.

$s_{sin} = 2.1\,m$ — Distance between the distancers

$l_{ef.curve} := 0.9 s_{sin}$ — Simply supported beam, uniformly distributed load — EN1995-1-1 tab. 6.1

Critical bendning stress, for softwood with solid rectangular cross-section

$$\sigma_{m.crit.curve} := \frac{0.78 \cdot b_{lvl}^{\,2}}{h_{lvl} \cdot l_{ef.curve}} \cdot E_{0.k.lvl} = 23.266 \cdot MPa$$ EN1995-1-1 eq. 6.32

Relative slenderness for bending

$$\lambda_{rel.m.curve} := \sqrt{\frac{f_{m.0.edge.k.lvl}}{\sigma_{m.crit.curve}}} = 1.375$$ EN1995-1-1 eq. 6.30

Factor considering reduced bending strength due to lateral buckling

$k_{crit} := 1$

<u>Calculate instability factor for the curved panel</u>

$$i_{z.curve} := \sqrt{\frac{I_{z.lvl}}{A_{lvl}}}$$ DTS 5.2 p. 26

$l_{e.curve} := s_{sin} = 2.1\,m$

Slenderness ratio

$$\lambda_{z.curve} := \frac{l_{e.curve}}{i_{z.curve}} = 134.715$$

$$\lambda_{rel.z.curve} := \frac{\lambda_{z.curve}}{\pi} \cdot \sqrt{\frac{f_{c.0.k.lvl}}{E_{0.k.lvl}}} = 2.355$$ EN1995-1-1 eq. 6.22

$$Control_{\lambda.rel.z.curve} := \begin{cases} \text{"Eq. 6.19, 6.20"} & \text{if } \lambda_{rel.z.curve} < 0.3 \\ \text{"Eq. 6.23, 6.24"} & \text{otherwise} \end{cases} = \text{"Eq. 6.23, 6.24"}$$

The stresses in z-direction increase due to deflection. Check capacity according to EN1995-1-1 ***eq. 6.24.***

$\beta_c := 0.1$ — EN1995-1-1 eq. 6.29

$$k_{z.curve} := 0.5 \cdot \left[1 + \beta_c \cdot \left(\lambda_{rel.z.curve} - 0.3\right) + \lambda_{rel.z.curve}^{\,2}\right] = 3.377$$ EN1995-1-1 eq. 6.28

$$k_{c.z.curve} := \frac{1}{k_{z.curve} + \sqrt{k_{z.curve}^{\,2} - \lambda_{rel.z.curve}^{\,2}}} = 0.173$$ EN1995-1-1 eq. 6.26

Panel in bending in one direction and compression

$$\eta_{m.d.curve.cz} := \frac{\sigma_{c.y.curve}}{k_{c.z.curve} \cdot f_{c.0.d.lvl}} + \left(\frac{\sigma_{m.d.curve.z}}{k_{crit} \cdot f_{m.0.edge.d.lvl}} \right)^2 = 0.34$$

EN 1995-1-1 eq. 6.35

Panel in bending inone direction, compression and induced deformations

Assume partly interaction

$k_{curve} := 0.7$

$$\eta_{m.d.curve.czd} := \frac{\sigma_{c.y.curve}}{k_{c.z.curve} \cdot f_{c.0.d.lvl}} + \left(\frac{\sigma_{m.d.curve.z}}{k_{crit} \cdot f_{m.0.edge.d.lvl}} \right)^2 + k_{curve} \cdot \frac{\sigma_{m.90.d}}{k_{r.lvl} \cdot f_{m.0.flat.d.lvl}} = 0.702$$

Control of bending and axial compression - whole cross-section

Largest unsupported span

$L_3 = 16.8\,m$

EN1995-1-1 tab. 6.1

Simply supported beam, uniformly distributed load

$l_{ef.deck} := 0.9 \cdot L$

Critical bendning stress, for softwood with solid rectangular cross-section

$$\sigma_{m.crit.deck} := \frac{0.78 \cdot \left(B - 2c_{lvl.s}\right)^2}{h_{lvl} \cdot l_{ef.curve}} \cdot E_{0.k.lvl} = 3.519 \times 10^4 \cdot MPa$$

EN1995-1-1 eq. 6.32

Relative slenderness for bending

$$\lambda_{rel.m.deck} := \sqrt{\frac{f_{m.0.edge.k.lvl}}{\sigma_{m.crit.deck}}} = 0.035$$

EN1995-1-1 eq. 6.30

$k_{crit} = 1$

Calculate instability factor for the whole bridge deck

$$i_{x.deck} := \sqrt{\frac{I_{x.tot}}{A_{tot}}} = 0.173\,m \qquad i_{z.deck} := \sqrt{\frac{I_{z.tot}}{A_{tot}}} = 0.865\,m$$

DTS 5.2 p. 26

$l_{e.x.deck} := s_{sin} = 2.1\,m \qquad l_{e.z.deck} := L$

$$\lambda_{x.deck} := \frac{l_{e.x.deck}}{i_{x.deck}} = 12.124 \qquad \lambda_{z.deck} := \frac{l_{e.z.deck}}{i_{z.deck}} = 31.561$$

$$\lambda_{rel.z.deck} := \frac{\lambda_{z.deck}}{\pi} \cdot \sqrt{\frac{f_{c.0.k.lvl}}{E_{0.k.lvl}}} = 0.552$$

EN1995-1-1 eq. 6.22

$$\lambda_{rel.x.deck} := \frac{\lambda_{x.deck}}{\pi} \cdot \sqrt{\frac{f_{c.0.k.lvl}}{E_{0.k.lvl}}} = 0.212$$

$$\text{Control}_{\lambda.rel.z.deck} := \begin{cases} \text{"Eq. 6.19, 6.20"} & \text{if } \lambda_{rel.z.deck} < 0.3 \\ \text{"Eq. 6.23, 6.24"} & \text{otherwise} \end{cases} = \text{"Eq. 6.23, 6.24"}$$

$$\text{Control}_{\lambda.rel.x.deck} := \begin{cases} \text{"Eq. 6.19, 6.20"} & \text{if } \lambda_{rel.x.deck} < 0.3 \\ \text{"Eq. 6.23, 6.24"} & \text{otherwise} \end{cases} = \text{"Eq. 6.19, 6.20"}$$

Both slenderness ratios must be <0.3 to use eq. 6.19-20.

*The stresses increase due to deflection. Check capacity according to **eq. 6.23, 24.***

$$k_{z.deck} := 0.5 \cdot \left[1 + \beta_c \cdot \left(\lambda_{rel.z.deck} - 0.3\right) + \lambda_{rel.z.deck}^2\right] = 0.665$$ EN1995-1-1 eq. 6.28

$$k_{x.deck} := 0.5 \cdot \left[1 + \beta_c \cdot \left(\lambda_{rel.x.deck} - 0.3\right) + \lambda_{rel.x.deck}^2\right] = 0.518$$

$$k_{c.z.deck} := \frac{1}{k_{z.deck} + \sqrt{k_{z.deck}^2 - \lambda_{rel.z.deck}^2}} = 0.966$$ EN1995-1-1 eq. 6.26

$$k_{c.x.deck} := \frac{1}{k_{x.deck} + \sqrt{k_{x.deck}^2 - \lambda_{rel.x.deck}^2}} = 1.009$$

Verify z-direction according to EN1995-1-1 eq. 6.24

$$\eta_{m.d.cz} := \frac{\sigma_{c.y}}{k_{c.z.deck} \cdot f_{c.0.d.lvl}} + \frac{\sigma_{m.d.z}}{f_{m.0.edge.d.lvl}} + k_m \cdot \frac{\sigma_{m.d.x}}{f_{m.0.flat.d.lvl}} = 0.493$$ EN1995-1-1 eq. 6.24

$$\eta_{m.d.cx} := \frac{\sigma_{c.y}}{k_{c.x.deck} \cdot f_{c.0.d.lvl}} + k_m \cdot \frac{\sigma_{m.d.z}}{f_{m.0.edge.d.lvl}} + \frac{\sigma_{m.d.x}}{f_{m.0.flat.d.lvl}} = 0.351$$ EN1995-1-1 eq. 6.23

Control of bending, axial compression and induced deformation - whole cross-section

Mainly bending in x-direction, eq. 6.23

$$\eta_{m.d.cxd} := \frac{\sigma_{c.y}}{k_{c.x.deck} \cdot f_{c.0.d.lvl}} + k_m \cdot \frac{\sigma_{m.d.z}}{f_{m.0.edge.d.lvl}} + \frac{\sigma_{m.d.x}}{f_{m.0.flat.d.lvl}} + k_{curve} \cdot \frac{\sigma_{m.90.d}}{k_{r.lvl} \cdot f_{m.0.flat.d.lvl}} = 0.714$$

Mainly bending in z-direction, eq. 6.24

$$\eta_{m.d.czd} := \frac{\sigma_{c.y}}{k_{c.z.deck} \cdot f_{c.0.d.lvl}} + \frac{\sigma_{m.d.z}}{f_{m.0.edge.d.lvl}} + k_m \cdot \frac{\sigma_{m.d.x}}{f_{m.0.flat.d.lvl}} + k_{curve} \cdot \frac{\sigma_{m.90.d}}{k_{r.lvl} \cdot f_{m.0.flat.d.lvl}} = 0.856$$

Design shear stresses

Shear stresses over the third support

$k_{cr} := 1.0$ LVL EN1995-1-1 eq. 6.13a

Assume interaction between the LVL panels and beams, verify for the whole cross-section area

$$A_{cr} := A_{tot} \cdot k_{cr} = 0.583\,m^2$$

$$\tau_{d.z} := \frac{V_{max.z}}{A_{cr}} = 0.458 \cdot MPa$$ Vertical laod

$$\tau_{d.x} := \frac{V_{max.x}}{A_{cr}} = 0.072 \cdot \text{MPa}$$

Transverse load

Verify according to EN 1995-1-1 eq. 6.13

$$\eta_{\tau.z} := \frac{\tau_{d.z}}{f_{v.0.edge.d.lvl}} = 0.268$$

$$\eta_{\tau.x} := \frac{\tau_{d.x}}{f_{v.0.flat.d.lvl}} = 0.075$$

Summary of utilisation ratios in ULS

Bending

Whole cross-section

Bending, z main

$\eta_{m.zx} = 0.485$

Bending, x main

$\eta_{m.xz} = 0.344$

One straight beam

Capacity ratio, bending z-dir

$\eta_{M.s.z} = 0.27$

Capacity ratio, bending x-dir

$\eta_{M.s.x} = 0.234$

One assumed straight panel

Capacity ratio, bending z-dir

$\eta_{M.curve.z} = 0.539$

Capacity ratio, bending x-dir

$\eta_{M.curve.x} = 0.935$

Induced deformation

One curved panel

$\eta_{m.90.d} = 0.518$

Compression

Whole cross-section

$\eta_{c.y} = 0.751 \cdot \%$

One straight beam

$\eta_{c.y.s} = 0.423 \cdot \%$

One assumed straight panel

$\eta_{c.y.curve} = 0.845 \cdot \%$

Bending + compression

Whole cross-section

Bending, z main

$\eta_{m.d.cz} = 0.493$

Bending, x main

$\eta_{m.d.cx} = 0.351$

One straight beam

Bending, z main

$\eta_{m.d.s.zx} = 0.402$

Bending, x main

$\eta_{m.d.s.xz} = 0.378$

One assumed straight panel

Bending, z-direction only

$\eta_{m.d.curve.cz} = 0.34$

Bending + compression + induced deformation

Whole cross-section

Bending, z main

$\eta_{m.d.czd} = 0.856$

Bending, x main

$\eta_{m.d.cxd} = 0.714$

One curved panel

Bending, z main

$\eta_{m.d.curve.czd} = 0.702$

Shear

Whole cross-section

$\eta_{\tau.z} = 0.268$

$\eta_{\tau.x} = 0.075$

SLS load combinations

Service class 3

$k_{def} := 2.0$ EN1995-1-1 tab. 3.2

Load combinations, vertical load

Partial factors for load combinations in SLS according to STR-2

$\gamma_{sls} := 1.0$ LH3 tab. 5.3

Load combination factors for variable loads on bridges in SLS

$\psi_{1.w} := 0.2$ Wind load frequent load EN1990 tab. A2.2

$\psi_{1.fk} := 0.4$ Traffic load frequent load

$\psi_{2.w} := 0$ Wind load quasi permanent load EN1990 tab. A2.2

$\psi_{2.fk} := 0$ Traffic load qasi permanent load

Load combinations, vertical load, permanent

Self-weight

$$q_{d.sls} := \gamma_{sls} \cdot G_k = 4.387 \cdot \frac{kN}{m}$$

Load combinations, vertical load, variable

Traffic load

$$LC1_{q.f} := \gamma_{sls} \cdot Q_{fk.z} = 10.236 \cdot \frac{kN}{m}$$

$$LC2_{q.f} := \gamma_{sls} \cdot \psi_{2.fk} \cdot Q_{fk.z} = 0 \cdot \frac{kN}{m}$$

$$q_{d.sls.q} := \max\left(LC1_{q.f}, LC2_{q.f}\right) = 10.236 \cdot \frac{kN}{m}$$

Calculate the deflection due to traffic load only (EN1995-2 7.2)

Use man values of density (EN1995-2 7.1 (1)).

Load response - permanent load in SLS

Distributed loads

Load distribution: self-weight is uniformly distributed in all spans.

$q_{1.SLS} := q_{d.sls}$

$q_{2.SLS} := q_{d.sls}$

$q_{3.SLS} := q_{d.sls}$

$q_{4.SLS} := q_{d.sls}$

Support moment

$M_{A.SLS} := 0kN \cdot m$

$M_{E.SLS} := 0 \cdot kN \cdot m$

$M_{C.guess} := 1000kN \cdot m$ Initial guess

$$M_{B.SLS}(M_{C.SLS}) := \frac{-\left(\frac{M_{A.SLS} \cdot L_1}{6} + \frac{q_{1.SLS} \cdot L_1^3}{24} + \frac{M_{C.SLS} \cdot L_2}{6} + \frac{q_{2.SLS} \cdot L_2^3}{24}\right)}{\left(\frac{L_1 + L_2}{3}\right)}$$

$$M_C = \frac{-\left(\frac{M_B \cdot L_2}{6} + \frac{q_2 \cdot L_2^3}{24} + \frac{M_D \cdot L_3}{6} + \frac{q_3 \cdot L_3^3}{24}\right)}{\left(\frac{L_2 + L_3}{3}\right)}$$

$$M_{D.SLS}(M_{C.SLS}) := \frac{-\left(\frac{M_{C.SLS} \cdot L_3}{6} + \frac{q_{3.SLS} \cdot L_3^3}{24} + \frac{M_{E.SLS} \cdot L_4}{6} + \frac{q_{4.SLS} \cdot L_4^3}{24}\right)}{\left(\frac{L_3 + L_4}{3}\right)}$$

$$M_{C.SLS} := \text{root}\left[M_{C.guess} + \frac{\left(\frac{M_{B.SLS}(M_{C.guess}) \cdot L_2}{6} + \frac{q_{2.SLS} \cdot L_2^3}{24} \dots + \frac{M_{D.SLS}(M_{C.guess}) \cdot L_3}{6} + \frac{q_{3.SLS} \cdot L_3^3}{24}\right)}{\left(\frac{L_2 + L_3}{3}\right)}, M_{C.guess}\right] = -100.316 \cdot kN \cdot m$$

$M_{B.SLS} := M_{B.SLS}(M_{C.SLS}) = 9.464 \cdot kN \cdot m$

$M_{D.SLS} := M_{D.SLS}(M_{C.SLS}) = -85.63 \cdot kN \cdot m$

$M_{max.s.SLS} := \min(M_{A.SLS}, M_{B.SLS}, M_{C.SLS}, M_{D.SLS}, M_{E.SLS}) = -100.316 \cdot kN \cdot m$

Reaction forces

$$R_{A.SLS} := \frac{-M_{A.SLS}}{L_1} + \frac{M_{B.SLS}}{L_1} + \frac{q_{1.SLS} \cdot L_1}{2} = 11.466 \cdot kN$$

$$R_{B1.SLS} := \frac{M_{A.SLS}}{L_1} + \frac{-M_{B.SLS}}{L_1} + \frac{q_{1.SLS} \cdot L_1}{2} = 6.96 \cdot kN$$

$$R_{B2.SLS} := \frac{-M_{B.SLS}}{L_2} + \frac{M_{C.SLS}}{L_2} + \frac{q_{2.SLS} \cdot L_2}{2} = -47.67 \cdot kN$$

$$R_{B.SLS} := R_{B1.SLS} + R_{B2.SLS} = -40.71 \cdot kN$$

$$R_{C1.SLS} := \frac{M_{B.SLS}}{L_2} + \frac{-M_{C.SLS}}{L_2} + \frac{q_{2.SLS} \cdot L_2}{2} = 56.883 \cdot kN$$

$$R_{C2.SLS} := \frac{-M_{C.SLS}}{L_3} + \frac{M_{D.SLS}}{L_3} + \frac{q_{3.SLS} \cdot L_3}{2} = 37.726 \cdot kN$$

$$R_{C.SLS} := R_{C1.SLS} + R_{C2.SLS} = 94.609 \cdot kN$$

$$R_{D1.SLS} := \frac{M_{C.SLS}}{L_3} + \frac{-M_{D.SLS}}{L_3} + \frac{q_{3.SLS} \cdot L_3}{2} = 35.977 \cdot kN$$

$$R_{D2.SLS} := \frac{-M_{D.SLS}}{L_4} + \frac{M_{E.SLS}}{L_4} + \frac{q_{4.SLS} \cdot L_4}{2} = 29.601 \cdot kN$$

$$R_{D.SLS} := R_{D1.SLS} + R_{D2.SLS} = 65.578 \cdot kN$$

$$R_{E.SLS} := \frac{M_{D.SLS}}{L_4} + \frac{-M_{E.SLS}}{L_4} + \frac{q_{4.SLS} \cdot L_4}{2} = -11.175 \cdot kN$$

$$R_{tot.SLS} := q_{1.SLS} \cdot L_1 + q_{2.SLS} \cdot L_2 + q_{3.SLS} \cdot L_3 + q_{4.SLS} \cdot L_4 = 119.768 \cdot kN$$ Total reaction force

$$R_{check.SLS} := R_{A.SLS} + R_{B.SLS} + R_{C.SLS} + R_{D.SLS} + R_{E.SLS} - R_{tot.SLS} = -1.455 \times 10^{-14} \cdot kN$$

$$R_{max.c.SLS} := \max\left(R_{A.SLS}, R_{B.SLS}, R_{C.SLS}, R_{D.SLS}, R_{E.SLS}\right) = 94.609 \cdot kN$$

$$R_{max.t.SLS} := \min\left(R_{A.SLS}, R_{B.SLS}, R_{C.SLS}, R_{D.SLS}, R_{E.SLS}\right) = -40.71 \cdot kN$$

Shear force distribution

$$V_{1.SLS}(x) := R_{A.SLS} - q_{1.SLS} \cdot x$$

$$V_{2.SLS}(x) := R_{A.SLS} + R_{B.SLS} - q_{1.SLS} \cdot L_1 - q_{2.SLS} \cdot \left(x - L_1\right)$$

$$V_{3.SLS}(x) := R_{A.SLS} + R_{B.SLS} + R_{C.SLS} - q_{1.SLS} \cdot L_1 - q_{2.SLS} \cdot L_2 - q_{3.SLS} \cdot \left[x - \left(L_1 + L_2\right)\right]$$

$$V_{4.SLS}(x) := R_{A.SLS} + R_{B.SLS} + R_{C.SLS} + R_{D.SLS} \cdots \\ + -q_{1.SLS} \cdot L_1 - q_{2.SLS} \cdot L_2 - q_{3.SLS} \cdot L_3 - q_{4.SLS} \cdot \left[x - \left(L_1 + L_2 + L_3\right)\right]$$

$$V_{SLS}(x) := \begin{cases} V_{1.SLS}(x) & \text{if } x \le L_1 \\ V_{2.SLS}(x) & \text{if } L_1 < x \le L_1 + L_2 \\ V_{3.SLS}(x) & \text{if } L_1 + L_2 < x \le L_1 + L_2 + L_3 \\ V_{4.SLS}(x) & \text{if } L_1 + L_2 + L_3 < x \le L_1 + L_2 + L_3 + L_4 \end{cases}$$

$$V_{A.x.SLS} := \begin{pmatrix} 0m \\ 0m \end{pmatrix} \qquad V_{A.y.SLS} := \begin{pmatrix} 0 \\ R_{A.SLS} \end{pmatrix} = \begin{pmatrix} 0 \\ 11.466 \end{pmatrix} \cdot kN$$

$$V_{B.x.SLS} := \begin{pmatrix} L_1 \\ L_1 \end{pmatrix} = \begin{pmatrix} 4.2 \\ 4.2 \end{pmatrix} m \qquad V_{B.y.SLS} := \begin{pmatrix} R_{B2.SLS} \\ -R_{B1.SLS} \end{pmatrix} = \begin{pmatrix} -47.67 \\ -6.96 \end{pmatrix} \cdot kN$$

$$V_{C.x.SLS} := \begin{pmatrix} L_1 + L_2 \\ L_1 + L_2 \end{pmatrix} = \begin{pmatrix} 6.3 \\ 6.3 \end{pmatrix} m \qquad V_{C.y.SLS} := \begin{pmatrix} R_{C2.SLS} \\ -R_{C1.SLS} \end{pmatrix} = \begin{pmatrix} 37.726 \\ -56.883 \end{pmatrix} \cdot kN$$

$$V_{D.x.SLS} := \begin{pmatrix} L_1 + L_2 + L_3 \\ L_1 + L_2 + L_3 \end{pmatrix} = \begin{pmatrix} 23.1 \\ 23.1 \end{pmatrix} m \qquad V_{D.y.SLS} := \begin{pmatrix} R_{D2.SLS} \\ -R_{D1.SLS} \end{pmatrix} = \begin{pmatrix} 29.601 \\ -35.977 \end{pmatrix} \cdot kN$$

$$V_{E.x.SLS} := \begin{pmatrix} L_1 + L_2 + L_3 + L_4 \\ L_1 + L_2 + L_3 + L_4 \end{pmatrix} = \begin{pmatrix} 27.3 \\ 27.3 \end{pmatrix} m \qquad V_{E.y.SLS} := \begin{pmatrix} -R_{E.SLS} \\ 0 \end{pmatrix} = \begin{pmatrix} 11.175 \\ 0 \end{pmatrix} \cdot kN$$

$$V_{max.SLS} := \max\left(V_{A.y.SLS}, V_{B.y.SLS}, V_{C.y.SLS}, V_{D.y.SLS}, V_{E.y.SLS}\right) = 37.726 \cdot kN$$

$$V_{min.SLS} := \min\left(V_{A.y.SLS}, V_{B.y.SLS}, V_{C.y.SLS}, V_{D.y.SLS}, V_{E.y.SLS}\right) = -56.883 \cdot kN$$

Moment distribution

$$M_{1.SLS}(x) := R_{A.SLS} \cdot x - q_{1.SLS} \cdot x \cdot \frac{x}{2}$$

$$M_{2.SLS}(x) := R_{A.SLS} \cdot x + R_{B.SLS} \cdot \left(x - L_1\right) - q_{1.SLS} \cdot L_1 \cdot \left(x - \frac{L_1}{2}\right) - q_{2.SLS} \cdot \left(x - L_1\right) \cdot \left(\frac{x - L_1}{2}\right)$$

$$M_{3.SLS}(x) := R_{A.SLS} \cdot x + R_{B.SLS} \cdot \left(x - L_1\right) + R_{C.SLS} \cdot \left[x - \left(L_1 + L_2\right)\right] \ldots$$
$$+ -q_{1.SLS} \cdot L_1 \cdot \left(x - \frac{L_1}{2}\right) - q_{2.SLS} \cdot L_2 \cdot \left[x - \left(L_1 + \frac{L_2}{2}\right)\right] - q_{3.SLS} \cdot \left[x - \left(L_1 + L_2\right)\right] \cdot \left[\frac{x - \left(L_1 + L_2\right)}{2}\right]$$

$$M_{4.SLS}(x) := R_{A.SLS} \cdot x + R_{B.SLS} \cdot \left(x - L_1\right) + R_{C.SLS} \cdot \left[x - \left(L_1 + L_2\right)\right] + R_{D.SLS} \cdot \left[x - \left(L_1 + L_2 + L_3\right)\right] \ldots$$
$$+ -q_{1.SLS} \cdot L_1 \cdot \left(x - \frac{L_1}{2}\right) - q_{2.SLS} \cdot L_2 \cdot \left[x - \left(L_1 + \frac{L_2}{2}\right)\right] - q_{3.SLS} \cdot L_3 \cdot \left[x - \left(L_1 + L_2 + \frac{L_3}{2}\right)\right] \ldots$$
$$+ -q_{4.SLS} \cdot \left[x - \left(L_1 + L_2 + L_3\right)\right] \cdot \left[\frac{x - \left(L_1 + L_2 + L_3\right)}{2}\right]$$

$$M_{SLS}(x) := \begin{cases} M_{1.SLS}(x) & \text{if } x \le L_1 \\ M_{2.SLS}(x) & \text{if } L_1 < x \le L_1 + L_2 \\ M_{3.SLS}(x) & \text{if } L_1 + L_2 < x \le L_1 + L_2 + L_3 \\ M_{4.SLS}(x) & \text{if } L_1 + L_2 + L_3 < x \le L_1 + L_2 + L_3 + L_4 \end{cases}$$

Field moment

$$x_{00} = 0$$

$$x_{0.1.SLS} := \text{Maximize}\left(M_{1.SLS}, x_{00}\right) = 2.614\,m$$

Point where shear force is zero

$$x_{0.2.SLS} := \text{Maximize}\left(M_{2.SLS}, x_{00}\right) = -6.666\,m$$

$$x_{0.3.SLS} := \text{Maximize}\left(M_{3.SLS}, x_{00}\right) = 14.899\,m$$

$$x_{0.4.SLS} := \text{Maximize}\left(M_{4.SLS}, x_{00}\right) = 29.847\,m$$

$$x_{0.1.SLS} := \begin{cases} x_{0.1.SLS} & \text{if } 0m \le x_{0.1.SLS} \le L_1 \\ 0m & \text{otherwise} \end{cases}$$

Check if zero shear force point is within the span, otherwise it is replaced with a dummy number.

$$x_{0.2.SLS} := \begin{cases} x_{0.2.SLS} & \text{if } L_1 \le x_{0.2.SLS} \le L_1 + L_2 \\ L_1 & \text{otherwise} \end{cases}$$

$$x_{0.3.SLS} := \begin{cases} x_{0.3.SLS} & \text{if } L_1 + L_2 \le x_{0.3.SLS} \le L_1 + L_2 + L_3 \\ L_1 + L_2 & \text{otherwise} \end{cases}$$

$$x_{0.4.SLS} := \begin{cases} x_{0.4.SLS} & \text{if } L_1 + L_2 + L_3 \le x_{0.4.SLS} \le L_1 + L_2 + L_3 + L_4 \\ L_{tot} & \text{otherwise} \end{cases}$$

$M_{f1.SLS} := M_{1.SLS}(x_{0.1.SLS}) = 14.984 \cdot kN \cdot m$

$M_{f2.SLS} := M_{2.SLS}(x_{0.2.SLS}) = 9.464 \cdot kN \cdot m$

$M_{f3.SLS} := M_{3.SLS}(x_{0.3.SLS}) = 61.891 \cdot kN \cdot m$

$M_{f4.SLS} := M_{4.SLS}(x_{0.4.SLS}) = -9.459 \times 10^{-14} \cdot kN \cdot m$

$M_{max.f.SLS} := \max(M_{f1.SLS}, M_{f2.SLS}, M_{f3.SLS}, M_{f4.SLS}) = 61.891 \cdot kN \cdot m$ Maximum field moment

Zero moment positions

$$x_{M0.1.SLS} := \mathrm{root}\left(M_{SLS}(x), x, 0, \frac{L_1}{2}\right) = 0\,m$$

$$x_{M0.2.SLS} := \mathrm{root}\left(M_{SLS}(x), x, \frac{L_1}{2}, L_1 + \frac{L_2}{2}\right) = 4.397\,m$$

$$x_{M0.3.SLS} := \mathrm{root}\left(M_{SLS}(x), x, L_1 + \frac{L_2}{2}, L_1 + L_2 + \frac{L_3}{2}\right) = 9.587\,m$$

$$x_{M0.4.SLS} := \mathrm{root}\left(M_{SLS}(x), x, L_1 + L_2 + \frac{L_3}{2}, L_1 + L_2 + L_3 + \frac{L_4}{2}\right) = 20.211\,m$$

$$x_{M0.5.SLS} := \mathrm{root}\left(M_{SLS}(x), x, L_1 + L_2 + L_3 + \frac{L_4}{2}, L_{tot}\right) = ▮$$

Deflection

$EI = 241.445 \cdot MPa \cdot m^4$ Flexural Rigidity

$$\kappa_{SLS}(x) := \frac{M_{SLS}(x)}{EI}$$ Curvature

$$\theta_{A.SLS} := \frac{\int_0^{L_1} \kappa_{SLS}(x)\cdot\left(L_1 - x\right)\,dx}{L_1} = 8.353 \times 10^{-5}$$

$$\theta_{B1.SLS} := \frac{\int_0^{L_1} \kappa_{SLS}(x)\cdot x\,dx}{L_1} = 1.11 \times 10^{-4}$$

$$\theta_{B2.SLS} := \frac{\int_{L_1}^{L_1+L_2} \kappa_{SLS}(x)\cdot\left(L_1 + L_2 - x\right)\,dx}{L_2} = -1.11 \times 10^{-4}$$

$$\theta_{C1.SLS} := \frac{\int_{L_1}^{L_1+L_2} \kappa_{SLS}(x)\cdot\left(x - L_1\right)\,dx}{L_2} = -2.701 \times 10^{-4}$$

$$\theta_{C2.SLS} := \frac{\int_{L_1+L_2}^{L_1+L_2+L_3} \kappa_{SLS}(x)\cdot\left(L_1 + L_2 + L_3 - x\right)\,dx}{L_3} = 2.701 \times 10^{-4}$$

$$\theta_{D1.SLS} := \frac{\int_{L_1+L_2}^{L_1+L_2+L_3} \kappa_{SLS}(x)\cdot\left(x - L_1 - L_2\right)\,dx}{L_3} = 4.404 \times 10^{-4}$$

$$\theta_{D2.SLS} := \frac{\int_{L_1+L_2+L_3}^{L_1+L_2+L_3+L_4} \kappa_{SLS}(x)\cdot\left(L_1 + L_2 + L_3 + L_4 - x\right)\,dx}{L_4} = -4.404 \times 10^{-4}$$

$$\theta_{E.SLS} := \frac{\int_{L_1+L_2+L_3}^{L_1+L_2+L_3+L_4} \kappa_{SLS}(x)\cdot\left(x - L_1 - L_2 - L_3\right)\,dx}{L_4} = -1.922 \times 10^{-4}$$

$$f_{1.SLS}(x) := \theta_{A.SLS}\cdot x - \int_0^x \int_0^x \kappa_{SLS}(x)\,dx\,dx$$

$$f_{2.SLS}(x) := \theta_{B2.SLS}\cdot\left(x - L_1\right) - \int_{L_1}^x \int_{L_1}^x \kappa_{SLS}(x)\,dx\,dx$$

$$f_{3.SLS}(x) := \theta_{C2.SLS}\cdot\left(x - L_1 - L_2\right) - \int_{L_1+L_2}^x \int_{L_1+L_2}^x \kappa_{SLS}(x)\,dx\,dx$$

$$f_{4.SLS}(x) := \theta_{D2.SLS} \cdot \left(x - L_1 - L_2 - L_3\right) - \int_{L_1+L_2+L_3}^{x} \int_{L_1+L_2+L_3}^{x} \kappa_{SLS}(x)\, dx\, dx$$

$$f_{SLS}(x) := \begin{vmatrix} f_{1.SLS}(x) & \text{if } x \le L_1 \\ f_{2.SLS}(x) & \text{if } L_1 < x \le L_1 + L_2 \\ f_{3.SLS}(x) & \text{if } L_1 + L_2 < x \le L_1 + L_2 + L_3 \\ f_{4.SLS}(x) & \text{if } L_1 + L_2 + L_3 < x \le L_1 + L_2 + L_3 + L_4 \end{vmatrix}$$

Maximum deflection

$x_{\theta 0.1.guess} = 2.1\,m$ Guess of where curvature is zero

$x_{\theta 0.2.guess} = 5.25\,m$

$x_{\theta 0.3.guess} = 14.7\,m$

$x_{\theta 0.4.guess} = 25.2\,m$

$$x_{\theta 0.1.SLS} := \text{root}\left(\int_{0}^{x_{\theta 0.1.guess}} \kappa_{SLS}(x)\, dx - \theta_{A.SLS}, x_{\theta 0.1.guess}\right) = 2.214\,m$$

Position where curvature is zero

$$x_{\theta 0.2.SLS} := \text{root}\left(\int_{L_1}^{x_{\theta 0.2.guess}} \kappa_{SLS}(x)\, dx - \theta_{B2.SLS}, x_{\theta 0.2.guess}\right) = 5.449\,m$$

$$x_{\theta 0.3.SLS} := \text{root}\left(\int_{L_1+L_2}^{x_{\theta 0.3.guess}} \kappa_{SLS}(x)\, dx - \theta_{C2.SLS}, x_{\theta 0.3.guess}\right) = 14.866\,m$$

$$x_{\theta 0.4.SLS} := \text{root}\left(\int_{L_1+L_2+L_3}^{x_{\theta 0.4.guess}} \kappa_{SLS}(x)\, dx - \theta_{D2.SLS}, x_{\theta 0.4.guess}\right) = 24.799\,m$$

$f_{max.1.SLS} := -f_{1.SLS}\left(x_{\theta 0.1.SLS}\right) = -0.117 \cdot mm$ Maximum field deflection

$f_{max.2.SLS} := -f_{2.SLS}\left(x_{\theta 0.2.SLS}\right) = 0.103 \cdot mm$

$f_{max.3.SLS} := -f_{3.SLS}\left(x_{\theta 0.3.SLS}\right) = -5.265 \cdot mm$

$f_{max.4.SLS} := -f_{4.SLS}\left(x_{\theta 0.4.SLS}\right) = 0.33 \cdot mm$

$f_{max.up.SLS} := \max\left(f_{max.1.SLS}, f_{max.2.SLS}, f_{max.3.SLS}, f_{max.4.SLS}\right) = 0.33 \cdot mm$

$f_{max.down.SLS} := \min\left(f_{max.1.SLS}, f_{max.2.SLS}, f_{max.3.SLS}, f_{max.4.SLS}\right) = -5.265 \cdot mm$

Summary of design load response - permanent load in SLS

Maximum support moment in support C
Maximum field moment in field 3

$$M_{max.sls.z} := \max\left(\left|M_{max.s.SLS}\right|, \left|M_{max.f.SLS}\right|\right) = 100.316 \cdot kN \cdot m$$

Maximum reaction force (compression) in support C
Maximum reaction force (tension) in support B

$$R_{max.c.sls.z} := R_{max.c.SLS} = 94.609 \cdot kN$$

$$R_{max.t.sls.z} := R_{max.t.SLS} = -40.71 \cdot kN$$

Maximum shear force in support C
Design shear force = negative shear

$$V_{max.sls.z} := \max\left(\left|V_{max.SLS}\right|, \left|V_{min.SLS}\right|\right) = 56.883 \cdot kN$$

Maximum deflection in span 3

$$\delta_{max.sls} := f_{max.down.SLS} = -5.265 \cdot mm$$

Load response - variable load in SLS

Distributed loads

Maximum deflection for variable load in span 1+3

$q_{1.SLS.q} := q_{d.sls.q}$ $\qquad$ $q_{3.SLS.q} := q_{d.sls.q}$

$q_{2.SLS.q} := 0$ $\qquad$ $q_{4.SLS.q} := 0$

Support moment

$M_{A.SLS.q} := 0kN\cdot m$

$M_{E.SLS.q} := 0\cdot kN\cdot m$

$M_{C.guess} := 1000kN\cdot m$ Initial guess

$$M_{B.SLS.q}(M_{C.SLS.q}) := \frac{-\left(\frac{M_{A.SLS.q}\cdot L_1}{6} + \frac{q_{1.SLS.q}\cdot L_1^{\,3}}{24} + \frac{M_{C.SLS.q}\cdot L_2}{6} + \frac{q_{2.SLS.q}\cdot L_2^{\,3}}{24}\right)}{\left(\frac{L_1 + L_2}{3}\right)}$$

$$M_C = \frac{-\left(\frac{M_B\cdot L_2}{6} + \frac{q_2\cdot L_2^{\,3}}{24} + \frac{M_D\cdot L_3}{6} + \frac{q_3\cdot L_3^{\,3}}{24}\right)}{\left(\frac{L_2 + L_3}{3}\right)}$$

$$M_{D.SLS.q}(M_{C.SLS.q}) := \frac{-\left(\frac{M_{C.SLS.q}\cdot L_3}{6} + \frac{q_{3.SLS.q}\cdot L_3^{\,3}}{24} + \frac{M_{E.SLS.q}\cdot L_4}{6} + \frac{q_{4.SLS.q}\cdot L_4^{\,3}}{24}\right)}{\left(\frac{L_3 + L_4}{3}\right)}$$

$$M_{C.SLS.q} := \mathrm{root}\left[M_{C.guess} + \frac{\left(\frac{M_{B.SLS.q}(M_{C.guess})\cdot L_2}{6} + \frac{q_{2.SLS.q}\cdot L_2^{\,3}}{24} \ldots + \frac{M_{D.SLS.q}(M_{C.guess})\cdot L_3}{6} + \frac{q_{3.SLS.q}\cdot L_3^{\,3}}{24}\right)}{\left(\frac{L_2 + L_3}{3}\right)}, M_{C.guess}\right] = -235.874\cdot kN\cdot m$$

$M_{B.SLS.q} := M_{B.SLS.q}(M_{C.SLS.q}) = 24.266\cdot kN\cdot m$

$M_{D.SLS.q} := M_{D.SLS.q}(M_{C.SLS.q}) = -194.54\cdot kN\cdot m$

$M_{max.s.SLS.q} := \min(M_{A.SLS.q}, M_{B.SLS.q}, M_{C.SLS.q}, M_{D.SLS.q}, M_{E.SLS.q}) = -235.874\cdot kN\cdot m$

Reaction forces

$$R_{A.SLS.q} := \frac{-M_{A.SLS.q}}{L_1} + \frac{M_{B.SLS.q}}{L_1} + \frac{q_{1.SLS.q}\cdot L_1}{2} = 27.272\cdot kN$$

$$R_{B1.SLS.q} := \frac{M_{A.SLS.q}}{L_1} + \frac{-M_{B.SLS.q}}{L_1} + \frac{q_{1.SLS.q}\cdot L_1}{2} = 15.717\cdot kN$$

$$R_{B2.SLS.q} := \frac{-M_{B.SLS.q}}{L_2} + \frac{M_{C.SLS.q}}{L_2} + \frac{q_{2.SLS.q} \cdot L_2}{2} = -123.876 \cdot kN$$

$$R_{B.SLS.q} := R_{B1.SLS.q} + R_{B2.SLS.q} = -108.159 \cdot kN$$

$$R_{C1.SLS.q} := \frac{M_{B.SLS.q}}{L_2} + \frac{-M_{C.SLS.q}}{L_2} + \frac{q_{2.SLS.q} \cdot L_2}{2} = 123.876 \cdot kN$$

$$R_{C2.SLS.q} := \frac{-M_{C.SLS.q}}{L_3} + \frac{M_{D.SLS.q}}{L_3} + \frac{q_{3.SLS.q} \cdot L_3}{2} = 88.439 \cdot kN$$

$$R_{C.SLS.q} := R_{C1.SLS.q} + R_{C2.SLS.q} = 212.316 \cdot kN$$

$$R_{D1.SLS.q} := \frac{M_{C.SLS.q}}{L_3} + \frac{-M_{D.SLS.q}}{L_3} + \frac{q_{3.SLS.q} \cdot L_3}{2} = 83.519 \cdot kN$$

$$R_{D2.SLS.q} := \frac{-M_{D.SLS.q}}{L_4} + \frac{M_{E.SLS.q}}{L_4} + \frac{q_{4.SLS.q} \cdot L_4}{2} = 46.319 \cdot kN$$

$$R_{D.SLS.q} := R_{D1.SLS.q} + R_{D2.SLS.q} = 129.838 \cdot kN$$

$$R_{E.SLS.q} := \frac{M_{D.SLS.q}}{L_4} + \frac{-M_{E.SLS.q}}{L_4} + \frac{q_{4.SLS.q} \cdot L_4}{2} = -46.319 \cdot kN$$

$$R_{tot.SLS.q} := q_{1.SLS.q} \cdot L_1 + q_{2.SLS.q} \cdot L_2 + q_{3.SLS.q} \cdot L_3 + q_{4.SLS.q} \cdot L_4 = 214.948 \cdot kN$$ Total reaction force

$$R_{check.SLS.q} := R_{A.SLS.q} + R_{B.SLS.q} + R_{C.SLS.q} + R_{D.SLS.q} + R_{E.SLS.q} - R_{tot.SLS.q} = -2.91 \times 10^{-14} \cdot kN$$

$$R_{max.c.SLS.q} := \max\left(R_{A.SLS.q}, R_{B.SLS.q}, R_{C.SLS.q}, R_{D.SLS.q}, R_{E.SLS.q}\right) = 212.316 \cdot kN$$

$$R_{max.t.SLS.q} := \min\left(R_{A.SLS.q}, R_{B.SLS.q}, R_{C.SLS.q}, R_{D.SLS.q}, R_{E.SLS.q}\right) = -108.159 \cdot kN$$

Shear force distribution

$$V_{1.SLS.q}(x) := R_{A.SLS.q} - q_{1.SLS.q} \cdot x$$

$$V_{2.SLS.q}(x) := R_{A.SLS.q} + R_{B.SLS.q} - q_{1.SLS.q} \cdot L_1 - q_{2.SLS.q} \cdot \left(x - L_1\right)$$

$$V_{3.SLS.q}(x) := R_{A.SLS.q} + R_{B.SLS.q} + R_{C.SLS.q} - q_{1.SLS.q} \cdot L_1 - q_{2.SLS.q} \cdot L_2 - q_{3.SLS.q} \cdot \left[x - \left(L_1 + L_2\right)\right]$$

$$V_{4.SLS.q}(x) := R_{A.SLS.q} + R_{B.SLS.q} + R_{C.SLS.q} + R_{D.SLS.q} \cdots \\ + -q_{1.SLS.q} \cdot L_1 - q_{2.SLS.q} \cdot L_2 - q_{3.SLS.q} \cdot L_3 - q_{4.SLS.q} \cdot \left[x - \left(L_1 + L_2 + L_3\right)\right]$$

$$V_{SLS.q}(x) := \left| \begin{array}{l} V_{1.SLS.q}(x) \ \text{ if } x \le L_1 \\ V_{2.SLS.q}(x) \ \text{ if } L_1 < x \le L_1 + L_2 \\ V_{3.SLS.q}(x) \ \text{ if } L_1 + L_2 < x \le L_1 + L_2 + L_3 \\ V_{4.SLS.q}(x) \ \text{ if } L_1 + L_2 + L_3 < x \le L_1 + L_2 + L_3 + L_4 \end{array} \right.$$

$$V_{A.x.SLS.q} := \begin{pmatrix} 0m \\ 0m \end{pmatrix}$$

$$V_{A.y.SLS.q} := \begin{pmatrix} 0 \\ R_{A.SLS.q} \end{pmatrix} = \begin{pmatrix} 0 \\ 27.272 \end{pmatrix} \cdot kN$$

$$V_{B.x.SLS.q} := \begin{pmatrix} L_1 \\ L_1 \end{pmatrix} = \begin{pmatrix} 4.2 \\ 4.2 \end{pmatrix} m$$

$$V_{B.y.SLS.q} := \begin{pmatrix} R_{B2.SLS.q} \\ -R_{B1.SLS.q} \end{pmatrix} = \begin{pmatrix} -123.876 \\ -15.717 \end{pmatrix} \cdot kN$$

$$V_{C.x.SLS.q} := \begin{pmatrix} L_1 + L_2 \\ L_1 + L_2 \end{pmatrix} = \begin{pmatrix} 6.3 \\ 6.3 \end{pmatrix} m$$

$$V_{C.y.SLS.q} := \begin{pmatrix} R_{C2.SLS.q} \\ -R_{C1.SLS.q} \end{pmatrix} = \begin{pmatrix} 88.439 \\ -123.876 \end{pmatrix} \cdot kN$$

$$V_{D.x.SLS.q} := \begin{pmatrix} L_1 + L_2 + L_3 \\ L_1 + L_2 + L_3 \end{pmatrix} = \begin{pmatrix} 23.1 \\ 23.1 \end{pmatrix} m \qquad V_{D.y.SLS.q} := \begin{pmatrix} R_{D2.SLS.q} \\ -R_{D1.SLS.q} \end{pmatrix} = \begin{pmatrix} 46.319 \\ -83.519 \end{pmatrix} \cdot kN$$

$$V_{E.x.SLS.q} := \begin{pmatrix} L_1 + L_2 + L_3 + L_4 \\ L_1 + L_2 + L_3 + L_4 \end{pmatrix} = \begin{pmatrix} 27.3 \\ 27.3 \end{pmatrix} m \qquad V_{E.y.SLS.q} := \begin{pmatrix} -R_{E.SLS.q} \\ 0 \end{pmatrix} = \begin{pmatrix} 46.319 \\ 0 \end{pmatrix} \cdot kN$$

$$V_{max.SLS.q} := \max\left(V_{A.y.SLS.q}, V_{B.y.SLS.q}, V_{C.y.SLS.q}, V_{D.y.SLS.q}, V_{E.y.SLS.q}\right) = 88.439 \cdot kN$$

$$V_{min.SLS.q} := \min\left(V_{A.y.SLS.q}, V_{B.y.SLS.q}, V_{C.y.SLS.q}, V_{D.y.SLS.q}, V_{E.y.SLS.q}\right) = -123.876 \cdot kN$$

Moment distribution

$$M_{1.SLS.q}(x) := R_{A.SLS.q} \cdot x - q_{1.SLS.q} \cdot x \cdot \frac{x}{2}$$

$$M_{2.SLS.q}(x) := R_{A.SLS.q} \cdot x + R_{B.SLS.q} \cdot \left(x - L_1\right) - q_{1.SLS.q} \cdot L_1 \cdot \left(x - \frac{L_1}{2}\right) - q_{2.SLS.q} \cdot \left(x - L_1\right) \cdot \left(\frac{x - L_1}{2}\right)$$

$$M_{3.SLS.q}(x) := R_{A.SLS.q} \cdot x + R_{B.SLS.q} \cdot \left(x - L_1\right) + R_{C.SLS.q} \cdot \left[x - \left(L_1 + L_2\right)\right] - q_{1.SLS.q} \cdot L_1 \cdot \left(x - \frac{L_1}{2}\right) \dots$$
$$+ -q_{2.SLS.q} \cdot L_2 \cdot \left[x - \left(L_1 + \frac{L_2}{2}\right)\right] - q_{3.SLS.q} \cdot \left[x - \left(L_1 + L_2\right)\right] \cdot \left[\frac{x - \left(L_1 + L_2\right)}{2}\right]$$

$$M_{4.SLS.q}(x) := R_{A.SLS.q} \cdot x + R_{B.SLS.q} \cdot \left(x - L_1\right) + R_{C.SLS.q} \cdot \left[x - \left(L_1 + L_2\right)\right] + R_{D.SLS.q} \cdot \left[x - \left(L_1 + L_2 + L_3\right)\right] \dots$$
$$+ -q_{1.SLS.q} \cdot L_1 \cdot \left(x - \frac{L_1}{2}\right) - q_{2.SLS.q} \cdot L_2 \cdot \left[x - \left(L_1 + \frac{L_2}{2}\right)\right] - q_{3.SLS.q} \cdot L_3 \cdot \left[x - \left(L_1 + L_2 + \frac{L_3}{2}\right)\right] \dots$$
$$+ -q_{4.SLS.q} \cdot \left[x - \left(L_1 + L_2 + L_3\right)\right] \cdot \left[\frac{x - \left(L_1 + L_2 + L_3\right)}{2}\right]$$

$$M_{SLS.q}(x) := \begin{cases} M_{1.SLS.q}(x) & \text{if } x \le L_1 \\ M_{2.SLS.q}(x) & \text{if } L_1 < x \le L_1 + L_2 \\ M_{3.SLS.q}(x) & \text{if } L_1 + L_2 < x \le L_1 + L_2 + L_3 \\ M_{4.SLS.q}(x) & \text{if } L_1 + L_2 + L_3 < x \le L_1 + L_2 + L_3 + L_4 \end{cases}$$

Field moment

$x_{00} = 0$

$x_{0.1.SLS.q} := \text{Maximize}\left(M_{1.SLS.q}, x_{00}\right) = 2.664\,m$ Point where shear force is zero

$x_{0.2.SLS.q} := \text{Maximize}\left(M_{2.SLS.q}, x_{00}\right) = ▮$

$x_{0.3.SLS.q} := \text{Maximize}\left(M_{3.SLS.q}, x_{00}\right) = 14.94\,m$

$x_{0.4.SLS.q} := \text{Maximize}\left(M_{4.SLS.q}, x_{00}\right) = ▮$

$$x_{0.1.SLS.q} := \begin{cases} x_{0.1.SLS.q} & \text{if } 0m \le x_{0.1.SLS.q} \le L_1 \\ 0m & \text{otherwise} \end{cases}$$

Check if zero shear force point is within the span, otherwise it is replaced with a dummy number.

$$x_{0.2.SLS.q} := \begin{cases} x_{0.2.SLS.q} & \text{if } L_1 \le x_{0.2.SLS.q} \le L_1 + L_2 \\ L_1 & \text{otherwise} \end{cases}$$

$$x_{0.3.SLS.q} := \begin{cases} x_{0.3.SLS.q} & \text{if } L_1 + L_2 \le x_{0.3.SLS.q} \le L_1 + L_2 + L_3 \\ L_1 + L_2 & \text{otherwise} \end{cases}$$

$$x_{0.4.SLS.q} := \begin{cases} x_{0.4.SLS.q} & \text{if } L_1 + L_2 + L_3 \le x_{0.4.SLS.q} \le L_1 + L_2 + L_3 + L_4 \\ L_{tot} & \text{otherwise} \end{cases}$$

$M_{f1.SLS.q} := M_{1.SLS.q}(x_{0.1.SLS.q}) = 36.333 \cdot kN \cdot m$

$M_{f2.SLS.q} := M_{2.SLS.q}(x_{0.2.SLS.q}) = \blacksquare \cdot kN \cdot m$

$M_{f3.SLS.q} := M_{3.SLS.q}(x_{0.3.SLS.q}) = 146.201 \cdot kN \cdot m$

$M_{f4.SLS.q} := M_{4.SLS.q}(x_{0.4.SLS.q}) = \blacksquare \cdot kN \cdot m$

$M_{max.f.SLS.q} := \max(M_{f1.SLS.q}, M_{f2.SLS.q}, M_{f3.SLS.q}, M_{f4.SLS.q}) = \blacksquare \cdot kN \cdot m$ Maximum field moment

$M_{max.f.SLS.q} := M_{f3.SLS.q} = 146.201 \cdot kN \cdot m$ Overwritten

Zero moment positions

$$x_{M0.1.SLS.q} := \mathrm{root}\left(M_{SLS.q}(x), x, 0, \frac{L_1}{2}\right) = 0\,m$$

$$x_{M0.2.SLS.q} := \mathrm{root}\left(M_{SLS.q}(x), x, \frac{L_1}{2}, L_1 + \frac{L_2}{2}\right) = 4.396\,m$$

$$x_{M0.3.SLS.q} := \mathrm{root}\left(M_{SLS.q}(x), x, L_1 + \frac{L_2}{2}, L_1 + L_2 + \frac{L_3}{2}\right) = 9.596\,m$$

$$x_{M0.4.SLS.q} := \mathrm{root}\left(M_{SLS.q}(x), x, L_1 + L_2 + \frac{L_3}{2}, L_1 + L_2 + L_3 + \frac{L_4}{2}\right) = 20.285\,m$$

$$x_{M0.5.SLS.q} := \mathrm{root}\left(M_{SLS.q}(x), x, L_1 + L_2 + L_3 + \frac{L_4}{2}, L_{tot}\right) = \blacksquare$$

Deflection

$EI = 241.445 \cdot MPa \cdot m^4$ Flexural Rigidity

$\kappa_{SLS.q}(x) := \dfrac{M_{SLS.q}(x)}{EI}$ Curvature

$$\theta_{A.SLS.q} := \frac{\int_0^{L_1} \kappa_{SLS.q}(x)\cdot\left(L_1 - x\right) dx}{L_1} = 2.012\times 10^{-4}$$

$$\theta_{B1.SLS.q} := \frac{\int_0^{L_1} \kappa_{SLS.q}(x)\cdot x\, dx}{L_1} = 2.716\times 10^{-4}$$

$$\theta_{B2.SLS.q} := \frac{\int_{L_1}^{L_1+L_2} \kappa_{SLS.q}(x)\cdot\left(L_1 + L_2 - x\right) dx}{L_2} = -2.716\times 10^{-4}$$

$$\theta_{C1.SLS.q} := \frac{\int_{L_1}^{L_1+L_2} \kappa_{SLS.q}(x)\cdot\left(x - L_1\right) dx}{L_2} = -6.487\times 10^{-4}$$

$$\theta_{C2.SLS.q} := \frac{\int_{L_1+L_2}^{L_1+L_2+L_3} \kappa_{SLS.q}(x)\cdot\left(L_1 + L_2 + L_3 - x\right) dx}{L_3} = 6.487\times 10^{-4}$$

$$\theta_{D1.SLS.q} := \frac{\int_{L_1+L_2}^{L_1+L_2+L_3} \kappa_{SLS.q}(x)\cdot\left(x - L_1 - L_2\right) dx}{L_3} = 1.128\times 10^{-3}$$

$$\theta_{D2.SLS.q} := \frac{\int_{L_1+L_2+L_3}^{L_1+L_2+L_3+L_4} \kappa_{SLS.q}(x)\cdot\left(L_1 + L_2 + L_3 + L_4 - x\right) dx}{L_4} = -1.128\times 10^{-3}$$

$$\theta_{E.SLS.q} := \frac{\int_{L_1+L_2+L_3}^{L_1+L_2+L_3+L_4} \kappa_{SLS.q}(x)\cdot\left(x - L_1 - L_2 - L_3\right) dx}{L_4} = -5.64\times 10^{-4}$$

$$f_{1.SLS.q}(x) := \theta_{A.SLS.q}\cdot x - \int_0^x \int_0^x \kappa_{SLS.q}(x)\, dx\, dx$$

$$f_{2.SLS.q}(x) := \theta_{B2.SLS.q}\cdot\left(x - L_1\right) - \int_{L_1}^x \int_{L_1}^x \kappa_{SLS.q}(x)\, dx\, dx$$

$$f_{3.SLS.q}(x) := \theta_{C2.SLS.q}\cdot\left(x - L_1 - L_2\right) - \int_{L_1+L_2}^x \int_{L_1+L_2}^x \kappa_{SLS.q}(x)\, dx\, dx$$

$$f_{4.SLS.q}(x) := \theta_{D2.SLS.q}\cdot\left(x - L_1 - L_2 - L_3\right) - \int_{L_1+L_2+L_3}^{x}\int_{L_1+L_2+L_3}^{x}\kappa_{SLS.q}(x)\,dx\,dx$$

$$f_{SLS.q}(x) := \begin{array}{|l} f_{1.SLS.q}(x) \ \text{ if } x \le L_1 \\ f_{2.SLS.q}(x) \ \text{ if } L_1 < x \le L_1 + L_2 \\ f_{3.SLS.q}(x) \ \text{ if } L_1 + L_2 < x \le L_1 + L_2 + L_3 \\ f_{4.SLS.q}(x) \ \text{ if } L_1 + L_2 + L_3 < x \le L_1 + L_2 + L_3 + L_4 \end{array}$$

Maximum deflection

$x_{\theta0.1.guess} = 2.1\,m$ Guess of where curvature is zero

$x_{\theta0.2.guess} = 5.25\,m$

$x_{\theta0.3.guess} = 14.7\,m$

$x_{\theta0.4.guess} = 25.2\,m$

$$x_{\theta0.1.SLS.q} := \mathrm{root}\left(\int_{0}^{x_{\theta0.1.guess}}\kappa_{SLS.q}(x)\,dx - \theta_{A.SLS.q}, x_{\theta0.1.guess}\right) = 2.221\,m$$ Position where curvature is zero

$$x_{\theta0.2.SLS.q} := \mathrm{root}\left(\int_{L_1}^{x_{\theta0.2.guess}}\kappa_{SLS.q}(x)\,dx - \theta_{B2.SLS.q}, x_{\theta0.2.guess}\right) = 5.443\,m$$

$$x_{\theta0.3.SLS.q} := \mathrm{root}\left(\int_{L_1+L_2}^{x_{\theta0.3.guess}}\kappa_{SLS.q}(x)\,dx - \theta_{C2.SLS.q}, x_{\theta0.3.guess}\right) = 14.898\,m$$

$$x_{\theta0.4.SLS.q} := \mathrm{root}\left(\int_{L_1+L_2+L_3}^{x_{\theta0.4.guess}}\kappa_{SLS.q}(x)\,dx - \theta_{D2.SLS.q}, x_{\theta0.4.guess}\right) = 24.875\,m$$

$f_{max.1.SLS.q} := -f_{1.SLS.q}\left(x_{\theta0.1.SLS.q}\right) = -0.284\cdot mm$ Maximum field deflection

$f_{max.2.SLS.q} := -f_{2.SLS.q}\left(x_{\theta0.2.SLS.q}\right) = 0.251\cdot mm$

$f_{max.3.SLS.q} := -f_{3.SLS.q}\left(x_{\theta0.3.SLS.q}\right) = -12.537\cdot mm$

$f_{max.4.SLS.q} := -f_{4.SLS.q}\left(x_{\theta0.4.SLS.q}\right) = 0.912\cdot mm$

$f_{max.up.SLS.q} := \max\left(f_{max.1.SLS.q}, f_{max.2.SLS.q}, f_{max.3.SLS.q}, f_{max.4.SLS.q}\right) = 0.912\cdot mm$

$f_{max.down.SLS.q} := \min\left(f_{max.1.SLS.q}, f_{max.2.SLS.q}, f_{max.3.SLS.q}, f_{max.4.SLS.q}\right) = -12.537\cdot mm$

Summary of design load response - variable load in SLS

Maximum support moment in support C
Maximum field moment in field 3

$$M_{max.sls.z.q} := \max\left(\left|M_{max.s.SLS.q}\right|, \left|M_{max.f.SLS.q}\right|\right) = 235.874 \cdot kN \cdot m$$

Maximum reaction force (compression) in support C
Maximum reaction force (tension) in support B

$$R_{max.c.sls.z.q} := R_{max.c.SLS.q} = 212.316 \cdot kN$$

$$R_{max.t.sls.z.q} := R_{max.t.SLS.q} = -108.159 \cdot kN$$

Maximum shear force in support C
Design shear force = negative shear

$$V_{max.sls.z.q} := \max\left(\left|V_{max.SLS.q}\right|, \left|V_{min.SLS.q}\right|\right) = 123.876 \cdot kN$$

Maximum deflection in span 3

$$\delta_{max.sls.q} := f_{max.down.SLS.q} = -12.537 \cdot mm$$

SLS capacity

Limited deflection

Limitation of deflection for pedestrian load

$$\delta_{lim} := \frac{1}{200}$$

EN1995-2 tab. 7.1

Deflection due to shear

Shear deflections should be checked for slender web panels. As the bridge deck is assumed to interact like a horizontal truss, the shear deflections can be neglected.

$$Control_{w.s} := \begin{cases} \text{"Check shear deflection"} & \text{if } \frac{L_3}{h_{lvl}} < 10 \\ \text{"Ignore shear deflection"} & \text{otherwise} \end{cases} = \text{"Ignore shear deflection"}$$

Instantaneous deformation, variable load

Deformation due to frequent load

$$u_{inst.Q} := f_{max.down.SLS.q} = -12.537 \cdot mm$$

Instantaneous deformation, permanent load

Deformation due to frequent load

$$u_{inst.G} := f_{max.down.SLS} = -5.265 \cdot mm$$

Final deformation

$$u_{fin} = u_{inst.Q} \cdot \left(1 + \psi_2 \cdot k_{def}\right) + u_{inst.G} \cdot \left(1 + k_{def}\right)$$

$$\psi_{2.w} = 0$$

$$\psi_{2.fk} = 0$$

$$u_{fin} := u_{inst.Q} + u_{inst.G} \cdot \left(1 + k_{def}\right) = -28.332 \cdot mm$$

Control final deformation, span 3

Span 1

$$\text{Control}_{u.fin} := \begin{cases} \text{"OK"} & \text{if } \left|u_{fin}\right| < \delta_{lim} \cdot L_3 \\ \text{"Not OK"} & \text{otherwise} \end{cases} = \text{"OK"}$$

Detailed design

Indata

$b_{beams} := B - 200mm \cdot 2 = 2.1\,m$ Distance between outer beams

Global load response

The load reactions are extracted for critical load responses, and corresponds to different load cases (see Chapter 7 in report).

Vertical load (permanent+variable, uls)	Transverse load (wind)
Shear force, support C	
$V_z := 281kN$	$V_x := 48.2kN$
Reaction force, support C	
$R_z := 459kN$	$R_x := 78.4kN$
Support moment, support C	
$M_{s.z} := 477kN \cdot m$	$M_{s.x} := 80.8kN \cdot m$
Field moment, span 3	
$M_{f.z} := 294kN \cdot m$	$M_{f.x} := 49.7kN \cdot m$

Prestressing force

The prestressing between the lamellas must be large enough to hold the bending stresses due to transverse bending, and hinder "glidning" due to transverse shear.
Calculate in ULS.

The force required to create the sinusoidal shape is calculated as a point load pushing down a continuous beam to the desired deflection. This can also be transferred into a simply supported beam with counteracting bending moments at the supports.

Dimensions, sectional constants

$p_1 := 70mm$ Wanted deflection

$L_{span} := s_{sin} \cdot 2 = 4.2\,m$ Distance between

$b_{lvl} = 54 \cdot mm$ Lamella thickness

$h_{lvl} = 600 \cdot mm$ Lamella height

$A_{lvl} = 32400 \cdot mm^2$ Lamella area

$I_{z.lvl} = 7873200 \cdot mm^4$ Second moment of area, around weak axis

$E_{m.0.flat} := 130MPa$ Modulus of elasticity for flatwise bending

$EI_P := E_{m.0.flat} \cdot I_{z.lvl} = 1.024 \cdot kN \cdot m^2$ Flexural rigidity

Calculate required point load for defleciton p

$$p_1 = \frac{M_1 \cdot L^2}{16 \cdot E \cdot I} + \frac{M_2 \cdot L^2}{16 \cdot E \cdot I} + \frac{P_1 \cdot L^3}{48 \cdot E \cdot I}$$

Deflection in mid span due to point load in middle of span and counteracting bending moments

$$P_1 = \frac{48 \cdot E \cdot I}{L^3} \cdot \left(p_1 - \frac{M_1 \cdot L^2}{16 \cdot E \cdot I} - \frac{M_2 \cdot L^2}{16 \cdot E \cdot I} \right)$$

Point load in middle of span for a specific deflection

$M_1(P_1) := -\frac{P_1}{2} \cdot \frac{L_{span}}{2} \cdot 0.5$ Left support moment due to pointload in middle of span

$M_2(P_1) := -\frac{P_1}{2} \cdot \frac{L_{span}}{2} \cdot 0.5$ Right support moment due to pointload in middle of span

$P_{1.guess} := 20N$ Guess of required point load to achieve wanted deflection

$$P_1 := \mathrm{root}\left[P_{1.guess} - \frac{48 \cdot EI_P}{L_{span}^3} \cdot \left(p_1 - \frac{M_1(P_{1.guess}) \cdot L_{span}^2}{16 \cdot EI_P} - \frac{M_2(P_{1.guess}) \cdot L_{span}^2}{16 \cdot EI_P}\right), P_{1.guess}\right]$$

$P_1 = 185.672\,N$ Required point load to reach wanted deflection

Compressive stress due to pre-stressing

The distancers are steel tubes in compression, threaded with a steel rod in tension. A steel plate distributes the compression forces from the steel tube to the LVL panel.

The long-term pre-stressing forces of a stress-laminated bridge deck is verified according to SS-EN 1995-2 Chp. 6.1.2

Dimensions Dywidag bar

$d_{bar} := 26.5mm$ Diameter pre-stressing bar

$f_{u.bar} := 1050MPa$ Hight-strength steel bar, Dywidag normally used in Sweden

$P_{max} := 646kN$ Max initial stressing force

$n_{layer.bar} := 2$ Number of bars over the height of the panels

$$A_{bar} := \frac{\pi \cdot d_{bar}^2}{4} = 5.515 \times 10^{-4}\,m^2$$

$$check_{hole} := \begin{cases} \text{"Disregard capacity check of holes"} & \text{if } \frac{d_{bar} \cdot 2}{h_{lvl}} < 20\% \\ \text{"Check capacity of holes"} & \text{otherwise} \end{cases} = \text{"Disregard capacity check of holes"}$$

Steel plate (between panel and compression tube)

$A_{plate.cs} := h_{plate} \cdot t_{plate}$ Cross-sectional area

$A_{plate.flat} := b_{plate} \cdot h_{plate} = 0.023\,m^2$ Face area

Effect of prestressing

Required presressing force

$$N = \max\left(\frac{1.5 \cdot V_t}{h \cdot \mu}, \frac{6M_t}{h^2}\right)$$

V.t = shear force between lamellas
M.t = bending due to uniformly distributed load on the deck (across)
h = height of lamella panel

Load effect load on the deck, transverse uniformly distributed load

Consider vertical load: self-weigt + traffic load (pedestrians)

Total permanent load across the deck

$$G_{k.across} := \frac{G_{k.bridge} + G_{k.deck}}{B} \cdot L = 47.907 \cdot \frac{kN}{m}$$

Total variable load across the deck

$$Q_{fk.z.across} := Q_{fk} \cdot L = 111.773 \cdot \frac{kN}{m}$$

Consider the deck as simply supported on the two outer, straight beams. Calculate the load effect due to uniformly distributed load across the deck

Calculate in SLS

$$q_t := \gamma_G \cdot G_{k.across} + \gamma_Q \cdot Q_{fk.z.across} = 225.148 \cdot \frac{kN}{m}$$

$$M_t := \frac{q_t \cdot b_{beams}^2}{8} = 124.113 \cdot kN \cdot m$$

$$V_t := \frac{q_t \cdot b_{beams}}{2} = 236.405 \cdot kN$$

Shear stress between lamellas

Consider the shear force in one bar.

$$V_{t.bar} := \frac{V_t}{2} = 118.203 \cdot kN$$

Friction coefficient

$$\mu_d := 0.40$$

Coefficient of friction, EC5-2 Table 6.1: planed timber to planed timber (MC >16%), perpendicular to grain.

Effective height of the cross-section:
The height of the shear connection correspond to the height of the steel plate, including the load path effect (45 deg)

$$h_{ef.v} := h_{plate} + 2 \cdot \frac{b_{lvl}}{\tan(45deg)} = 258 \cdot mm$$

Obs overlap with the other plate!

$$b_{ef.v} := b_{plate} + 2 \cdot \frac{b_{lvl}}{\tan(45deg)} = 0.258\,m$$

$$A_{ef.v} := h_{ef.v} \cdot b_{ef.v} = 0.067\,m^2$$

$$2 \cdot h_{ef.v} < h_{lvl} = 1$$

OBS the effective height of two plates are larger than the height of the LVL panels

$$\tau_v := \frac{1.5 \cdot V_{t.bar}}{A_{ef.v} \cdot \mu_d} = 6.659 \cdot MPa$$

Bending stress in the upper part of the lamellas

Consider the bending stresses at the edge of the panels (conservative, more exact would be to use the bending stress in the point of the tension rod).

$$h_{ef.b} := h_{lvl} = 0.6\,m$$

$$b_{ef.b} := b_{ef.v} = 258 \cdot mm$$

$$W_{ef.b} := \frac{b_{ef.b} \cdot h_{ef.b}^{2}}{6}$$

$$\sigma_b := \frac{M_t}{W_{ef.b}} = 8.018 \cdot MPa$$

<u>Required compression force on the lamellas</u>

Minimum required compression stress

$$\sigma_{c.t} := \max\left(\tau_v, \sigma_b\right) = 8.018 \cdot MPa$$

Bending stresses are dimensioning for the required compression force

Minimum required compression force on the panels

$$N_c := \sigma_{c.t} \cdot b_{ef.b} \cdot h_{ef.b} = 1.241 \times 10^{3} \cdot kN$$

Corresponding required tension force from two steel bars

$$N_{c.bar} := \sigma_{c.t} \cdot 2A_{bar} = 8.844 \cdot kN$$

Minimum required compression force in one steel tube

$$N_{c.tube} := \frac{N_{c.bar}}{2} = 4.422 \cdot kN$$

<u>Verify the compression capacity in LVL</u>

Corresponding compression stress from the steel plate to the panel

$$\sigma_{c.panel} := \sigma_{c.t} \cdot \frac{h_{ef.v} \cdot b_{ef.v}}{h_{ef.b} \cdot b_{ef.b}} = 3.448 \cdot MPa$$

$$\eta_{\sigma.panel} := \frac{\sigma_{c.panel}}{f_{c.0.d.lvl}} = 23.641 \cdot \%$$

<u>Verify the tension capacity of the steel bar</u>

$$\eta_{\sigma.bar} := \frac{N_{c.bar}}{P_{max}} = 1.369 \cdot \%$$

Maximum allowed pretension of the tension bar is 70% of the ultimate tension capacity.

$$\eta_{N.bar} := \frac{N_{c.bar}}{f_{u.bar} \cdot 2A_{bar}} = 0.764 \cdot \%$$

<u>Verify that the compression force is larger than the required point load on the panels</u>

$$check_{N.c.bar} := \left| \begin{array}{l} \text{"OK"} \quad \text{if } P_1 < N_{c.bar} \\ \text{"NOT OK"} \quad \text{otherwise} \end{array} \right. = \text{"OK"}$$

Check buckling of compression tubes

Sectional constants

$$I_{x.tube} := \frac{\pi}{64}\cdot\left(D_1^{\,4} - d_1^{\,4}\right) = 1.006\times 10^{-6}\,m^4$$

$$I_{z.tube} := \frac{\pi}{64}\cdot\left(D_1^{\,4} - d_1^{\,4}\right) = 1.006\times 10^{-6}\,m^4$$

$$l_{0.tube} := 0.5\cdot L_{tube} = 45\cdot mm$$ Effective length

Check slenderness

$$\lambda_{tube} := \frac{l_{0.tube}}{\sqrt{\frac{I_{x.tube}}{A_{tube}}}} = 1.856$$ Slenderness

$$N_{cr} := \frac{\pi^2\cdot E_{steel}\cdot I_{x.tube}}{l_{0.tube}^{\,2}} = 1.03\times 10^6\cdot kN$$

$$\lambda_{bar} := \sqrt{\frac{A_{tube}\cdot f_y}{N_{cr}}} = 0.021$$

$$check_{slenderness} := \left|\begin{array}{l}\text{"NO Buckling occurs"} \quad \text{if } \lambda_{bar} \le 0.2 \\ \text{"Buckling needs to be checked"} \quad \text{otherwise}\end{array}\right. = \text{"NO Buckling occurs"}$$

Verfiy

Minimum required compression force on the panels = compression force on the steel tubes

$$\sigma_{tube} := \frac{N_{c.tube}}{A_{tube}} = 2.584\cdot MPa$$

$$check_{\sigma.tube} := \left|\begin{array}{l}\text{"OK"} \quad \text{if } \sigma_{tube} \le f_y \\ \text{"NOT OK"} \quad \text{otherwise}\end{array}\right. = \text{"OK"}$$

$$\eta_{tube} := \frac{\sigma_{tube}}{f_y} = 0.9\cdot\%$$